Chromosome Dynamics of the Early Meiotic Cell Cycle in *S. cerevisiae*

by

Hannah G. Blitzblau

Sc.B. Biochemistry
Brown University, 1999

Submitted to the Department of Biology in partial fulfillment
of the requirements for the degree of

Doctor of Philosophy in Biology

at the

Massachusetts Institute of Technology

February 2008

Signature of Author: _____
Department of Biology
January 11, 2008

Certified by: _____
Stephen P. Bell
Professor of Biology
Thesis Supervisor

Accepted by: _____
Stephen P. Bell
Professor of Biology
Chair, Committee for Graduate Students

Chromosome Dynamics of the Early Meiotic Cell Cycle in *S. cerevisiae*

By

Hannah G. Blitzblau

Submitted to the Department of Biology in partial fulfillment of the requirements for the degree of Doctor of Philosophy in Biology

Abstract

In every cell cycle the genetic material must be duplicated and transmitted to the daughter cells. Meiosis is a developmental program that allows a diploid cell to produce haploid progeny. The reduction in chromosome number obtained during meiosis requires specialized mechanisms that are absent during the canonical mitotic cell cycle. Although previous studies found strong similarities between pre-mitotic and pre-meiotic DNA replication, pre-meiotic S phase is longer than pre-mitotic S phase, suggesting that meiosis-specific events regulate the rate of DNA replication. Additionally, after DNA replication, homologous recombination is initiated by the introduction of hundreds DNA double-strand breaks (DSBs) into the genome to produce physical DNA exchnges, or crossovers, between homologous chromosomes. To investigate the chromosome dynamics of the early meiotic cell cycle, I performed comprehensive analysis of pre-meiotic DNA replication and DSB formation in budding yeast.

Genome-wide studies of pre-meiotic DNA replication confirmed that the same replication origins are selected and activated in pre-meiotic and pre-mitotic cells, although replication was delayed at a large number of origins. These results indicate that the regulation of DNA replication is similar in the meiotic and mitotic cell cycles, but that the replication-timing program differs. Elimination of meiosis-specific cohesion or homologous recombination had no effect on the number or identity of early pre-meiotic origins. Analysis of cells sporulated in the presence of the replication inhibitor HU revealed a Cln3-dependent inhibition of meiotic entry.

To map the locations of meiotic DSBs, I developed a method to detect meiotic ssDNA. Examination of the sites of ssDNA enrichment indicated that DSBs occur mainly in the promoters of active genes, consistent with previous studies of individual DSB sites. Global analysis of the most common DSB sites revealed a non-random distribution of DSB "hotspots." In particular, DSB hotspots are over-enriched close to chromosome ends, which could explain why small chromosomes have a higher DSB density than large chromosomes. This mechanism could help ensure that all homologous chromosomes receive at least one crossover and segregate properly in meiosis. These studies also indicated that suppression of recombination at telomeres, centromeres and around the rDNA occurs by 3 distinct mechanisms.

Thesis advisor: Stephen P. Bell, Professor of Biology

To Sister, Anjakat and Menalie,

for their inspiration and support

Acknowledgements

This work could not have been completed without the help and support of a large number of people. Thank you to the past and present members of the Bell Lab family for creating a stimulating environment for scientific discovery and extracurricular hobbies. I am also indebted to past and present members of the Amon lab, particularly those in the meiosis group, for providing me with reagents, protocols, ideas and genuine friendship. Thank you to Andreas, as our collaboration has been great fun and the kind of success that the faculty told us would magically happen if we spent enough time together in the Pit (and Starbucks). My classmates in Biograd 2000 have become friends and colleagues in pursuits inside the lab, as well as dim sum, supper club, girls' night, river walks etc. My friends and family outside of MIT have constantly reminded me that I am part of a larger world that requires an excess of love, patience and creative vision to go 'round. I cannot thank my roommates, sister, Phil and Anna, enough for being there for me through this process as only the best of friends and family can.

I am extremely grateful to past and present members of my thesis committee, Anja-Katrin Bielinsky, Frank Solomon, Terry Orr-Weaver and Rick Young, who have always imparted scientific and life advice when it was needed.

I would like to specially acknowledge Angelika Amon, who has supported me ceaselessly as a mentor, second advisor, role model and friend.

Thank you especially to Steve, who, from start to finish, entrusted me with the means and freedom to follow my whims, wherever they took us. I have enjoyed his sound advice, stimulating scientific discussions, ability to be understanding, and generous nature, which make the Bell Lab a great place to work.

Table of Contents

Summary 3

Acknowledgements 7

Table of Contents 9

Chapter I: Introduction 11

Meiosis: a specialized cell division 13
Regulation of cell cycle entry 17
Regulation of DNA replication 20
The intra-S phase checkpoint 23
Regulation of replication timing 24
Pre-meiotic DNA replication 27
Initiation of homologous recombination 28
Repair of meiotic DSBs 31
Regulation of crossover formation 32
Co-regulation of DNA replication and recombination 35
Thesis Summary 37
References 38

Chapter II: Characterization of a slow S phase: pre-meiotic DNA replication in yeast 45

Summary 47
Introduction 49
Results 52
Differential pre-RC formation at a subset of pre-meiotic origins 52
The same origins are active in the meiotic and mitotic cell cycles 55
Replication initiation is delayed for some pre-meiotic origins 58
Hydroxyurea inhibits meiotic cell cycle entry 60
Initiation timing differs in the meiotic and mitotic cell cycles 64
Replication timing, cohesion and homolgous recombination 67
Discussion 70
Transcription regulated pre-RC assembly at a subset of origins 70
HU inhibits meiotic entry in a Cln3-dependent manner 72
Fewer early replicating origins during pre-meiotic S phase 73
Pre-meiotic and pre-mitotic DNA replication kinetics differ 74
Why a slow S phase? 77
Materials and Methods 78
Supplemental Data 80
References 104

Chapter III: Mapping of meiotic ssDNA reveals double-strand break hotspots near centromeres and telomeres 107

Summary 109
Introduction 111
Results 113
Labeling of ssDNA reveals DSB sites 113
Hotspots mapped by ssDNA versus Spo11 localization 117
DSBs are enriched in the promoters of active genes 120
Strong hotspots in the pericentromeric regions 123
Hotspot distribution near the rDNA and telomeres 125
Discussion 133
Acknowledgements 139
Materials and Methods 140
Supplemental Data 142
References 169

Chapter IV: Discussion and Future Directions 173
Key conclusions 175
Regulation of replication complex assembly 176
Regulation of replication timing in meiosis 177
The intra-S phase checkpoint in meiosis 179
Global distribution of DSB activity 181
Suppression of homologous recombination 182
References 184

Chapter I

Introduction

Meiosis: a specialized cell division

The survival of all species depends on their ability to reproduce and adapt to a changing environment. Sexually reproducing organisms have an evolutionary advantage because they can give rise to a genetically distinct offspring in each reproductive cycle through the fusion of gametes with half the genetic material of the parents. The reduction in chromosome number required for gamete production is carried out during a specialized cell division called meiosis, in which a single round of DNA replication precedes two successive chromosome segregation events. The most common problem encountered during meiosis is the failure of chromosomes to properly segregate, which leads to gametes with an inappropriate chromosome number and results in aneuploid offspring. In humans, more than 20% of conceptions fail because of meiotic errors and the rate of such errors increases with age (Hassold and Hunt 2001). Both genetic and environmental factors have been implicated in meiotic chromosome non-disjunction (Hunt and Hassold 2002). However, a mechanistic understanding of these effects has been impeded by the relative lack of understanding of mammalian meiosis. In contrast, many key insights into meiotic chromosome segregation have been revealed by recent work in both budding and fission yeast. The high degree of conservation of many meiotic regulators across eukaryotic species implies that understanding meiosis in the relatively simple yeast system will contribute to our understanding of human fertility.

Meiosis shares many characteristics with the well-studied mitotic cell division cycle, but instead of conserving chromosome number, meiosis allows cells to reduce the chromosome number by half (Figure 1). In mitosis, a single DNA replication event precedes the segregation of replicated chromosomes, termed sister chromatids, away from each other. Mitosis produces two

cells with identical genetic material to the progenitor. Meiosis is comprised of a single DNA replication event, followed by two consecutive chromosome segregations. In the first meiotic division, homologous chromosomes are separated and in the second division, sister chromatids segregate. DNA replication and the second meiotic division closely resemble the mitotic cell cycle and are regulated by many of the same factors. In contrast, the segregation of homologous chromosomes is unique to meiosis and requires specialized machinery and regulation.

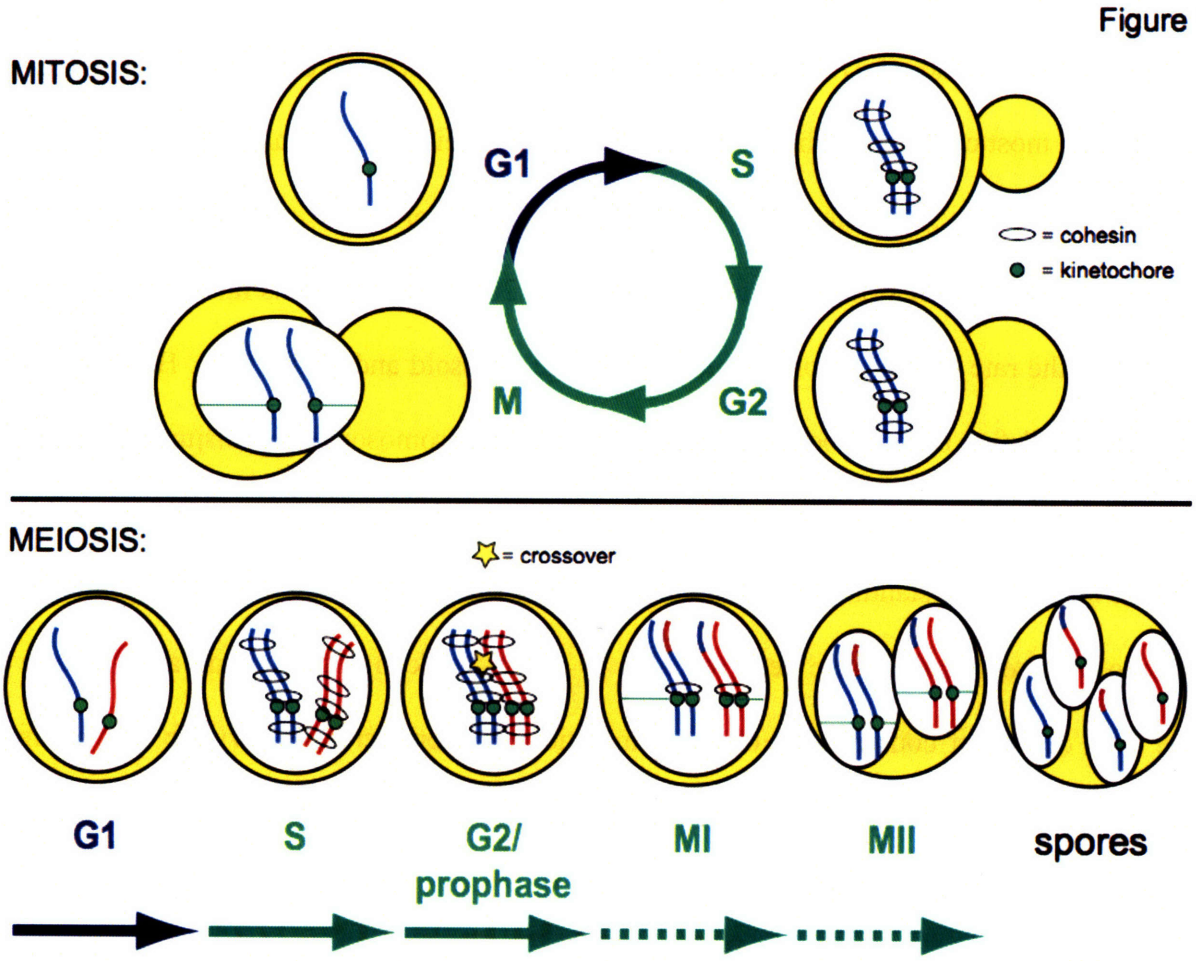

Figure 1. The mitotic and meiotic cell cycles

The major events of each stage of the mitotic and meiotic cell cycles are depicted. Red and blue indicate homologous chromosomes.

The alignment and faithful segregation of chromosomes is highly regulated to prevent lethal chromosome loss events. Chromosome segregation requires the attachment of the kinetochores of the two chromosomes to spindles emanating from opposite poles (Figure 1, mitosis). Cells sense the bipolar attachment of chromosomes because the chromosomes are physically attached to each other, such that when microtubules from opposite poles provide a pulling force on the chromosomes, tension is generated. In mitotically dividing cells, sister chromatids are segregated away from each other. Sister chromatids are bound together by the cohesion complex (cohesin) as they are replicated (Michaelis, Ciosk et al. 1997; Uhlmann and Nasmyth 1998) (Figure 1). Thus, when the kinetochores attach to microtubules from opposite poles in mitosis, the existing physical connection between sister chromatids allows tension to be generated and chromosomes can be faithfully segregated. In contrast, homologous chromosomes have no predetermined interaction and must become properly aligned and physically connected before they can satisfy the tension requirement of the spindle checkpoint in meiosis. The alignment and attachment of homologous chromosomes is accomplished by the process of meiotic homologous recombination. During recombination, at least one set of sister chromatids from each homologous chromosome pair undergoes a physical DNA exchange, or crossover (Figure 1, yellow star).

The faithful segregation of homologous chromosomes also requires meiosis-specific cohesin and kinetochore-associated factors. Because the sister chromatids of each homolog are held together by cohesion after they are replicated, the cohesin complexes distal to the crossover physically hold chromosomes together and allow tension to be generated when homologous chromosome attach to the meiotic spindle in metaphase I (Figure 1, meiotic G2/prophase).

Furthermore, special protein complexes located at the kinetochores ensure that the sister chromatids of each homolog attach to spindles from the same pole, so that homologs, but not sisters, are separated (Toth, Rabitsch et al. 2000; Rabitsch, Petronczki et al. 2003; Lee, Kiburz et al. 2004) (Figure 1, meiosis I). Following segregation of homologs in meiosis I, sister chromatids are segregated without either an intervening DNA replication event or new establishment of cohesion (meiosis II). Cohesion distal to the crossovers must be removed for chromosomes to separate in meiosis I, but for the second division to occur properly, cohesion at centromeres must be retained between sister chromatids until they have properly aligned at metaphase II. This step-wise removal of cohesin differs from that of mitosis and is carried out, in part, through the use of distinct cohesin complexes in meiosis (Buonomo, Clyne et al. 2000) and specialized proteins that protect cohesin around centromeres (Kerrebrock, Moore et al. 1995; Kitajima, Kawashima et al. 2004; Lee, Kiburz et al. 2004; Marston, Tham et al. 2004; Kiburz, Reynolds et al. 2005; Watanabe 2005).

Following the segregation of homologous chromosomes in meiosis I, sister chromatids are bioriented on the meiosis II spindle (Figure 1, meiosis II). Segregation of sister chromatids produces four haploid nuclei, which are packaged into spores in yeast. Cells then exit the cell cycle and meiosis is completed. The need for both homologous recombination and special regulation of cohesin and kinetochore components obliges meiotic cells to undertake a discrete and highly regulated developmental program. In this thesis, I will focus on the chromosome dynamics that occur early in the meiotic program. Specifically, I will focus on measuring pre-meiotic DNA replication and the initiation of recombination.

Regulation of cell cycle entry

The decision to undergo the meiotic program is regulated by external cellular signals in all organisms. In higher eukaryotes, meiosis is reserved for the production of gametes and occurs only in specialized organs. In this case, temporal and spatially restricted signals control the meiotic entry of a specific subset cells called germ cells. In yeast, the decision to enter either the mitotic or meiotic cell cycles is nutritionally regulated (Figure 2). When nutrients are plentiful, cells grow until they reach a sufficient size and then enter the mitotic cell cycle. In contrast, when nutrients are limiting, yeast can either enter G0 and cease cell division or, if they are diploid, enter the meiotic cell cycle. Yeast sporulate when they are starved of fermentable carbon and nitrogen. The spores that result from yeast meiosis enter a dormant state in which they can survive nutritional deprivation for long periods of time.

The meiotic developmental program is determined by altered transcription and protein synthesis. Altogether, ~1600 genes (>25% of the yeast genome) are differentially expressed between sporulating and non-sporulating cells (Chu, DeRisi et al. 1998; Primig, Williams et al. 2000). These changes in gene expression prevent mitosis-specific events such as budding and promote meiotic processes necessary for segregation of homologous chromosomes and spore formation. Meiosis-specific transcriptional activators implement the altered transcription program. Entry into meiosis is regulated by the synthesis and stability of the Ime1 transcription factor, which activates genes necessary for DNA replication and homologous recombination (Smith, Su et al. 1990). After homologous recombination, the Ndt80 transcription factor activates the expression of genes necessary for meiotic chromosome segregation (Chu and Herskowitz 1998).

Figure 2

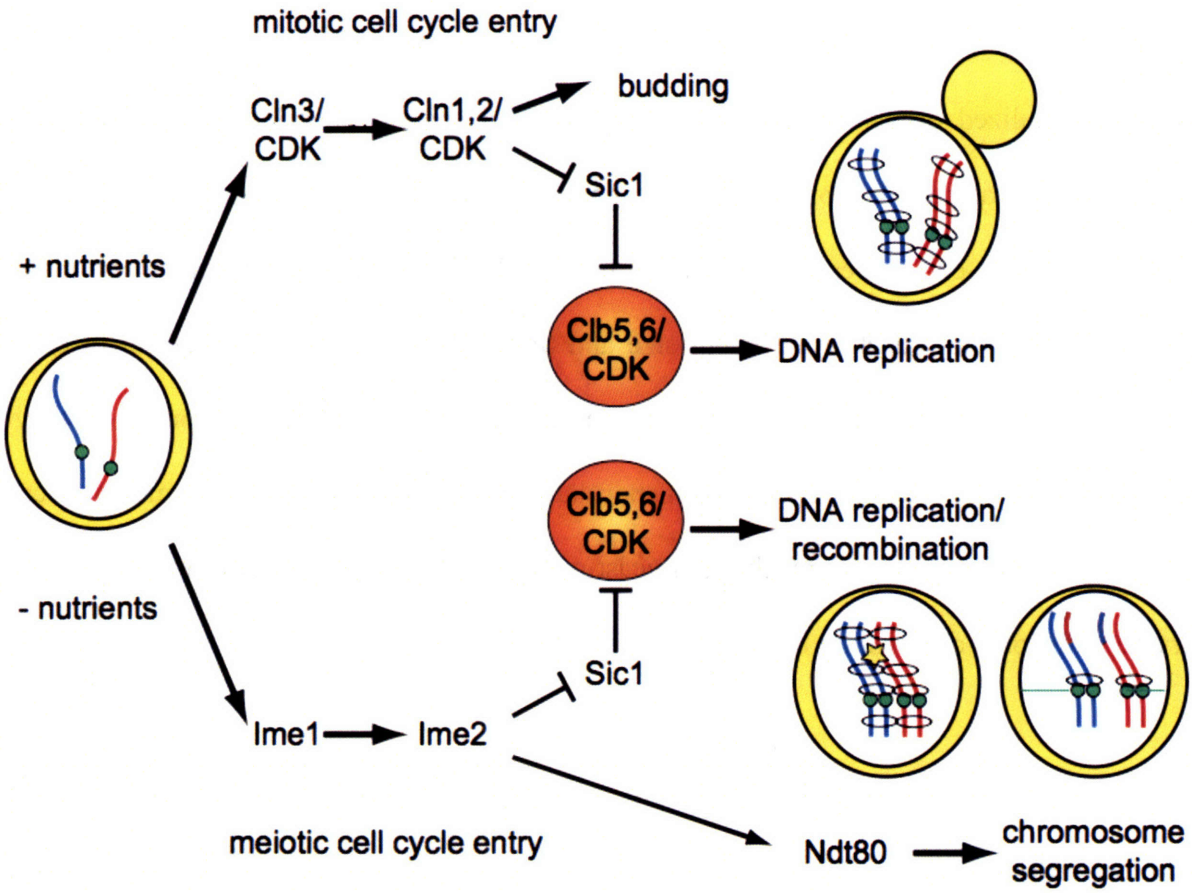

Figure 2: Cell cycle entry

The processes of mitotic and meiotic cell cycle entry are depicted. The presence or absence of fermentable carbon and nitrogen sources determines whether cells will enter the mitotic or meiotic cell cycle. Different mechanisms of activating Clb/CDK are shown.

In yeast, both the mitotic and meiotic cell cycles are regulated by the activity of the single cyclin-dependent kinase (CDK), Cdc28. Cdc28 promotes all DNA replication and chromosome segregation events in a complex with one of the six B-type cyclins, or Clbs. Clb5 and Clb6 are synthesized in G1, but remain inactive due to the presence of the B-type CDK inhibitor Sic1

(Schwob, Bohm et al. 1994). At the G1/S phase transition, Sic1 is degraded and Clb-CDK is activated. Clb5/Clb6-associated CDK activity promotes DNA replication (Kuhne and Linder 1993; Schwob and Nasmyth 1993). Prior to mitosis, four other B type cyclins, Clbs1-4, are synthesized and their activity regulates the single chromosome segregation (Surana, Robitsch et al. 1991; Fitch, Dahmann et al. 1992). CDK regulation is similar in sporulating cells, with a few exceptions. Clb5 and Clb6 are essential for both DNA replication and homologous recombination in early meiosis (Dirick, Goetsch et al. 1998; Stuart and Wittenberg 1998; Benjamin, Zhang et al. 2003). Clbs1, 3, 4 and 5 are synthesized prior to the two meiotic chromosome segregation events, but expression of *CLB2* is highly repressed in meiosis (Grandin and Reed 1993; Dahmann and Futcher 1995). After both mitosis and meiosis, the complete inactivation of Clb-CDK leads to spindle disassembly and cell cycle exit, allowing cells to reenter the next G1 phase. Therefore, the proper regulation of CDK activity is critical to all aspects of cell cycle progression in yeast.

The decision to activate CDK and enter either the meiotic or mitotic cell cycle occurs during the G1 phase when cells sense nutrient availability (Figure 2). When nutrients are plentiful, the mitotic cell cycle is initiated by the association of Cdc28 with the G1-specific cyclins Cln1, Cln2 and Cln3. Cln-CDK activity drives cell cycle progression by promoting both budding and Clb-CDK activation (Dirick, Bohm et al. 1995). Phosphorylation of Sic1 by Cln-CDK targets Sic1 for degradation, activating Clb-CDK and stimulating entry into S phase/DNA synthesis. Cln3 is the first cyclin to be activated during mitotic G1 and it both stimulates Cln1, Cln2, Clb5 and Clb6 synthesis and prevents cells from entering meiosis (Colomina, Gari et al. 1999). When nutrients are limiting, Cln3 is never activated. Instead, Ime1 induces transcription

of the gene for the meiosis-specific kinase, Ime2. Ime2 is homologous to Cdc28, but does not require a cyclin subunit for activation. Ime2 substrate specificity differs from Cdc28 (Clifford, Marinco et al. 2004; Holt, Hutti et al. 2007), allowing it to differentially regulate events of the early meiotic cell cycle. For example, Ime2 does not promote mitosis specific events such as budding, whereas Ime2 specifically promotes meiosis-specific functions such as activation of the Ndt80 transcription factor (Benjamin, Zhang et al. 2003; Honigberg and Purnapatre 2003). In some cases, Ime2 performs the same function as Cln-CDK, although it does so by phosphorylating substrates on distinct residues. For example, Ime2 is required to target Sic1 for degradation and thereby promote Clb-CDK activation in meiosis (Benjamin, Zhang et al. 2003), but it does so through the utilization of alternate sites on Sic1 than CDK uses (Sedgwick, Rawluk et al. 2006; Sawarynski, Kaplun et al. 2007).

Regulation of DNA replication

Activation of Clb-CDK drives cells into S phase. In both mitotic and meiotic cell cycles it is critical that the DNA is fully duplicated prior to its segregation into daughter cells. This ensures that each progeny receives a full complement of the genetic material. Additionally, faithful chromosome segregation in mitosis and meiosis require cohesion between sister chromatids that is established during S phase as the DNA is replicated (Uhlmann and Nasmyth 1998). The regulation of DNA replication during the mitotic cell cycle has been relatively well-characterized. The conservation of many of the key regulators of DNA replication in meiosis suggests that similar mechanisms probably function in pre-meiotic DNA replication.

The duplication of large eukaryotic genomes requires the coordination of hundreds of replication forks distributed throughout the genome. DNA replication begins at specific sites in the DNA termed origins of replication, and bidirectional replication forks proceed away from each origin. The region duplicated by the forks emanating from a single origin is termed a replicon. The duplication of large eukaryotic genomes that contain multiple chromosomes requires many replicons. The average eukaryotic replicon is ~40-100 kb, which is less than the length of even the smallest chromosome in yeast. Replicon size is limited both by stability of the replication fork assemblies and cell growth rate. Because replication usually initiates from origins, if forks collapse they are generally not able to reinitiate (Labib, Tercero et al. 2000). Additionally, utilization of multiple origins of replication allows DNA replication to be completed in a timely manner, providing a growth advantage to cells. However, replication forks must be coordinated such that each piece of DNA in the cell is duplicated only once per cell cycle, since over- or under-replication leads to genome instability and death (DePamphilis, Blow et al. 2006).

The initiation of DNA replication occurs in two steps; selection of potential replication origins and initiation of DNA replication (Figure 3) (Diffley and Labib 2002). Origins are selected during the G1 phase of the cell cycle by the association of a complex containing the replicative helicase with all potential origins of replication. Helicase loading is initiated by the multifunctional origin recognition complex (ORC), which binds to yeast replication origins in a sequence-specific manner throughout the cell cycle (Bell and Dutta 2002). When cells enter G1, the Cdc6 and Cdt1 proteins associate with ORC, and together ORC, Cdc6 and Cdt1 load the replicative helicase, the Mcm2-7 complex, onto DNA (Bowers, Randell et al. 2004; DePamphilis

2005; Randell, Bowers et al. 2006). The resulting "pre-replicative" complex (pre-RC), marks all potential replication origins. When cells progress into S phase, two kinases, Clb-CDK and Dbf4-Cdc7 (DDK), are activated, which promotes the origin association of additional proteins, including polymerases and regulatory factors (Zou and Stillman 2000). These proteins assemble into a pair of bidirectional replication forks that initiate the replication process. Existing pre-RCs are dismantled during initiation or when their associated DNA is replicated. CDK activation also prevents further pre-RC formation for the remainder of the cell cycle by multiple mechanisms involving phosphorylation of pre-RC components (Dahmann, Diffley et al. 1995; Nguyen, Co et al. 2001). The separation of pre-RC formation in G1 and replication initiation in S phase ensures that each origin is replicated only once, (Diffley 2004).

Figure 3

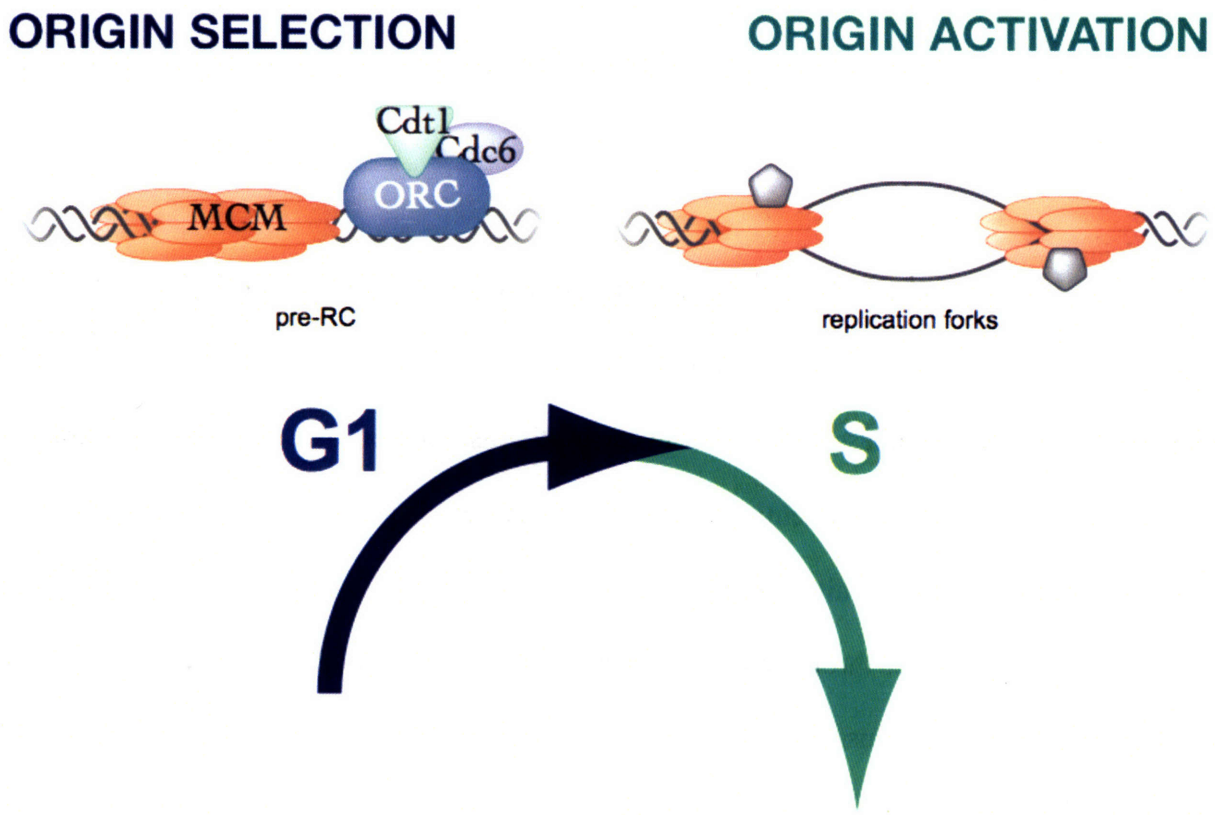

Figure 3: Cell cycle regulation of DNA replication initiation

During G1 with Clb/CDK activity is low (blue arrow), Cdc6 and Cdt associate with ORC and load the Mcm2-7 complex onto origin DNA. When cells enter S phase and Clb/CDK increases (green arrow), polymerases and accessory factors associate with origins (grey pentagons) and repliation initiates.

When cells enter S phase, DNA replication proceeds in an ordered fashion. Each origin initiates replication with a particular efficiency (the percentage of cells in which the origin initiates) and at a certain time during S phase. Forks progress away from origins at a relatively constant rate, leading to a reproducible temporal program of genomic replication. Multiple techniques have been used to measure local and genome-wide replication timing in mitotic cells and have led to a model in which different origins initiate replication at distinct times throughout S phase (Raghuraman, Winzeler et al. 2001; Yabuki, Terashima et al. 2002). It is unclear why all origins do not initiate replication as soon as cells enter S phase. Current models postulate either a limited supply of replication initiation factors or an advantage of reserving initiation from some origins until later in S phase in case existing forks stall or encounter DNA damage.

The intra-S phase checkpoint

When cells encounter problems during DNA replication, such as DNA damage or limiting nucleotide pools, they initiate the intra-S phase checkpoint to arrest cell cycle progression until DNA replication is completed. This checkpoint is distinct from other DNA damage checkpoints, because DNA replication intermediates share characteristics with other types of damage (e.g. the presence of ssDNA) and thus a different threshold must be set for checkpoint response during S phase (Shimada, Pasero et al. 2002). It is thought that the sensors

of the checkpoints are components of the replication fork and both fork stalling and excessive exposure of ssDNA are signals of replication stress (Paulovich and Hartwell 1995; Foiani, Pellicioli et al. 2000; Tercero, Longhese et al. 2003). The function of the checkpoint is carried out through the activation of the ATM-like kinase Mec1, and subsequently the Chk2-related kinase Rad53 (Cocker, Piatti et al. 1996; Santocanale and Diffley 1998; Shirahige, Hori et al. 1998). The intra-S phase checkpoint is distinct from the DNA damage checkpoint that prevents entry into mitosis in a Chk1-dependent manner (Sanchez, Bachant et al. 1999; Melo and Toczyski 2002). The Rad53 kinase can also be activated by the DNA damage checkpoint factors during S phase (Branzei and Foiani 2005). Rad53 activation leads to stabilization of stalled replication forks, inhibition of further initiation of DNA replication, and inhibition of spindle formation and progression into mitosis (Lopes, Cotta-Ramusino et al. 2001; Tercero and Diffley 2001; Branzei and Foiani 2005).

Regulation of replication timing

Activation of the intra-S phase checkpoint regulates of the kinetics of DNA replication at the levels of both the initiation and elongation of replication. Two well-characterized replication inhibitors have been used to study the effects of replication stress on replication progression: (1) hydroxyurea (HU) is an inhibitor if ribonucleotide reductase (RNR) that exerts an effect by decreasing intracellular dNTP levels; and (2) methylmethane sulfonate (MMS), which inhibits replication by methylating the DNA bases. Under both conditions, the effect of the inhibitor is sensed during S phase when forks stall due to either low nucleotide levels or DNA damage (Tercero, Longhese et al. 2003). The stalled forks activate the intra-S phase checkpoint, which leads to a decrease in the rate of DNA replication through both the inhibition of replication

initiation from origins that have not yet begun replication, as well as slowed replication fork progression (Shirahige, Hori et al. 1998; Tercero and Diffley 2001). When synchronized cells enter S phase in the presence of HU or MMS, origins that have already initiated replication before activation of the checkpoint are termed "early" origins (Yabuki, Terashima et al. 2002). These are the same origins that normally initiate replication early and efficiently in an unperturbed S phase (Raghuraman, Winzeler et al. 2001; Yabuki, Terashima et al. 2002). Therefore, the intra-S phase checkpoint has been used to separate origins that initiate DNA replication at different times in S phase into two functional classes; early origins that initiate DNA replication efficiently in the presence of replication inhibitors and late origins that do not.

Decreased levels of replication factors that function in both pre-RC formation and replication initiation can also lead to altered replication kinetics. Insufficient pre-RC formation leads to inefficient origin activation and protracted S phase progression due to the utilization of a smaller number of origins. Similarly, reduction of CDK levels through the deletion of the Clb5 cyclin inhibits replication initiation from late origins and therefore slows S phase progression (Donaldson, Raghuraman et al. 1998).

Chromatin structure has also been implicated in the regulation of replication timing. Elimination of the histone deacetylase Rpd3 was reported to alter replication efficiency and the timing of replication initiation (Vogelauer, Rubbi et al. 2002; Aparicio, Viggiani et al. 2004). However, gene expression is dramatically altered in *rpd3Δ* cells, thus, it is unclear whether the effect of Rpd3 removal on replication timing is through changes in origin proximal chromatin structure or because the expression of genes necessary for replication initiation is reduced in the

mutant background. A more direct test of the role of local chromatin structure was provided by experiments in which a histone acetylase was targeted to a late initiating origin of replication. Intriguingly, this modification resulted in an earlier time of replication intiation at that site, suggesting that local chromatin structure can influence origin activity (Vogelauer, Rubbi et al. 2002). Despite these findings, genome-wide analysis of histone occupancy and modification have not yet uncovered any correlation between local chromatin structure and the timing or efficiency of replication initiation.

The rate of DNA replication is also regulated during development. During the early cell divisions of *Drosophila* or *Xenopus* embryos when little transcription of the genome is occurring, DNA replication occurs very rapidly through the utilization of a large number of closely spaced origins (Coverley and Laskey 1994). Under these conditions of very rapid cell growth, there appears to be no S phase or DNA damage checkpoint, indicating that it is advantageous for cells to divide as quickly as possible at the expense of fidelity. Such a mechanism is tolerated because these organisms generate many embryos per mating. It is also likely that when replicon size is small, forks are less likely to stall because they do not need to process as far. As development proceeds and the transcription of many more genes occurs, the cell cycle length increases dramatically, fewer origins of replication are utilized and the intra-S phase checkpoint functions to ensure proper replication prior to chromosome segregation (Hyrien, Maric et al. 1995). Meiosis is an obligate developmental program in all sexually reproducing species. Interestingly, in every organism studied to date, pre-meiotic DNA replication lasts longer than mitotic DNA replication (Zickler and Kleckner 1999). Meiosis is not a proliferative cycle, but rather a single cell division that produces gametes that must fuse with each other or germinate before they can

proliferate. Thus there is little cost to the organism if the meiotic cell cycle is longer than the mitotic cell cycle, but there could be an important benefit to decreasing the rate of S phase during meiosis. This observation suggests that meiosis-specific events may regulate the timing of pre-meiotic DNA replication.

Pre-meiotic DNA replication

Pre-meiotic S phase in yeast takes approximately twice as long as mitotic S phase (Williamson, Johnston et al. 1983; Padmore, Cao et al. 1991), although the mechanism of DNA replication seems to be largely conserved. DNA replication mainly initiates at the same origins during both cell cycles (Collins and Newlon 1994; Mori and Shirahige 2007) and is dependent on the same members of the pre-RC, including ORC, Mcm2-7 and Cdc6 (Murakami and Nurse 2001; Lindner, Gregan et al. 2002; Ofir, Sagee et al. 2004; Hochwagen, Tham et al. 2005). Additionally, S phase in meiosis requires Clb5-CDK activation (Dirick, Goetsch et al. 1998; Stuart and Wittenberg 1998; Benjamin, Zhang et al. 2003). In contrast, DDK has been reported to be dispensable for pre-meiotic DNA replication (Schild and Byers 1978; Hollingsworth and Sclafani 1993; Wan, Zhang et al. 2006), although these results may be due to incomplete inactivation of the Cdc7 kinase. Because the basic mechanisms of DNA replication are similar in meiosis and mitosis, the longer pre-meiotic S phase could be the effect of decreases in the timing or efficiency of replication initiation or a slower replication fork rate during sporulation.

Obvious candidates for the meiosis-specific events that could influence DNA replication timing are the cohesin and recombination factors that are present only in the meiotic cell cycle. Cohesion is established between sister chromatids during pre-meiotic DNA replication, however,

the composition of the cohesin complex is altered in meiosis. The Rec8 protein replaces the Scc1 subunit in most cohesin complexes. Rec8-containing cohesin is essential for both meiotic recombination and the step-wise loss of cohesion during chromosome segregation (Klein, Mahr et al. 1999; Toth, Rabitsch et al. 2000). Similarly, some of the proteins required for homologous recombination begin to associate with chromosomes during pre-meiotic S phase (Smith and Roeder 1997; Leu, Chua et al. 1998; Blat, Protacio et al. 2002; Tsubouchi and Roeder 2002). Rec8 and Spo11, the endonuclease that makes DSBs during homologous recombination, have been implicated in the regulation of S phase length in sporulating yeast (Cha, Weiner et al. 2000), although the mechanism of such an effect is unknown. Studies of these effects have been hampered by the difficulty in measuring the length of pre-meiotic S phase in yeast. Entry into the meiotic cell cycle is not easily synchronized, therefore, within a population, indvidual cells start and finish S phase at different times. Although the average length of S phase in the population can be estimated from FACS measurements of DNA content, the length of pre-meiotic S phase in individual cells has not been calculated.

Initiation of homologous recombination

Directly after pre-meiotic DNA replication, the process of homologous recombination begins. The ultimate goal of homologous recombination is to create a physical DNA linkage between at least one set of sister chromatids for every homologous chromosome pair, because this serves to hold the chromosomes together during the first meiotic division. Homologous recombination proceeds in several steps. Double-strand breaks (DSBs) are formed across the genome, homologous chromosomes pair and form stable interactions and mature recombination

products are formed (Figure 4). The cytological results of the physical DNA exchanges between homologous chromosomes are chiasmata.

Homologous recombination is initiated during meiotic G2/prophase by the regulated introduction of at least 200 DSBs into the 16 chromosomes of the yeast genome. A large number of proteins are required for DSB formation in yeast (Keeney 2001; Arora, Kee et al. 2004; Prieler, Penkner et al. 2005), and a subset of these factors begin to associate with chromosomes prior to DSB formation. During meiotic G2/prophase, chromosomes begin to condense and some potential DSB sites undergo a "chromatin transition" and become sensitive to nucleolytic cleavage (Ohta, Shibata et al. 1994). This finding indicates that DSB site selection occurs prior to DNA cleavage. DSB formation also requires the activity of CDK and DDK (Hochwagen, Tham et al. 2005; Wan, Zhang et al. 2006).

DSBs are made by a topoisomerase-VI-related protein, Spo11, along with several accessory factors (Keeney 2001). Spo11 is widely conserved, with orthologs present in a wide variety of eukaryotic species including yeast, plants and humans. Spo11 is thought to cleave the DNA through a covalent intermediate, in which the 5' end of the DNA is attached to a catalytic tyrosine via a phosphodiester bond, similar to topoisomerases (Bergerat, de Massy et al. 1997) (Figure 4). A non-null mutation in the protein Rad50, termed rad50S, and null alleles of *SAE2/COM1* block cells at this stage of DSB formation (Alani, Padmore et al. 1990; McKee and Kleckner 1997; Prinz, Amon et al. 1997). In a wild-type cell, Spo11 is removed from the chromosome by cleavage of the DNA strand attached to Spo11, allowing for repair of the DSB (Neale, Pan et al. 2005).

Figure 4

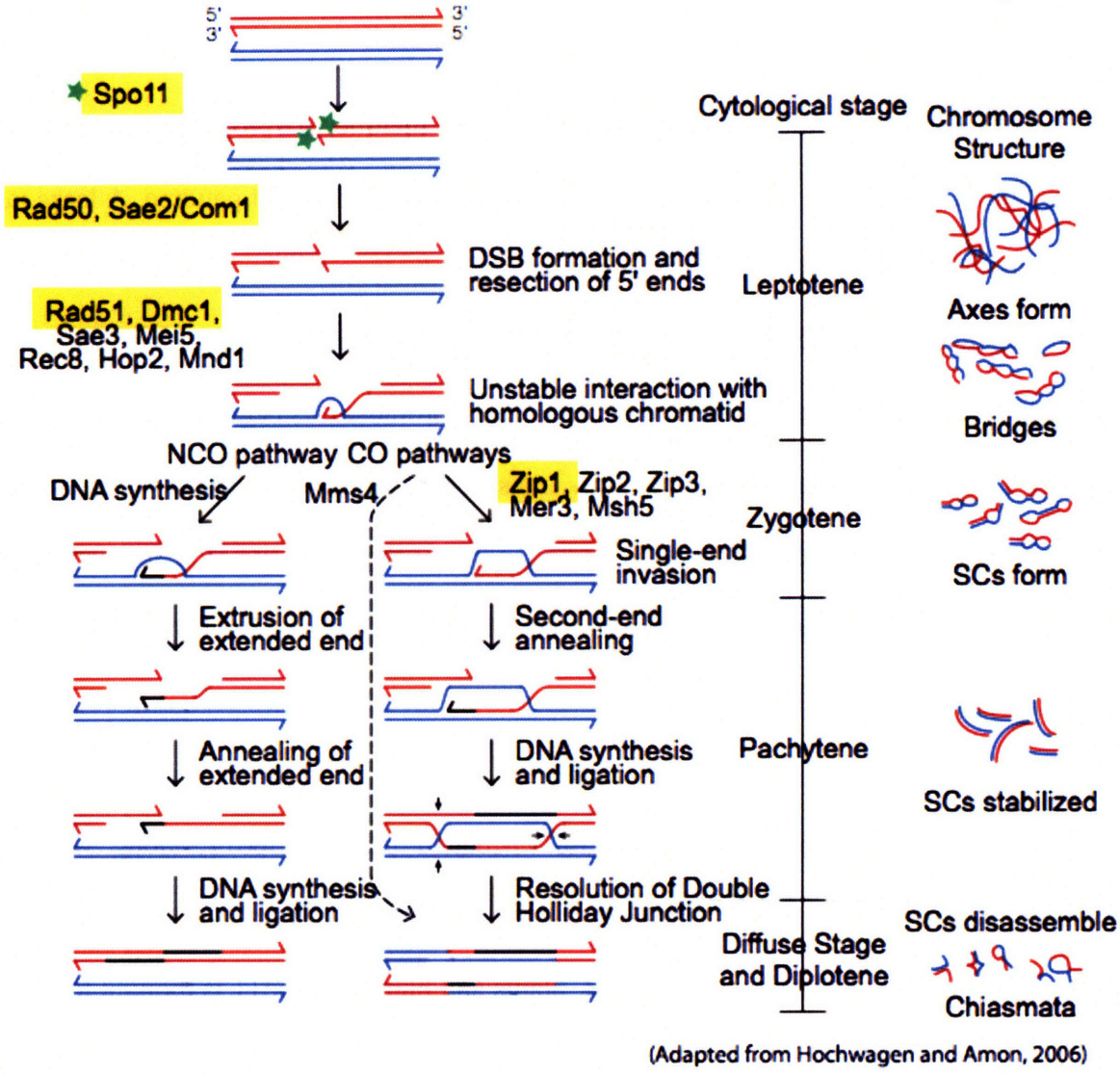

Figure 4: Control of meiotic homologous recombination

The mechanism and key regulators of homologous recombination are depicted on the left panel. The molecular reactions occur during the cytological stage indicated. The accompanying changes in chromosome structure that occur during meiotic Gs/prophase are shown on the far fight.

Repair of meiotic DSBs

In meiosis, DSB repair occurs almost exclusively through recombination, instead of non-homologous end joining or other repair pathways that are observed in other cell types. The first intermediate produced is ssDNA, via the 5'-3' resection of one strand of DNA on either side of the DSB site (Figure 4). Approximately ~600 bp of ssDNA are generated on either side of the DSB site, which nucleates the binding of several repair factors including the recA homologs, Rad51 and Dmc1. Once loaded on the DNA, these factors form a nucleoprotein filament and initiate the search for homologous DNA with which to repair the break. In mitotic cells, the Rad51 protein normally directs repair to the sister-chromatid. In meiosis, the Dmc1 protein directs the strand invasion step of repair to the homolog instead. Cells lacking Dmc1 or Rad51 arrest with long stretches (>1kb) of unrepaired ssDNA at DSB sites.

In the meiotic cell cycle, the repair of DSBs occurs preferentially from the homologous chromosome, with only 20% of repair events occurring from the sister chromatid (Schwacha and Kleckner 1997). Repair from the homolog can lead to either a non-crossover (NCO) or crossover (CO) recombination product, depending on how the repair intermediates are resolved (Figure 4). The traditional model for homologous recombination depicts a double Holliday junction (DHJ), which has an equal likelihood to be resolved by one of two recombination events to produce CO or NCOs. Analysis of mutants that specifically affect CO or NCO production indicate that *in vivo*, the production of NCOs occurs before mature CO recombinants are produced and NCOs arise via a transient interaction with the homologous chromosome, in which there is no stable strand exchange (Storlazzi, Xu et al. 1995; Hunter and Kleckner 2001)(Allers and Lichten 2001). Stable strand exchange and the production of DHJs occurs only during crossover production

(Figure 4). An alternate pathway to crossover formation that may not require DHJ formation exists, and this pathway is not regulated by crossover interference (see below).

DSB repair facilitates the interaction between homologous chromosomes, although chromosome pairing can occur slowly in the absence of DSB formation (Weiner and Kleckner 1994). Homologous chromosomes establish a stable interaction through the process of CO recombination and a protein complex known as the synaptonemal complex (SC) associates along their length. The exact role of the SC is not well-understood. SC formation is nucleated at CO sites, indicating that its assembly occurs after the CO decision is made. Mutants in SC components, such as the Zip1 protein, show reduced levels of CO formation, indicating that the SC may stabilize stable strand exchange and CO designation until DHJs are resolved. In G2/prophase, the telomeres of all chromosomes congress in a few discrete clusters known as the bouquet. Bouquet formation is dependent on the protein Ndj1 and in its absence, chromosome pairing is delayed, indicating that the bouquet also plays an ill-defined role in chromosome synapsis (Trelles-Sticken, Dresser et al. 2000).

Regulation of crossover formation

Ultimately, each pair of homologous chromosomes should have at least one CO to be properly segregated during the first meiotic division. The regulation of CO distribution in the genome is regulated in at least two ways. First, DSBs must occur on all chromosomes. Second, a mechanism exists to distribute crossovers to all chromosomes. Only ~90 COs occur per cell in yeast and these must be distributed to all of the 16 chromosomes (Mortimer, Schild et al. 1991).

The phenomenon of crossover interference prevents multiple CO recombinants from occurring in close proximity on the same chromosome.

DSBs occur more frequently at some genomic loci termed "hotspots." Studies of several individual DSB sites indicated that DSBs occur most frequently in intergenic regions that contain promoters (Baudat and Nicolas 1997). Some DSB hotspots contain binding sites for transcription factors and their activity is increased by transcription factor binding, but other hotspots do not depend on transcription factors (Petes 2001). Some of the determinants of hotspots activity seem to be encoded in *cis*, since a DSB hotspot that was moved to a "cold" region retained some hotspot activity, albeit at a lower level than at the endogenous locus (Wu and Lichten 1995). Deletion experiments indicated that no single sequence within a DSB hotspot was essential for hotspot activity, and at individual hotspots all break do not occur in the same location, consistent with the idea that there is no simple consensus sequence that determines hotspot activity (De Massy, Baudat et al. 1994). Furthermore, the movement of hotspots in the genome indicated that altering the DSB activity at one locus can increase or decrease DSB activity at nearby hotspots. These experiments indicate that large scale chromosome organization or competition may also regulate DSB activity.

Alleles that arrest DSB formation with Spo11 linked to the DNA have allowed the genome-wide mapping of DSB hotspots in yeast, via the purification of Spo11-associated DNA (Gerton, DeRisi et al. 2000; Borde, Lin et al. 2004). Spo11 sites were found to be distributed across all chromosomes. No sequence or chromatin determinants of DSB site selection could be identified. A slight correlation with elevated GC-content was observed, although GC-content

was calculated for relatively large (5kb) windows and the breaks did not necessarily occur in the GC-rich sequences themselves. It is worth noting that all of these experiments were all carried out in the *rad50S* or *sae2Δ/com1Δ* background. The efficiency of DSBs at specific loci is altered in the *rad50S* background compared to wild-type cells (Borde, Goldman et al. 2000), suggesting that not all DSB hotspots were identified in the Spo11 localization studies.

Although DSBs occur preferentially in some loci, other genomic regions are repressed for homologous recombination through multiple mechanisms. DSBs are under-represented near repeat-rich regions such as telomeres and the rDNA. Homologous recombination within repetitive DNA at chromosome ends could lead to CO formation with the incorrect chromosome. Additionally, since cohesin distal to the CO is required to hold chromosomes together during metaphase I in meiosis, a CO at the very end of the DNA molecule could cause chromosome non-disjunction because of the lack of cohesin distal to the CO. Homologous recombination within the rDNA is also prevented, because unequal exchanges between homologs can lead to rDNA loss and death. Finally, CO formation close to centromeres is prevented, and genome-wide studies of Spo11 localization indicated that DSBs are under-represented in these regions (Gerton, DeRisi et al. 2000). CO formation close to centromeres is associated with increased levels of non-disjunction, suggesting that crossovers in this region are detrimental to faithful chromosome segregation (Lambie and Roeder 1988; Sears, Hegemann et al. 1995; Lamb, Sherman et al. 2005; Rockmill, Voelkel-Meiman et al. 2006). It is thought that CO formation within this region disrupts the specialized structure necessary for chromosome segregation in meiosis.

Alternate mechanisms exist to distribute at least one CO to all chromosomes. Some species have a far larger number of CO than chromosomes, and in this case CO are randomly distributed. These species also lack SC, suggesting that the SC plays a role in CO distribution. For other organisms, such as yeast, it has been observed that COs are limiting in number, non-randomly distributed and do not occur close together, a phenomenon termed CO interference. Members of the SC including Zip1 have been implicated in CO interference, because genetically they appear to lack CO interference, although they probably function downstream of the initial CO selection to stablize CO intermediates (Borner, Kleckner et al. 2004; Fung, Rockmill et al. 2004). Not all crossovers are subject to crossover interference, however, indicating that at least two pathways exist to regulate CO formation. For example, cells containing a version of Spo11 that makes fewer DSBs than average maintain a wild-type level of COs and exhibit fewer NCO events (Martini, Diaz et al. 2006). The COs that are not affected by interference are regulated by distinct factors (Hollingsworth and Brill 2004). This suggests that a basal level of CO are produced on all chromosomes in the absence of interference, and that additional CO are distributed through an interference-dependent mechanism.

Co-regulation of DNA replication and recombination

The proper execution of any cell cycle requires that cells complete one process before beginning the next, for example completing DNA replication before attempting to segregate chromosomes. Several checkpoints operate in meiosis to ensure the integrity of the DNA prior to chromosome segregation. Because the initiation of homologous recombination involves the introduction of hundreds of DSBs into the yeast genome, it can be viewed as a form of severe DNA damage. If this occurred prior to or during DNA replication, it would lead to activation of

the intra-S phase checkpoint and replication arrest. Additionally, intermediates produced during errors in DNA replication and during recombination share many structural similarities (such as ssDNA), and the cell might not differentiate between them. Therefore, cells must complete DNA replication, at least on a local level, before DSBs are formed. To test this coordination, a form of chromosome III was created that experiences severely delayed replication on one arm, due to the deletion of several origins. Both the chromatin transition and DSB formation occur later on the delayed replicating chromosome arm than on the wild-type arm, indicating that DSB formation is delayed in response to the delay in the replication of the local DNA (Borde, Goldman et al. 2000; Murakami, Borde et al. 2003). Although these studies indicate that replication and DSB formation are separated, the mechanism of coupling is unknown.

One candidate for ensuring complete replication before the initiation of recombination is the intra-S phase checkpoint, which can monitor the process of DNA replication. The intra-S phase checkpoint has been reported to function during meiosis, similar to during mitotic cell division (Stuart and Wittenberg 1998). Studies indicate that neither mitotic nor meiotic cells monitor DNA replication by counting the number of chromosomes, but instead by sensing ongoing DNA replication by the presence of replication forks or replication intermediates such as ssDNA. Cells lacking Cdc6 that never initiate DNA replication progress in the cell cycle in both mitosis and meiosis, and these cells make DSBs in the absence of DNA replication. A basic understanding of pre-meiotic DNA replication and recombination is be required to better determine how these two processes are regulated.

Thesis summary

In this thesis, I describe the characterization of pre-meiotic DNA replication and DSB formation across the *S. cerevisiae* genome. I present a model for the protracted pre-meiotic S phase arising as a result of both inefficient initiation of DNA replication and slower fork progression rates. I find no evidence that the altered replication kinetics during pre-meiotic DNA replication are regulated by or related to either cohesion or recombination, suggesting that the link between pre-meiotic DNA replication and homologous recombination affects only the kinetics of DSB formation. Analysis of DSB distribution revealed significant differences in the mechanisms of inhibition of recombination at telomeres, centromeres and near the rDNA. Additionally, this study revealed a non-random distribution of DSB hotspots, which explains how chromosomes of all sizes receive a sufficient number of DSBs to form at least one crossover during homologous recombination.

References

Alani, E., R. Padmore, et al. (1990). "Analysis of Wild-Type and rad50 Mutants of Yeast Suggests an Intimate Relationship between Meiotic Chromosome Synapsis and Recombination." Cell **61**: 419-436.

Allers, T. and M. Lichten (2001). "Differential Timing and Control of Noncrossover and Crossover Recombination during Meiosis." Cell **106**: 47-57.

Aparicio, J. G., C. J. Viggiani, et al. (2004). "The Rpd3-Sin3 histone deacetylase regulates replication timing and enables intra-S origin control in Saccharomyces cerevisiae." Mol Cell Biol **24**(11): 4769-80.

Arora, C., K. Kee, et al. (2004). "Antiviral protein Ski8 is a direct partner of Spo11 in meiotic DNA break formation, independent of its cytoplasmic role in RNA metabolism." Mol Cell **13**(4): 549-59.

Baudat, F. and A. Nicolas (1997). "Clustering of meiotic double-strand breaks on yeast chromosome III." Proc Natl Acad Sci U S A **94**(10): 5213-8.

Bell, S. P. and A. Dutta (2002). "DNA replication in eukaryotic cells." Annu Rev Biochem **71**: 333-74.

Benjamin, K. R., C. Zhang, et al. (2003). "Control of landmark events in meiosis by the CDK Cdc28 and the meiosis-specific kinase Ime2." Genes Dev **17**(12): 1524-39.

Bergerat, A., B. de Massy, et al. (1997). "An Atypical Topoisomerase II from Archaea with Implications for Meiotic Recombination." Nature **386**: 414-417.

Blat, Y., R. U. Protacio, et al. (2002). "Physical and functional interactions among basic chromosome organizational features govern early steps of meiotic chiasma formation." Cell **111**(6): 791-802.

Borde, V., A. S. Goldman, et al. (2000). "Direct coupling between meiotic DNA replication and recombination initiation." Science **290**(5492): 806-9.

Borde, V., W. Lin, et al. (2004). "Association of Mre11p with double-strand break sites during yeast meiosis." Mol Cell **13**(3): 389-401.

Borner, G. V., N. Kleckner, et al. (2004). "Crossover/noncrossover differentiation, synaptonemal complex formation, and regulatory surveillance at the leptotene/zygotene transition of meiosis." Cell **117**(1): 29-45.

Bowers, J. L., J. C. Randell, et al. (2004). "ATP hydrolysis by ORC catalyzes reiterative Mcm2-7 assembly at a defined origin of replication." Mol Cell **16**(6): 967-78.

Branzei, D. and M. Foiani (2005). "The DNA damage response during DNA replication." Curr Opin Cell Biol **17**(6): 568-75.

Buonomo, S. B., R. K. Clyne, et al. (2000). "Disjunction of homologous chromosomes in meiosis I depends on proteolytic cleavage of the meiotic cohesin Rec8 by separin." Cell **103**(3): 387-98.

Cha, R. S., B. M. Weiner, et al. (2000). "Progression of meiotic DNA replication is modulated by interchromosomal interaction proteins, negatively by Spo11p and positively by Rec8p." Genes Dev **14**(4): 493-503.

Chu, S., J. DeRisi, et al. (1998). "The transcriptional program of sporulation in budding yeast." Science **282**(5389): 699-705.

Chu, S. and I. Herskowitz (1998). "Gametogenesis in Yeast Is Regulated by a Transcriptional Cascade Dependent on Ndt80." Mol. Cell **1**: 685-696.

Clifford, D. M., S. M. Marinco, et al. (2004). "The meiosis-specific protein kinase Ime2 directs phosphorylation of replication protein A." J Biol Chem **279**(7): 6163-70.
Cocker, J. H., S. Piatti, et al. (1996). "An essential role for the Cdc6 protein in forming the pre-replicative complexes of budding yeast." Nature **379**(6561): 180-2.
Collins, I. and C. S. Newlon (1994). "Chromosomal DNA replication initiates at the same origins in meiosis and mitosis." Mol Cell Biol **14**(5): 3524-34.
Colomina, N., E. Gari, et al. (1999). "G1 cyclins block the Ime1 pathway to make mitosis and meiosis incompatible in budding yeast." Embo J **18**(2): 320-9.
Coverley, D. and R. A. Laskey (1994). "Regulation of eukaryotic DNA replication." Annu Rev Biochem **63**: 745-76.
Dahmann, C., J. F. Diffley, et al. (1995). "S-phase-promoting cyclin-dependent kinases prevent re-replication by inhibiting the transition of replication origins to a pre-replicative state." Curr Biol **5**(11): 1257-69.
Dahmann, C. and B. Futcher (1995). "Specialization of B-type cyclins for mitosis or meiosis in S. cerevisiae." Genetics **140**(3): 957-63.
De Massy, B., F. Baudat, et al. (1994). "Initiation of recombination in Saccharomyces cerevisiae haploid meiosis." Proc Natl Acad Sci U S A **91**(25): 11929-33.
DePamphilis, M. L. (2005). "Cell cycle dependent regulation of the origin recognition complex." Cell Cycle **4**(1): 70-9.
DePamphilis, M. L., J. J. Blow, et al. (2006). "Regulating the licensing of DNA replication origins in metazoa." Curr Opin Cell Biol **18**(3): 231-9.
Diffley, J. F. (2004). "Regulation of early events in chromosome replication." Curr Biol **14**(18): R778-86.
Diffley, J. F. and K. Labib (2002). "The chromosome replication cycle." J Cell Sci **115**(Pt 5): 869-72.
Dirick, L., T. Bohm, et al. (1995). "Roles and regulation of Cln-Cdc28 kinases at the start of the cell cycle of Saccharomyces cerevisiae." Embo J **14**(19): 4803-13.
Dirick, L., L. Goetsch, et al. (1998). "Regulation of meiotic S phase by Ime2 and a Clb5,6-associated kinase in Saccharomyces cerevisiae." Science **281**(5384): 1854-7.
Donaldson, A. D., M. K. Raghuraman, et al. (1998). "CLB5-dependent activation of late replication origins in S. cerevisiae." Mol Cell **2**(2): 173-82.
Fitch, I., C. Dahmann, et al. (1992). "Characterization of four B-type cyclin genes of the budding yeast Saccharomyces cerevisiae." Mol Biol Cell **3**(7): 805-18.
Foiani, M., A. Pellicioli, et al. (2000). "DNA damage checkpoints and DNA replication controls in Saccharomyces cerevisiae." Mutat Res **451**(1-2): 187-96.
Fung, J. C., B. Rockmill, et al. (2004). "Imposition of crossover interference through the nonrandom distribution of synapsis initiation complexes." Cell **116**(6): 795-802.
Gerton, J. L., J. DeRisi, et al. (2000). "Inaugural article: global mapping of meiotic recombination hotspots and coldspots in the yeast Saccharomyces cerevisiae." Proc Natl Acad Sci U S A **97**(21): 11383-90.
Grandin, N. and S. I. Reed (1993). "Differential function and expression of Saccharomyces cerevisiae B-type cyclins in mitosis and meiosis." Mol Cell Biol **13**(4): 2113-25.
Hassold, T. and P. Hunt (2001). "To err (meiotically) is human: the genesis of human aneuploidy." Nat Rev Genet **2**(4): 280-91.

Hochwagen, A., W. H. Tham, et al. (2005). "The FK506 binding protein Fpr3 counteracts protein phosphatase 1 to maintain meiotic recombination checkpoint activity." Cell **122**(6): 861-73.

Hollingsworth, N. M. and S. J. Brill (2004). "The Mus81 solution to resolution: generating meiotic crossovers without Holliday junctions." Genes Dev **18**(2): 117-25.

Hollingsworth, R. E., Jr. and R. A. Sclafani (1993). "Yeast pre-meiotic DNA replication utilizes mitotic origin ARS1 independently of CDC7 function." Chromosoma **102**(6): 415-20.

Holt, L. J., J. E. Hutti, et al. (2007). "Evolution of Ime2 phosphorylation sites on Cdk1 substrates provides a mechanism to limit the effects of the phosphatase Cdc14 in meiosis." Mol Cell **25**(5): 689-702.

Honigberg, S. M. and K. Purnapatre (2003). "Signal pathway integration in the switch from the mitotic cell cycle to meiosis in yeast." J Cell Sci **116**(Pt 11): 2137-47.

Hunt, P. A. and T. J. Hassold (2002). "Sex matters in meiosis." Science **296**(5576): 2181-3.

Hunter, N. and N. Kleckner (2001). "The single-end invasion: an asymmetric intermediate at the double-strand break to double-holliday junction transition of meiotic recombination." Cell **106**(1): 59-70.

Hyrien, O., C. Maric, et al. (1995). "Transition in specification of embryonic metazoan DNA replication origins." Science **270**(5238): 994-7.

Keeney, S. (2001). "Mechanism and control of meiotic recombination initiation." Curr Top Dev Biol **52**: 1-53.

Kerrebrock, A. W., D. P. Moore, et al. (1995). "Mei-S332, a Drosophila protein required for sister-chromatid cohesion, can localize to meiotic centromere regions." Cell **83**(2): 247-56.

Kiburz, B. M., D. B. Reynolds, et al. (2005). "The core centromere and Sgo1 establish a 50-kb cohesin-protected domain around centromeres during meiosis I." Genes Dev **19**(24): 3017-30.

Kitajima, T. S., S. A. Kawashima, et al. (2004). "The conserved kinetochore protein shugoshin protects centromeric cohesion during meiosis." Nature **427**(6974): 510-7.

Klein, F., P. Mahr, et al. (1999). "A Central Role for Cohesins in Sister Chromatid Cohesion, Formation of Axial Elements and Recombination during Yeast Meiosis." Cell **98**: 91-103.

Kuhne, C. and P. Linder (1993). "A new pair of B-type cyclins from Saccharomyces cerevisiae that function early in the cell cycle." Embo J **12**(9): 3437-47.

Labib, K., J. A. Tercero, et al. (2000). "Uninterrupted MCM2-7 function required for DNA replication fork progression." Science **288**(5471): 1643-7.

Lamb, N. E., S. L. Sherman, et al. (2005). "Effect of meiotic recombination on the production of aneuploid gametes in humans." Cytogenet Genome Res **111**(3-4): 250-5.

Lambie, E. J. and G. S. Roeder (1988). "A yeast centromere acts in cis to inhibit meiotic gene conversion of adjacent sequences." Cell **52**(6): 863-73.

Lee, B. H., B. M. Kiburz, et al. (2004). "Spo13 maintains centromeric cohesion and kinetochore coorientation during meiosis I." Curr Biol **14**(24): 2168-82.

Leu, J.-Y., P. R. Chua, et al. (1998). "The Meiosis-Specific Hop2 Protein of S. cerevisiae Ensures Synapsis between Homologous Chromosomes." Cell **94**: 375-386.

Lindner, K., J. Gregan, et al. (2002). "Essential role of MCM proteins in premeiotic DNA replication." Mol Biol Cell **13**(2): 435-44.

Lopes, M., C. Cotta-Ramusino, et al. (2001). "The DNA replication checkpoint response stabilizes stalled replication forks." Nature **412**(6846): 557-61.

Marston, A. L., W. H. Tham, et al. (2004). "A genome-wide screen identifies genes required for centromeric cohesion." Science **303**(5662): 1367-70.

Martini, E., R. L. Diaz, et al. (2006). "Crossover homeostasis in yeast meiosis." Cell **126**(2): 285-95.

McKee, A. H. and N. Kleckner (1997). "A general method for identifying recessive diploid-specific mutations in Saccharomyces cerevisiae, its application to the isolation of mutants blocked at intermediate stages of meiotic prophase and characterization of a new gene SAE2." Genetics **146**(3): 797-816.

Melo, J. and D. Toczyski (2002). "A unified view of the DNA-damage checkpoint." Curr Opin Cell Biol **14**(2): 237-45.

Michaelis, C., R. Ciosk, et al. (1997). "Cohesins: Chromosomal Proteins that Prevent Premature Separation of Sister Chromatids." Cell **91**: 35-45.

Mori, S. and K. Shirahige (2007). "Perturbation of the activity of replication origin by meiosis-specific transcription." J Biol Chem **282**(7): 4447-52.

Mortimer, R. K., D. Schild, et al. (1991). "Genetic and physical maps of Saccharomyces cerevisiae." Methods Enzymol **194**: 827-63.

Murakami, H., V. Borde, et al. (2003). "Correlation between premeiotic DNA replication and chromatin transition at yeast recombination initiation sites." Nucleic Acids Res **31**(14): 4085-90.

Murakami, H. and P. Nurse (2001). "Regulation of premeiotic S phase and recombination-related double-strand DNA breaks during meiosis in fission yeast." Nat Genet **28**(3): 290-3.

Neale, M. J., J. Pan, et al. (2005). "Endonucleolytic processing of covalent protein-linked DNA double-strand breaks." Nature **436**(7053): 1053-7.

Nguyen, V. Q., C. Co, et al. (2001). "Cyclin-dependent kinases prevent DNA re-replication through multiple mechanisms." Nature **411**(6841): 1068-73.

Ofir, Y., S. Sagee, et al. (2004). "The role and regulation of the preRC component Cdc6 in the initiation of premeiotic DNA replication." Mol Biol Cell **15**(5): 2230-42.

Ohta, K., T. Shibata, et al. (1994). "Changes in chromatin structure at recombination initiation sites during yeast meiosis." Embo J **13**(23): 5754-63.

Padmore, R., L. Cao, et al. (1991). "Temporal comparison of recombination and synaptonemal complex formation during meiosis in S. cerevisiae." Cell **66**(6): 1239-56.

Paulovich, A. G. and L. H. Hartwell (1995). "A checkpoint regulates the rate of progression through S phase in S. cerevisiae in response to DNA damage." Cell **82**(5): 841-7.

Petes, T. D. (2001). "Meiotic recombination hot spots and cold spots." Nat Rev Genet **2**(5): 360-9.

Prieler, S., A. Penkner, et al. (2005). "The control of Spo11's interaction with meiotic recombination hotspots." Genes Dev **19**(2): 255-69.

Primig, M., R. M. Williams, et al. (2000). "The Core Meiotic Transcriptome in Budding Yeasts." Nat. Genet. **26**: 415-423.

Prinz, S., A. Amon, et al. (1997). "Isolation of COM1, a new gene required to complete meiotic double-strand break-induced recombination in Saccharomyces cerevisiae." Genetics **146**(3): 781-95.

Rabitsch, K. P., M. Petronczki, et al. (2003). "Kinetochore recruitment of two nucleolar proteins is required for homolog segregation in meiosis I." Dev Cell **4**(4): 535-48.

Raghuraman, M. K., E. A. Winzeler, et al. (2001). "Replication dynamics of the yeast genome." Science **294**(5540): 115-21.

Randell, J. C., J. L. Bowers, et al. (2006). "Sequential ATP hydrolysis by Cdc6 and ORC directs loading of the Mcm2-7 helicase." Mol Cell **21**(1): 29-39.
Rockmill, B., K. Voelkel-Meiman, et al. (2006). "Centromere-proximal crossovers are associated with precocious separation of sister chromatids during meiosis in Saccharomyces cerevisiae." Genetics **174**(4): 1745-54.
Sanchez, Y., J. Bachant, et al. (1999). "Control of the DNA damage checkpoint by chk1 and rad53 protein kinases through distinct mechanisms." Science **286**(5442): 1166-71.
Santocanale, C. and J. F. Diffley (1998). "A Mec1- and Rad53-dependent checkpoint controls late-firing origins of DNA replication." Nature **395**(6702): 615-8.
Sawarynski, K. E., A. Kaplun, et al. (2007). "Distinct activities of the related protein kinases Cdk1 and Ime2." Biochim Biophys Acta **1773**(3): 450-6.
Schild, D. and B. Byers (1978). "Meiotic effects of DNA-defective cell division cycle mutations of Saccharomyces cerevisiae." Chromosoma **70**(1): 109-30.
Schwacha, A. and N. Kleckner (1997). "Interhomolog bias during meiotic recombination: meiotic functions promote a highly differentiated interhomolog-only pathway." Cell **90**(6): 1123-35.
Schwob, E., T. Bohm, et al. (1994). "The B-type cyclin kinase inhibitor p40SIC1 controls the G1 to S transition in S. cerevisiae." Cell **79**(2): 233-44.
Schwob, E. and K. Nasmyth (1993). "CLB5 and CLB6, a new pair of B cyclins involved in DNA replication in Saccharomyces cerevisiae." Genes Dev **7**(7A): 1160-75.
Sears, D. D., J. H. Hegemann, et al. (1995). "Cis-acting determinants affecting centromere function, sister-chromatid cohesion and reciprocal recombination during meiosis in Saccharomyces cerevisiae." Genetics **139**(3): 1159-73.
Sedgwick, C., M. Rawluk, et al. (2006). "Saccharomyces cerevisiae Ime2 phosphorylates Sic1 at multiple PXS/T sites but is insufficient to trigger Sic1 degradation." Biochem J **399**(1): 151-60.
Shimada, K., P. Pasero, et al. (2002). "ORC and the intra-S-phase checkpoint: a threshold regulates Rad53p activation in S phase." Genes Dev **16**(24): 3236-52.
Shirahige, K., Y. Hori, et al. (1998). "Regulation of DNA-replication origins during cell-cycle progression." Nature **395**(6702): 618-21.
Smith, A. V. and G. S. Roeder (1997). "The Yeast Red1 Protein Localizes to the Cores of Meiotic Chromosomes." J. Cell Biol. **136**: 957-967.
Smith, H. E., S. S. Su, et al. (1990). "Role of IME1 expression in regulation of meiosis in Saccharomyces cerevisiae." Mol Cell Biol **10**(12): 6103-13.
Storlazzi, A., L. Xu, et al. (1995). "Crossover and noncrossover recombination during meiosis: timing and pathway relationships." Proc Natl Acad Sci U S A **92**(18): 8512-6.
Stuart, D. and C. Wittenberg (1998). "CLB5 and CLB6 Are Required for Premeiotic DNA Replication and Activation of the Meiotic S/M Checkpoint." Genes Dev **12**: 2698-2710.
Surana, U., H. Robitsch, et al. (1991). "The role of CDC28 and cyclins during mitosis in the budding yeast S. cerevisiae." Cell **65**(1): 145-61.
Tercero, J. A. and J. F. Diffley (2001). "Regulation of DNA replication fork progression through damaged DNA by the Mec1/Rad53 checkpoint." Nature **412**(6846): 553-7.
Tercero, J. A., M. P. Longhese, et al. (2003). "A central role for DNA replication forks in checkpoint activation and response." Mol Cell **11**(5): 1323-36.
Toth, A., K. P. Rabitsch, et al. (2000). "Functional genomics identifies monopolin: a kinetochore protein required for segregation of homologs during meiosis i." Cell **103**(7): 1155-68.

Trelles-Sticken, E., M. E. Dresser, et al. (2000). "Meiotic Telomere Protein Ndj1 Is Required for Meiosis-Specific Telomere Distribution, Bouquet Formation and Efficient Homolog Pairing." J. Cell Biol. **151**: 95-106.

Tsubouchi, H. and G. S. Roeder (2002). "The Mnd1 Protein Forms a Complex with Hop2 to Promote Homologous Chromosome Pairing and Meiotic Double-Strand Break Repair." Mol. Cell Biol. **22**: 3078-3088.

Uhlmann, F. and K. Nasmyth (1998). "Cohesion between Sister Chromatids Must Be Established during DNA Replication." Curr. Biol. **8**: 1095-1101.

Vogelauer, M., L. Rubbi, et al. (2002). "Histone acetylation regulates the time of replication origin firing." Mol Cell **10**(5): 1223-33.

Wan, L., C. Zhang, et al. (2006). "Chemical inactivation of cdc7 kinase in budding yeast results in a reversible arrest that allows efficient cell synchronization prior to meiotic recombination." Genetics **174**(4): 1767-74.

Watanabe, Y. (2005). "Sister chromatid cohesion along arms and at centromeres." Trends Genet **21**(7): 405-12.

Weiner, B. M. and N. Kleckner (1994). "Chromosome Pairing via Multiple Interstitial Interactions before and during Meiosis in Yeast." Cell **77**: 977-991.

Williamson, D. H., L. H. Johnston, et al. (1983). "The timing of the S phase and other nuclear events in yeast meiosis." Exp Cell Res **145**(1): 209-17.

Wu, T. C. and M. Lichten (1995). "Factors that affect the location and frequency of meiosis-induced double-strand breaks in Saccharomyces cerevisiae." Genetics **140**(1): 55-66.

Yabuki, N., H. Terashima, et al. (2002). "Mapping of early firing origins on a replication profile of budding yeast." Genes Cells **7**(8): 781-9.

Zickler, D. and N. Kleckner (1999). "Meiotic chromosomes: integrating structure and function." Annu Rev Genet **33**: 603-754.

Zou, L. and B. Stillman (2000). "Assembly of a complex containing Cdc45p, replication protein A, and Mcm2p at replication origins controlled by S-phase cyclin-dependent kinases and Cdc7p-Dbf4p kinase." Mol Cell Biol **20**(9): 3086-96.

Chapter II

Characterization of a slow S phase: pre-meiotic DNA replication in yeast

Summary

Pre-meiotic S phase is longer than pre-mitotic S phase, suggesting that replication kinetics are regulated by the meiotic developmental program. To understand how the slower S phase is accomplished, we measured replication origin selection and replication kinetics in sporulating yeast. Consistent with a similar mechanism of origin selection in pre-meiotic and pre-mitotic S phase, we found that the sites of pre-replicative complex assembly were nearly identical during both cell cycles. To identify early initiating origins of replication, we sporulated cells in the presence of hydroxyurea (HU) to arrest cells in early pre-meiotic S. We found that cells sporulated with HU arrested in pre-meiotic G1 phase with unreplicated DNA in a Cln3-dependent manner. In the absence of Cln3, cells initiated pre-meiotic DNA synthesis in the presence of HU. However, we detected fewer early replicating origins in sporulating cells than in mitotically growing cells. Analysis of DNA replication profiles from cells undergoing a synchronous pre-meiotic S phase confirmed that replication initiation was delayed for a large number of origins during pre-meiotic S phase. The altered replication timing program was not affected by the meiosis-specific cohesion or DSB factors Rec8 and Spo11. We conclude that the mechanisms governing DNA replication are conserved between the meiotic and mitotic cell cycles, but that delayed replication initiation at a significant number of origins leads to a prolonged pre-meiotic S phase.

Introduction

In every eukaryotic cell cycle the DNA is duplicated prior to its segregation into daughter cells. Replication of large genomes requires coordinating the initiation of DNA replication from many sites along each chromosome, termed origins of replication. In many organisms, the length of S phase is developmentally modulated to accommodate cell cycles of different lengths. For example, during the rapid cell cycles of early *Drosophila* and *Xenopus* embryogenesis, cells complete chromosome duplication quickly by initiating replication from many closely spaced origins (Coverley and Laskey 1994). Later in development when cells divide more slowly, replication initiates from a smaller number of origins (Hyrien, Maric et al. 1995). Intriguingly, in every organism studied to date, meiotic S phase is longer than that of the mitotic cell cycle (Zickler and Kleckner 1999). This conservation suggests that meiosis-specific events alter the DNA replication program, but how this occurs is unknown.

DNA replication is highly regulated during the cell cycle. In G1, origins are selected by formation of the pre-replicative complex (pre-RC) at specific sites along each chromosome (Mendez and Stillman 2003). Pre-RC assembly requires DNA binding by the origin recognition complex (ORC), which, together with other factors, loads the minichromosome maintenance (Mcm2-7) complex onto origins (DePamphilis 2003; Bowers, Randell et al. 2004). The Mcm2-7 complex is required for the initiation and elongation stages of DNA replication, most likely because it is the replicative helicase (Lei and Tye 2001). As cells progress from G1 into S phase, the activity of the single yeast cyclin-dependent kinase (CDK) promotes the initiation of DNA replication (Diffley 2004).

The kinetics of genome duplication are determined by a combination of the location and time of initiation of replication origins, as well as by replication fork progression rates. A subset of potential replication origins initiate replication during S phase, whereas other potential replication origins assemble pre-RCs during G1, but do not initiate replication during S phase. Each active origin initiates replication at characteristic time during S phase and with a given efficiency (the percentage of cells in which the origin initiates replication), leading to a reproducible temporal program of genome duplication. Genome-wide studies have enabled the comprehensive description of replication in yeast. Potential replication origins were identified by genome-wide location analysis of ORC and Mcm2-7 (Wyrick, Aparicio et al. 2001). The average replication time for sites across the genome has been determined using microarray techniques that measure DNA synthesis during a synchronous S phase (Raghuraman, Winzeler et al. 2001; Yabuki, Terashima et al. 2002). These studies defined a set of active origins by identifying sites that replicated before neighboring loci, indicating a replication initiation event. Active origins are frequently termed either "early" or "late" replicating origins based on their relative times of initiation during S phase.

Frequently, early and late replicating origins are functionally distinguished by how they respond to perturbations in DNA replication. For example, reduction of S phase CDK activity by deletion of the B-type cyclin Clb5 specifically reduces replication initiation from late replicating origins (Donaldson, Raghuraman et al. 1998). Addition of exogenous replication inhibitors or DNA damaging agents can also perturb S-phase progression by impeding replication fork progression. For example, the replication inhibitor hydroxyurea (HU) inhibits ribonucleotide reductase (RNR) and prevents the increase in dNTP levels that usually occurs during S phase,

leading to slow replication fork progression. Stalled replication forks activate the intra-S phase checkpoint, which results in the inhibition of cell cycle progression until replication is completed and stabilization of existing replication forks. When the intra-S phase checkpoint is initiated, early origins have already initiated DNA replication, but initiation from late origins is delayed in a checkpoint-dependent manner (Santocanale and Diffley 1998; Shirahige, Hori et al. 1998; Feng, Collingwood et al. 2006). Exposure of cells to HU has been used to map a set of early replicating origins and these correspond to the first origins that initiate replication in an unperturbed cell cycle (Yabuki, Terashima et al. 2002). Thus far, replication timing has been studied in cells treated with replication inhibitors and in the presence of mutant proteins. Meiosis has a slow S phase that occurs in wild-type cells and thus provides an interesting biological alternative to study changes in replication timing.

Meiosis is a specialized cell cycle, consisting of a single DNA replication event, followed by two rounds of chromosome segregation. The alignment and faithful segregation of homologous chromosomes requires both a specialized form of cohesion that is established between sister chromatids during S phase (Klein, Mahr et al. 1999) and a homologous recombination event, in which every homologous chromosome undergoes at least one physical DNA exchange. Pre-meiotic S phase is at least twice as long as pre-mitotic S phase (Williamson, Johnston et al. 1983; Padmore, Cao et al. 1991), yet the majority of the origins on chromosomes III and VI initiate DNA replication during both cell cycles (Collins and Newlon 1994; Mori and Shirahige 2007). Proteins involved in meiosis-specific cohesion and recombination have been implicated in the regulation of pre-meiotic S phase length (Cha, Weiner et al. 2000). Conversely, replication has also been reported to influence the timing of the initiation of homologous

recombination (Borde, Goldman et al. 2000), suggesting that the processes are functionally linked. However, the mechanisms that regulate the kinetics of early meiotic cell cycle progression remain elusive.

To better understand why pre-meiotic S phase is slower, we used genome-wide assays to localize pre-meiotic replication origins and characterize the temporal program of pre-meiotic DNA replication. Although most potential replication origins are identical in the meiotic and mitotic cell cycles, we identified a class of origins that is regulated by the meiotic transcriptional program. Examination of cells treated with the replication inhibitor HU indicated that, unlike during the mitotic cell cycle when HU arrests cells in early S phase, HU prevented entry into the meiotic cell cycle. We observed that the same origins are active during the meiotic and mitotic cell cycles, although origin firing is either slower or less efficient and the average fork rate is decreased in meiosis. Both of these changes are likely to contribute to the protracted pre-meiotic S phase. Finally, we observed no effect of the removal the meiosis-specific factors Rec8 and Spo11 on the altered replication timing in pre-meiotic S phase, indicating that the altered replication timing program in pre-meiotic S phase is not regulated by meiosis-specific cohesion or DSB formation.

Results

Differential pre-RC formation at a subset of pre-meiotic origins

To determine whether the initial selection of potential replication origins differed in the meiotic and mitotic cell cycles, we performed genome-wide location analysis for the Mcm2-7 complex, using high-density microarrays (Figure 1A and Supplemental Figure 1). In all experiments we observed a reproducible pattern of Mcm2-7 enrichment at loci that have been

previously identified as potential replication origins in other strain backgrounds (Supplemental Table 2). Comparison of the pre-mitotic and pre-meiotic Mcm2-7 binding sites revealed that the majority of origins (407/427 total origins) assembled pre-RCs in both cell cycles (Supplemental Table 2). These data imply that the mechanism of origin selection is identical in both cell cycles.

Although most potential origins formed pre-RCs in both the meiotic and the mitotic cell cycle, we observed 14 mitosis-specific and 6 meiosis-specific Mcm2-7 binding sites. We examined the location of these potential origins and found that most of these binding sites (17/20) clearly overlapped with open reading frames. In contrast, we observed few differences in Mcm2-7 binding between meiotic and mitotic cell cycles at intergenic sites, where most origins of replication are located (Wyrick, Aparicio et al. 2001; Nieduszynski, Knox et al. 2006; Xu, Aparicio et al. 2006). To determine why Mcm2-7 binding differed at some loci in the meiotic and mitotic cell cycles, we examined the expression pattern of the genes overlapping the potential origins. In 13/14 cases, we found that the mitosis-specific Mcm2-7 binding sites were located within the coding region of a gene that is transcriptionally induced during the meiotic cell cycle (Chu, DeRisi et al. 1998; Primig, Williams et al. 2000)(Table 1). We expect that these loci are permissible for pre-RC formation during mitotic growth in rich media when they are not transcribed, but activation of transcription during starvation and sporulation prevents pre-RC association. For example, one mitosis specific origin was located in the *SPO22* coding region (Figure 1B). SPO22 is a well-characterized meiosis-specific gene that is transcriptionally silent during mitotic growth, but is strongly activated as cells enter meiosis (Primig, Williams et al. 2000). Four of the six of meiosis-specific Mcm2-7 binding sites were found in genes that are repressed during sporulation. These results indicate that a subset of potential replication origins

are located within transcribed regions, and replication complex assembly at these sites is incompatible with transcription of the locus.

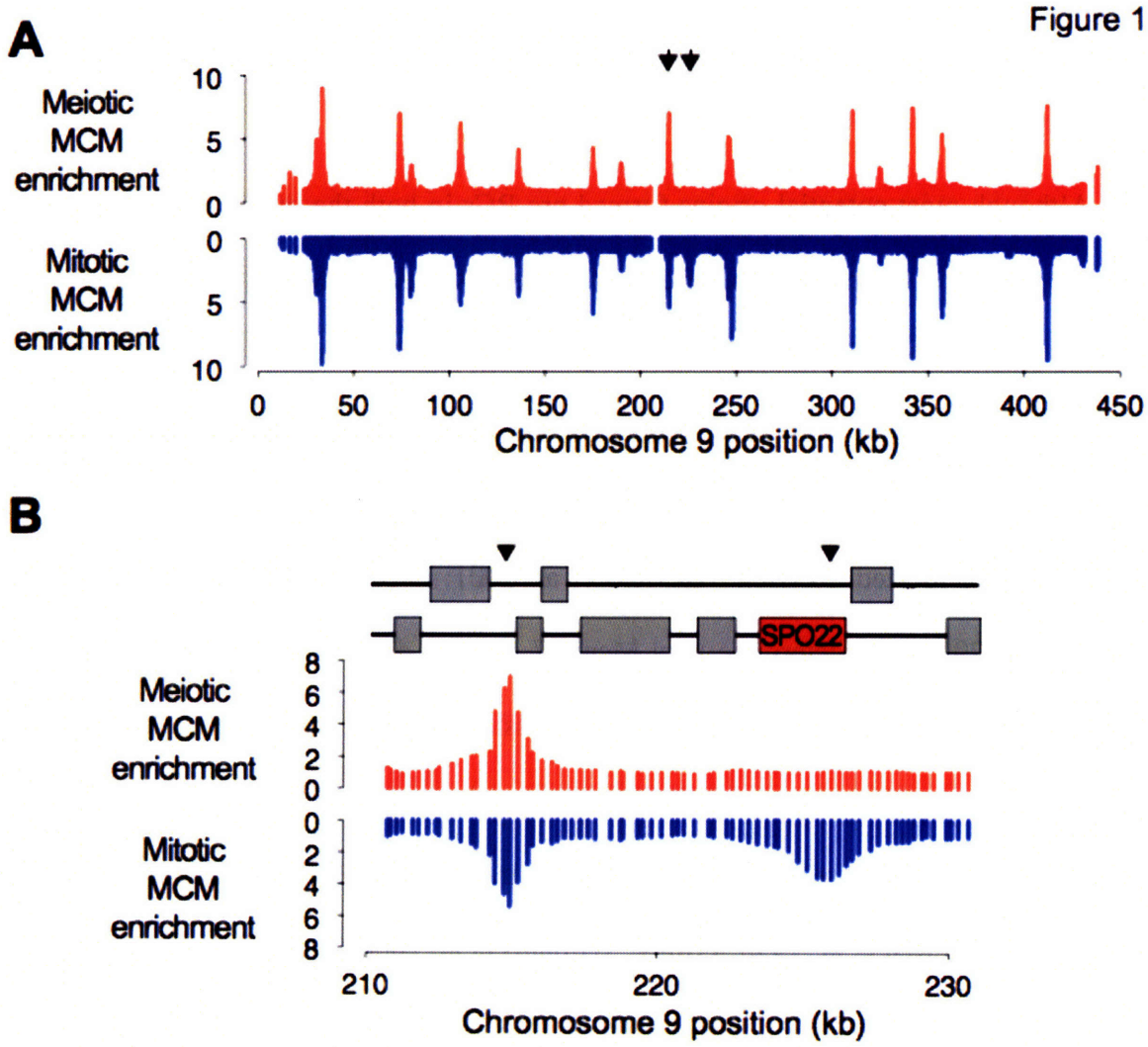

Figure 1. Transcription influences origin selection

(A) MCM localization was performed for a wild-type SK1 strains in mitosis (yHB65) and meiosis (yHB95). For meiotic analysis, cells were induced to undergo synchronous sporulation and cells were collected after 1 hour in sporulation medium. Mitotic cells were arrested with 5μg/ml alpha-factor prior to sample collection. MCM enrichment is plotted versus chromosome position for Chromosome IX for meiotic cells (red, enrichment is upwards) and mitotic cells

(blue, enrichment is downwards). Arrowheads indicate the positions of ARS913 and the *SPO22* ARS.

(B) As in (A), except a detailed view of ARS913 (left) and the *SPO22* ARS (right) are shown, arrowheads indicate positions. Grey boxes indicate coding regions on each DNA strand of the chromosome.

The same origins are active in the meiotic and mitotic cell cycles

To determine which potential replication origins are activated during pre-meiotic S phase, we measured the average time of replication across the genome. To synchronize cells, we used an analog-sensitive allele of the Ime2 kinase, *ime2-as1*, which can be inactivated by an ATP-analog inhibitior (Benjamin, Zhang et al. 2003). Ime2 is essential for meiotic cell cycle entry and pre-meiotic DNA replication (Dirick, Goetsch et al. 1998; Benjamin, Zhang et al. 2003). Thus, *ime2-as1* cells inoculated into sporulation medium containing the inhibitor did not initiate DNA replication (Figure 2A, 0 minutes). When the inhibitor was removed, cells progressed relatively synchronously through pre-meiotic S phase, as measured by FACS (Figure 2A). To determine the relative time of DNA replication, we measured the relative DNA abundance of a pool of samples collected every 7.5 minutes throughout pre-meiotic S phase. The quantity of the DNA doubles when a site is replicated. Therefore, sites that replicate earlier in S phase are enriched in the pooled DNA compared to sites that replicate later (Figure 2A) and the relative abundance of a given site in the S phase DNA pool is proportional to its average relative time of replication during S phase (Yabuki, Terashima et al. 2002). Genomic DNA from the pooled S phase samples and from a control population of G1 cells that had not yet initiated replication was differentially labeled and co-hybridized to a high-density microarray (Figure 2A). The results were visualized by plotting a replication timing curve, which is the relative enrichment in the S phase sample

compared to the G1 sample for all points along a given chromosome (Figure 2B, red line). The most enriched sites were those that replicated earliest in S phase. A peak in the profile represents the location of an origin that initiated replication during pre-meiotic S phase, because it is a site that replicated before neighboring sequences.

To compare the kinetics of pre-meiotic and pre-mitotic DNA replication, we created pre-mitotic replication profiles for SK1 cells using alpha-factor synchronized cultures (Figure 2B, blue line). The pre-mitotic replication profiles were very similar to those obtained in other *S. cerevisiae* strain backgrounds (data not shown), indicating that our method works comparably to those previous published. Although the pre-meiotic and pre-mitotic replication profiles looked comparable after smoothing the data, the raw data for the pre-meiotic profiles consistently had a lower signal to noise ratio (data not shown). This was expected, given that the synchrony of the meiotic cultures was not as high as that of the mitotic cultures. The presence of a population of non-replicating cells (see Figure 2A) resulted in a lower absolute enrichment in copy number, and more noise in the profiles. To measure the level random noise inherent in the copy number technique, we performed a control co-hybridization of two G1 DNA samples (Figure 2B, grey line). We found that the absolute levels of enrichment in the G1 versus G1 hybridizations were much lower than in the pre-meiotic replication profiles, indicating that there was significant and specific copy number enrichment in the pre-meiotic replication profiles. The peaks in both the pre-meiotic and pre-mitotic DNA replication profiles were associated sites of Mcm2-7 binding (Figure 2B, inverted triangles), indicating that we could identify origins in both profiles. In general, the same peaks were present in both the pre-meiotic and pre-mitotic replication profiles,

extending previous observations that the same origins are active during both cell cycles.

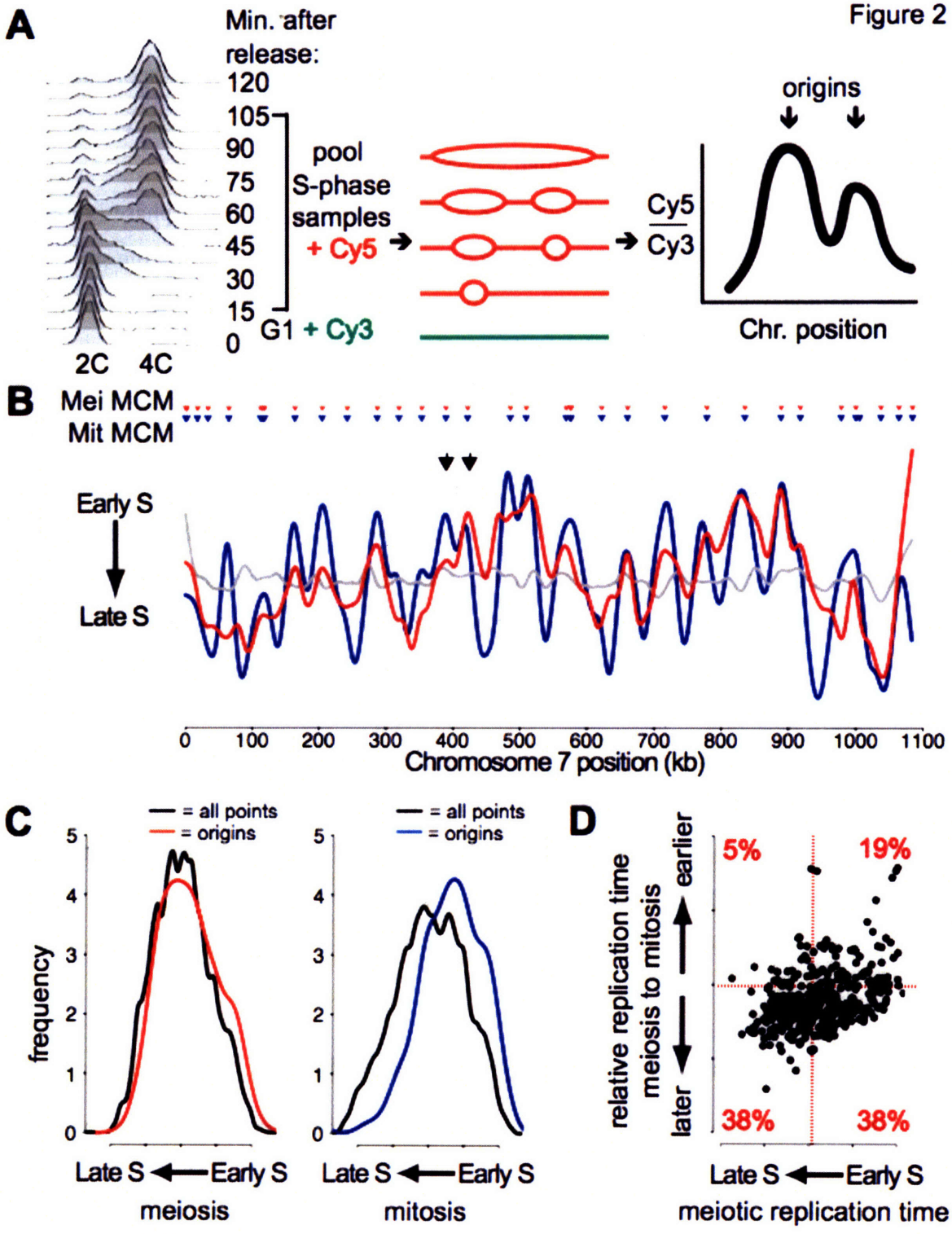

Figure 2

Figure 2. Meiotic DNA replication profiles

(A) The experimental procedure is indicated. Ime2-as1-myc homozygous diploids (KBY518) were induced to undergo synchronous sporulation in media containing 20μM 1-Na-PP1 inhibitor. After 4 hours, inhibitor was removed and cells were released in sporulation media. DNA samples were collected every 7.5 minutes. Resulting samples were pooled and co-hybridized with a G1 DNA sample to a tiled genomic microarray.

(B) Replication profiles for meiotic S phase (KBY518, red line), mitotic S phase (yHB65, blue line) and control G1 vs. G1 (grey line) hybridizations were created by plotting the smoothed $\log_2$ ratio (see methods) versus chromosome position. Triangles indicate the positions of MCM binding sites in meiosis (red) and mitosis (blue). Black arrowheads indicate sites with disparate replication time in meiosis and mitosis. Sites within 10kb of chromosome ends were excluded from analysis because of the inability to smooth the data accurately at the chromosome ends.

(C) The frequency distribution of the average replication time of all MCM binding sites was calculated for meiotic (left panel) and mitotic (right panel) S phase. Black lines indicate the frequency of $\log_2$ ratios for all points, colored lines indicate the frequency of $\log_2$ ratios for potential replication origins for each profile. Sites within 10kb of chromosome ends (single copy sequence) were excluded from analysis because of the inability to smooth the data accurately at the chromosome ends.

(D) The relative replication time in meiotic and mitotic S phase was plotted versus replication time in meiosis for all potential replication origins (meiotic MCM binding sites). Sites within 10kb of chromosome ends were excluded from analysis. The percentage of total potential replication origins in each quadrant is indicated in red.

Replication initiation is delayed for some pre-meiotic origins

Although the same origins are active in pre-meiotic and pre-mitotic S phase, we observed significant differences in the relative timing of replication of at some origins. At a large number of loci, the peak was lower in meiotic cells than in mitotic cells, indicating that the average replication time of that origin was delayed in pre-meiotic S phase. In some cases sequences that

replicated at a similar time in mitotic cells showed substantially different average replication time in meiotic cells (Figure 2B, arrows), indicating that pre-meiotic S phase is not simply a delayed pre-mitotic S phase. To qualitatively assess the apparent differences in replication time between pre-meiotic and pre-mitotic origins, we examined the distribution of replication time of all potential replication origins during S phase (Figure 2C). We chose to examine all potential origins because in many cases it was not possible to unambiguously assign peaks to a particular Mcm2-7 binding site due to the lack of spatial resolution in the replication profiles. In mitotically dividing cells, 75% of potential origins had replication times earlier than the average site in the genome, causing a significant shift in the timing (Figure 2C, blue curve versus black curve). This is consistent with the idea that many of these sites are active origins that replicate before neighboring chromosomal loci. In contrast, only 60% of origins replicated before the average site during pre-meiotic S phase, such that the average replication time of potential origins in pre-meiotic S phase was similar to bulk replication during S phase (Figure 2C, red curve versus black curve). These data indicate that a significant number of potential origins did not initiate replication before the majority of genomic replication occurred in meiotic cells, consistent with a model of later or less efficient replication initiation.

To determine how the replication time at individual origins was altered during pre-meiotic S phase, we determined the change in replication time (relative to S phase as a whole) between pre-meiotic and pre-mitotic S phase for each potential origin (Figure 2D, Y axis). Because the replication profiles were adjusted to the same mean, the average replication time was the same for both profiles. We observed that 75% of potential origins replicated relatively proportionally later in the meiotic cell cycle compared to the mitotic cell cycle (Figure 2D,

bottom two quadrants). To determine whether early and late replicating origins were equally likely to experience delayed replication during pre-meiotic S, we plotted the relative replication time in the two cell cycles versus the time of replication on the meiotic profile (Figure 2D). We found that an equal number of early and late replicating origins exhibited delayed replication in pre-meiotic S phase. Of the 100 potential origins that replicated relatively earlier in the meiotic cell cycle, 73 were early replicating on the timing curve (Figure 2D, top two quadrants). These results indicate that a subset of early mitotic origins also initiate replication in an early and efficient manner in pre-meiotic S phase, but that the majority of origins are replicated later.

Hydroxyurea inhibits meiotic cell cycle entry

To confirm the apparent differences in the timing of replication initiation that we observed in the replication profiles, we sought to compare the number and location of early replicating origins in pre-meiotic S phase. To this end, we wanted to arrest cells early in pre-meiotic S phase using HU to trigger the intra-S phase checkpoint, as has been done previously for mitotcally dividing cells. Cells were inoculated in sporulation medium in the presence or absence of 200mM HU for 7 hours. In the absence of HU, most cells had completed pre-meiotic DNA replication at this time point, but cells treated with HU arrested with mainly unreplicated DNA (Figure 3B, wild-type cells). DNA samples from the sporulating cells exposed to HU were co-hybridized with a G1 DNA sample to produce an HU replication profile, indicative of the extent of replication in the population of cells at that single time point. We were unable to detect any significant enrichment at specific chromosomal loci in the HU treated cells when compared to the G1 versus G1 hybridization (Figure 3A, compare red histogram with grey line). In a control experiment in which mitotic cells were released from alpha-factor into 200mM HU, we

were able to detect the firing of early origins in a pattern consistent with published results (data not shown), indicating that the smaller amounts of DNA replication that occur in the presence of HU are detectable with this method. The mechanism of cell cycle arrest in mitotic cells exposed to HU depends on replication forks that sense the reduced nucleotide levels. Thus, all cells must complete a significant amount of replication to trigger the intra-S phase checkpoint and slow cell cycle progression. Therefore, our inability to detect replication in sporulating cells exposed to HU suggested that the cells were not arrested in S phase via the intra-S phase checkpoint.

To understand what effect HU treatment had on sporulating cells, we examined meiotic cell cycle progression during HU treatment by multiple methods. Although cells sporulated in the absence of HU largely completed DNA replication during the time course, cells incubated in the presence of 200mM HU failed to undergo any detectable DNA replication as measured by FACS analysis (Figure 3B, wild-type cells in SPO), consistent with either a G1 or early S phase arrest. When HU-arrested cells were released into sporulation medium without HU, they completed sporulation, indicating they were reversibly arrested and remained viable during the HU treatment (data not shown). It has been reported that cells sporulated in the presence of HU have reduced levels of early meiotic transcripts, including *IME2* (Lamb and Mitchell 2001). We measured the induction of transcripts required for pre-meiotic S phase by RT-PCR. In cells sporulated in the absence of HU, we were able to detect the efficient induction of several early meiotic transcripts, including *IME1*, *IME2* and *CLB5*. In cells sporulated in the presence of HU, *IME2* and *CLB5* expression was severely impaired (Figure 3C) suggesting that these cells were arrested in G1 prior to meiotic entry.

Figure 3

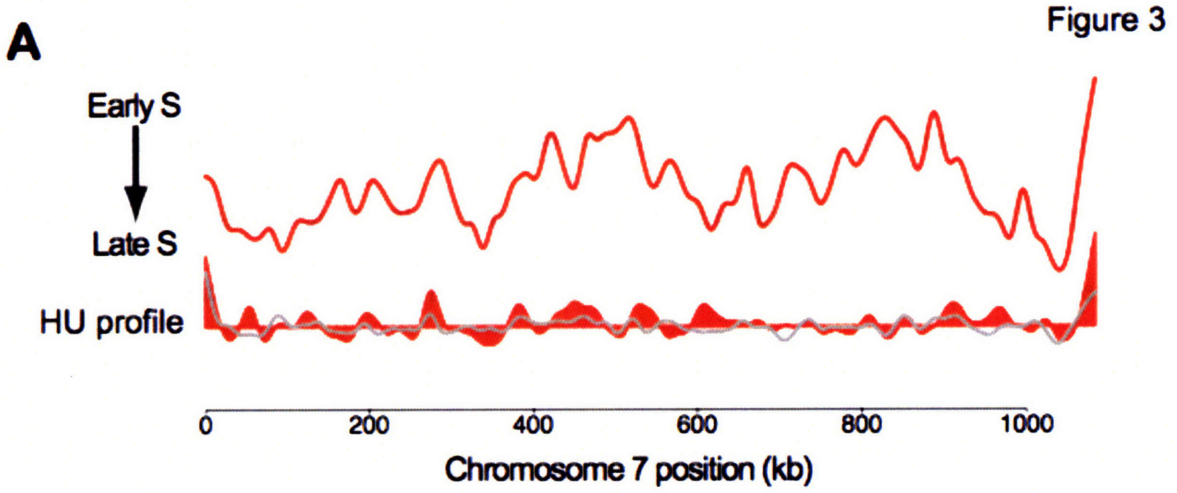
A
Early S
Late S
HU profile
0
200
400
600
800
1000
Chromosome 7 position (kb)

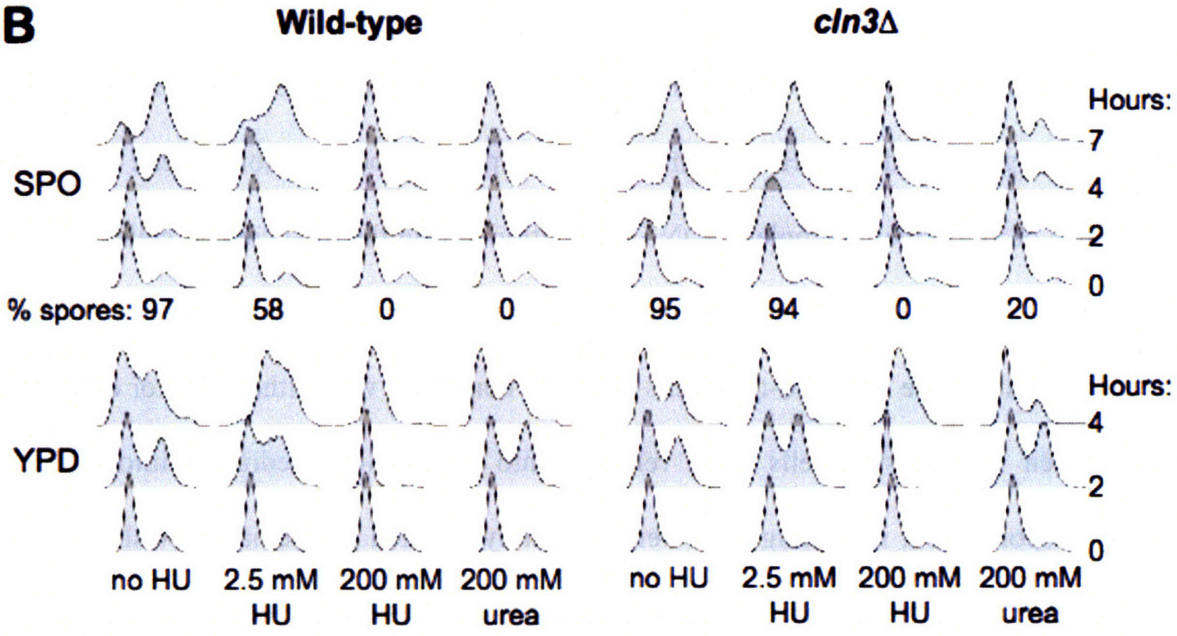
B
Wild-type
cln3Δ
SPO
Hours:
7
4
2
0
% spores: 97
58
0
0
95
94
0
20
YPD
Hours:
4
2
0
no HU
2.5 mM HU
200 mM HU
200 mM urea
no HU
2.5 mM HU
200 mM HU
200 mM urea

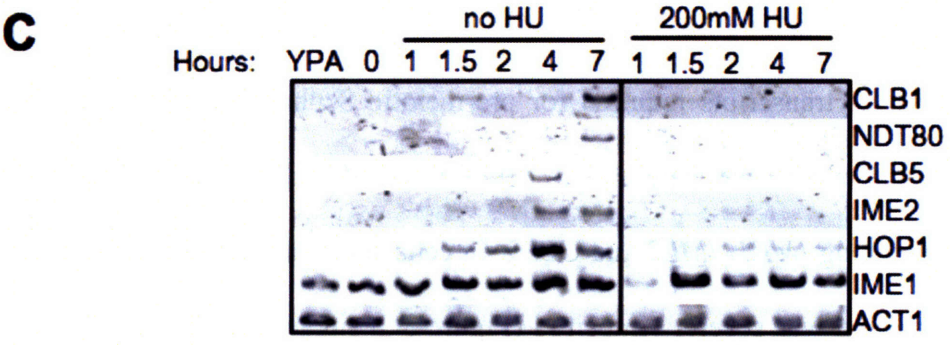
C
no HU
200mM HU
Hours:
YPA
0
1
1.5
2
4
7
1
1.5
2
4
7
CLB1
NDT80
CLB5
IME2
HOP1
IME1
ACT1

Figure 3. HU inhibits meiotic entry

(A) The wild-type strain (yHB95) was induced to undergo synchronous meiosis for 4 hours in the presence of 200mM HU. Total genomic DNA was cohybridized with G1 DNA to a tiled genomic microarray and smoothed data were plotted versus chromosome position (red histogram, bottom). For comparison, the meiotic replication timing profile (red line, above) and G1 vs. G1 profile (grey line, bottom) are shown.

(B) Wild-type cells (yHB95) were synchronized for meiosis. At time 0, cells were inocolated into either sporulation media or YPD containing 0, 2.5 or 200 mM HU or 200 mM urea. Samples were removed for FACS analysis of DNA replication at the indicated times. Sporulation efficiency was counted after 24 hours.

(C) RT-PCR analysis of RNA prepared from cells grown as in (B) was performed for wild type cells grown in 0 or 100 mM HU. Samples were collected at the indicated intervals and RT-PCR was performed with primers specific for the indicated genes.

Yeast must be starved of both fermentable carbon and nitrogen sources to induce sporulation. Thus, we hypothesized that the addition of a high concentration of HU to sporulating cultures could inhibit meiotic entry independently of any affect on DNA replication because of the nitrogen-rich nature of the compound. To eliminate the role of DNA replication in the G1 arrest we observed in cells sporulated in the presence of HU, we sporulated cells in the presence of 200mM urea, a similarly nitrogen-rich compound that is not known to have any effect on DNA replication. Cells sporulated in the presence of urea arrested prior to pre-meiotic DNA replication with 2C DNA content (Figure 3B, wild-type cells in SPO), and also failed to induce IME2 or CLB5 transcripts (data not shown). Addition of 200mM urea to mitotic cultures had no effect on growth rate or cell cycle progression (Figure 3B, wild-type cells in YPD, and data not shown), consistent with urea not acting as a general inhibitor of DNA replication or S phase

entry. Together, these results indicate the G1 arrest of wild-type cells exposed to HU or urea was meiosis-specific.

The G1 cyclin Cln3 has a role in inhibiting meiotic entry in the presence of nitrogen sources (Colomina, Gari et al. 1999). To test whether the inhibition of meiotic entry in cells treated with HU or urea was *CLN3* dependent, we sporulated *cln3Δ* cells in the absence or presence of both compounds. In medium containing either low concentrations of HU (2.5 mM) or 200mM urea, *cln3Δ* cells sporulated more efficiently than wild-type cells (Figure 3B). We did not see a complete rescue of the sporulation efficiency to the levels of cells without HU, (Figure 3B) which may be due the presence of other G1 cyclins, Cln1 and Cln2. Strikingly, when we performed DNA copy number analysis on *cln3Δ* cells sporulated in the presence of high concentrations of HU (200mM), we were able to detect replication from a set of early replicating origins (Figure 4A). Together, these data imply that HU inhibits meiotic entry via the nitrogen-sensing pathway.

Initiation timing differs in the meiotic and mitotic cell cycles

Using the *cln3Δ* strain, we compared the replication profiles of pre-mitotic and pre-meiotic cells arrested in early S phase with 200mM HU. To create as similar a situation as possible, we synchronized *cln3Δ* cells in G1 in acetate-based rich medium (Padmore, Cao et al. 1991). Cultures were divided and cells were inoculated into either sporulation medium (to induce meiosis) or rich medium (to induce mitosis). In each case the media contained 200mM HU. In both the meiotic and mitotic cell cycles we were able to detect the DNA replication at many early origins of replication in cells arrested in HU (Figure 4 and Supplemental Figure 3,

asterisks). The extent of replication in HU for each origin had a high correlation to the timing of origins in the S-phase replication profile; the tallest peaks in the HU profiles almost always coincided with the tallest peaks in the corresponding replication timing curve (Figure 4 and Supplemental Figure 3, compare histograms with curves). This indicates that both methods reliably detected the locations of early replicating origins.

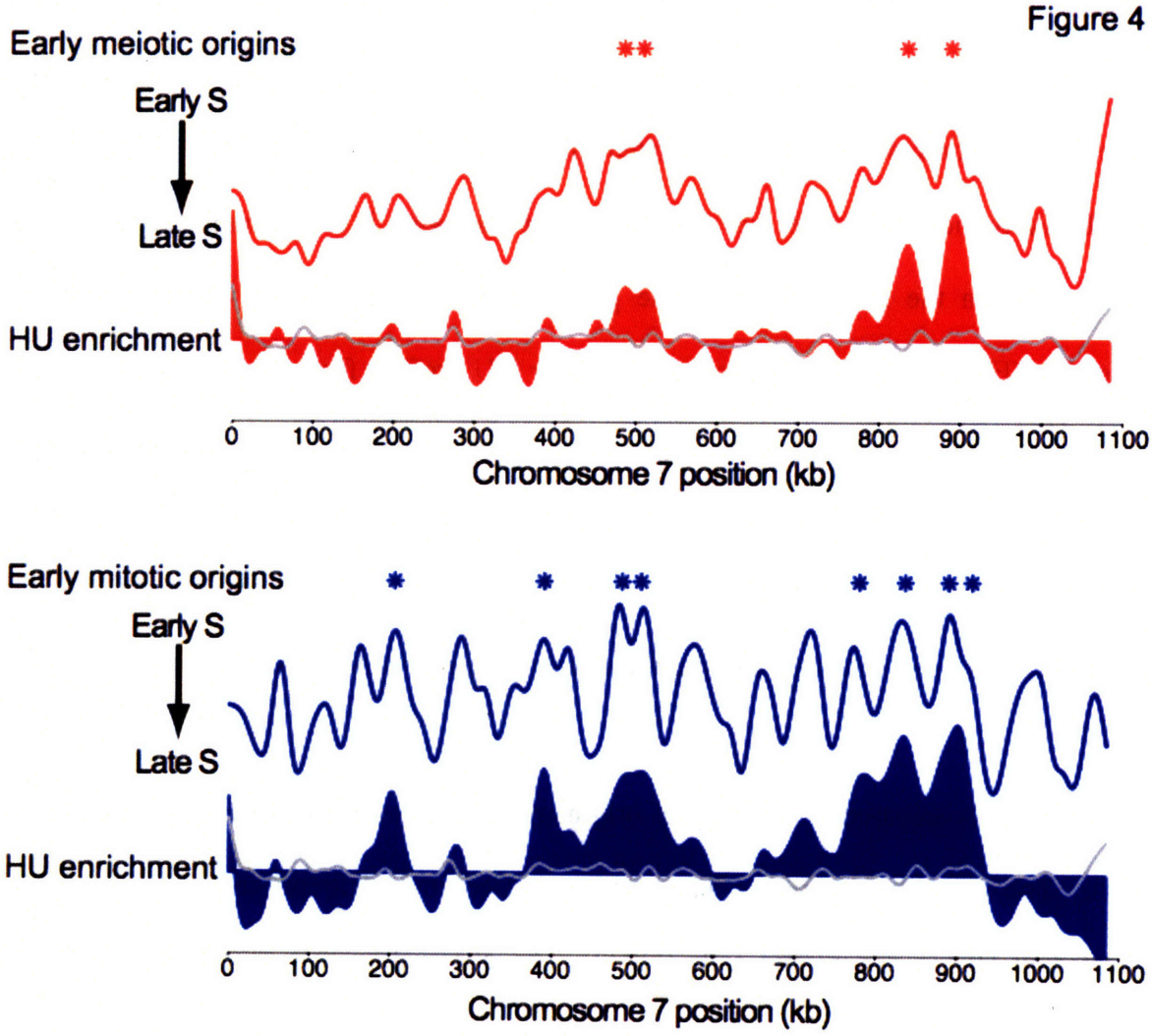

Figure 4. Fewer early origins in meiosis than mitosis

cln3Δ cells were induced to undergo synchronous sporulation in the presence of 200 mM HU and DNA replication was analyzed as in Figure 3A. Replication in HU is indicated by the histogram on the bottom of each plot. The meiotic replication profile (red line), mitotic

replication profile (blue line) and the G1 versus G1 profile (grey lines) are indicated. Asterisks indicate the position of origins that are considered replicated in the HU replication profile.

When we compared the pre-meiotic and pre-mitotic replication profiles for *cln3Δ* cells in 200mM HU, we noted that the nature of the replication arrests differed. Cells sporulated in 200mM HU showed similar replication profiles after 4 and 7 hours, indicating that they had fully arrested replication in early S phase (representative 7hr data shown in Figure 4A and FACS in Figure 3B). In contrast, the cells inoculated into rich medium with 200mM HU did not fully arrest DNA replication, since we saw significant increases in copy number throughout the genome between the 2 and 4 hour time points (data not shown), as well as in the FACS progression (Figure 3B). We compared the 4 hour HU profiles from *cln3Δ* pre-mitotic cells to the *cln3Δ* pre-meiotic HU profiles. These results revealed that many fewer origins initiated replication in HU in meiotic cells (133 versus 72, respectively, Supplemental Table 2). While in each profile the earliest initiating origins are enriched, we conclude that 200mM HU inhibits DNA replication more effectively in pre-meiotic cells than pre-mitotic cells.

We next compared the identity of origins replicated in meiotic and mitotic cells exposed to HU. The majority of origins that were replicated in HU in pre-meiotic cells were also replicated in HU in pre-mitotic cells (68/72). The observation that sporulating cells arrested replication more effectively than mitotic cells in the presence of HU suggested that the origins that we detected in sporulating cells in HU might correspond to the earliest pre-mitotic origins. To identify earliest pre-mitotic origins, we released mitotic cells from alpha-factor into HU for a short time (70 minutes, data not shown). In this case, we detected 56 early origins, all of which

were also detected in mitotic cells after the long 4 hour HU exposure. Comparison of the earliest pre-mitotic and pre-meiotic origins revealed that only 36 of these origins were replicated in the presence of HU in both cell cycles. This result indicates that the pre-meiotic HU profile is not identical to an early pre-mitotic S phase profile. Rather the earliest replicating origins are different in the mitotic and meiotic cell cycles, indicating differences in the regulation of replication initiation. This finding is consistent with the changes in origin replication timing observed in the pre-meiotic and pre-mitotic DNA replication profiles.

Replication timing, cohesion and homologous recombination

We next tested whether early meiosis-specific processes, such as establishment of cohesion and initiation of recombination, influenced meiotic DNA replication timing. To determine whether meiosis-specific cohesin or recombination regulate replication timing in the meiotic cell cycle, we deleted the *REC8* and *SPO11* genes in a *cln3Δ* background and measured early replication in HU. We observed similar HU replication profiles in sporulating *cln3Δ*, *cln3Δrec8Δ* and *cln3Δspo11Δ* cells (Figure 5A). Similarly, we compared the identity of the early origins of replication in each HU profile. We found that 60 of the early origins were replicated in all three strains (of the 72, 73 and 72 early origins identified for each strain, respectively). These data indicate that Rec8 and Spo11 are not primarily responsible for the changes in replication origin timing that we observed in meiotic cells.

Finally, we asked whether sites that differed in their replication timing in mitosis and meiosis were enriched for DSB sites. We expected that if recombination influenced replication timing, DSB sites would be enriched at sites that experience the biggest changes in replication

Figure 5

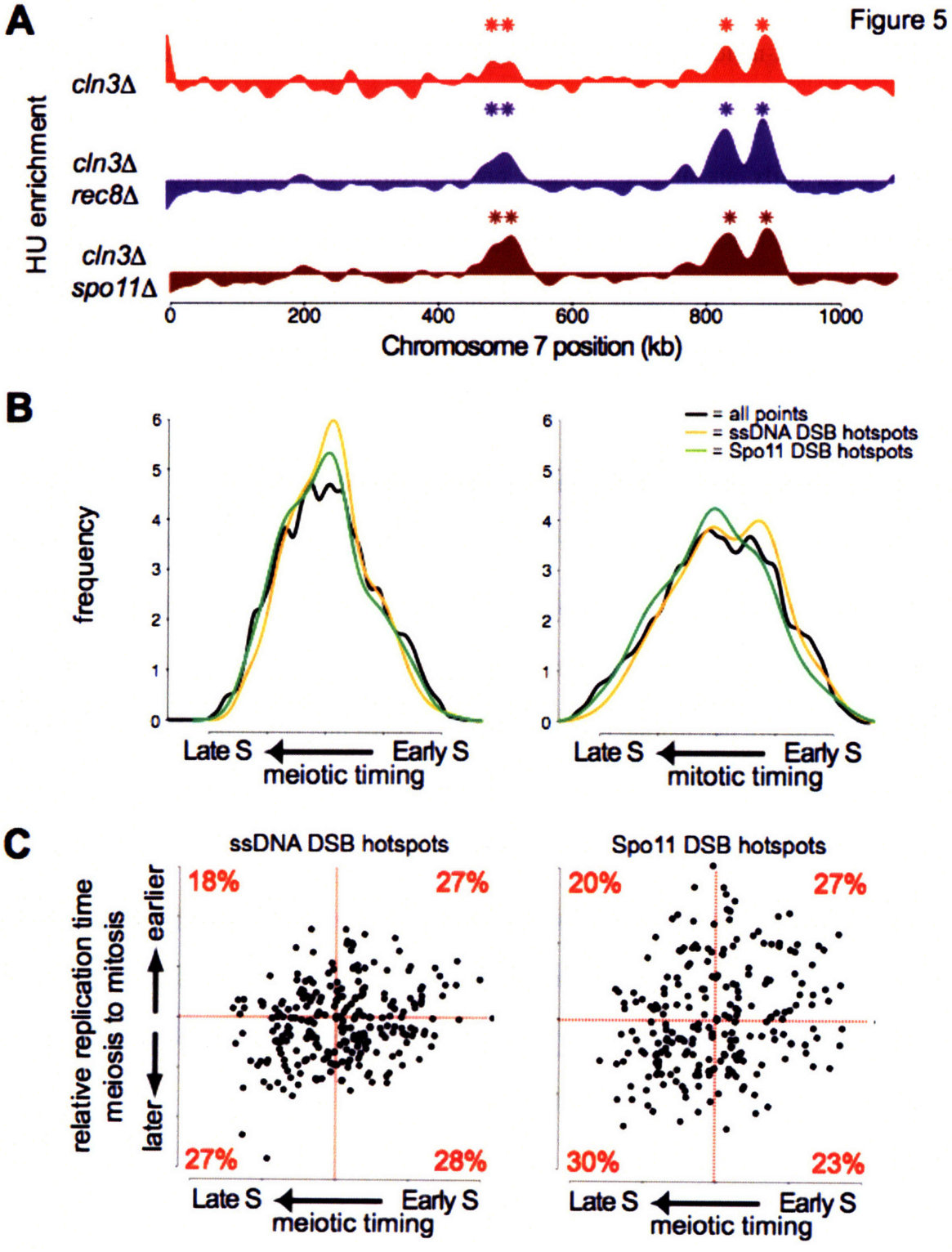
A
HU enrichment
cln3Δ
cln3Δ rec8Δ
cln3Δ spo11Δ
0
200
400
600
800
1000
Chromosome 7 position (kb)
B
frequency
= all points
= ssDNA DSB hotspots
= Spo11 DSB hotspots
Late S
Early S
meiotic timing
mitotic timing
C
ssDNA DSB hotspots
Spo11 DSB hotspots
relative replication time
meiosis to mitosis
earlier
later
18%
27%
27%
28%
20%
27%
30%
23%

Figure 5. Random distribution of DSB sites with respect to replication timing

(A) Replication profiles for cells sporulated in the presence of 200mM HU are shown for *cln3Δ* (4224), *cln3Δ rec8Δ* (YHB153) and *cln3Δ spo11Δ* (YHB150) cells. Asterisks indicate the position of origins that are considered replicated in each strain.

(B) The frequency distribution of replication timing (log_2 ratios) was plotted for all points (black line), and for DSB sites mapped by Spo11 attachment (green line) and by ssDNA enrichment (orange line) as in Figure 2C.

(C) Similar to Figure 3D, the relative replication time in meiotic and mitotic S phase was plotted versus replication time in meiosis for DSB sites mapped by Spo11 attachment (left panel) and ssDNA enrichment (right panel). The percentage of total DSB sites is indicated in red.

---

replication timing between the meiotic and mitotic cell cycles. We recently mapped DSB sites by Spo11 localization in a *rad50S* strain and by a novel method that detects DSB site-associated ssDNA (see Chapter III). We first compared the replication time of DSB sites mapped by both Spo11-localization and ssDNA enrichment to the meiotic and mitotic replication timing distribution. (Figure 5B). This analysis revealed that DSB sites were randomly distributed with respect to either pre-meiotic or pre-mitotic replication time (Figure 5B) and did not change between the two cell cycles. Therefore replication time is likely not a determinant of DSB site selection, nor is replication time systematically altered at DSB hotspots. Second, we determined the relative replication time of each DSB sites in meiosis versus mitosis (Figure 5C, Y axis). We found that DSB sites were equally likely to be replicated earlier or later in pre-meiotic S phase compared to pre-mitotic S phase (43% versus 53%, respectively). We also observed that DSB sites that were replicated early and late in pre-meiotic S phase were equally likely to experience relatively earlier or later replication timing (Figure 5C, X axis) during pre-meiotic S phase. This result was different from that observed for replication origins, which were more likely to be replicated later during the meiotic cell cycle than the mitotic cell cycle. Together, these data

indicate that the replication timing of potential DSB sites is not specifically altered during pre-meiotic DNA replication compared to average for all genomic loci during. However, we cannot exlude the possibility that recombination factors exert a more subtle effect on S phase progression that was not measured in these studies.

Discussion

The study described here reveals differences in the regulation of meiotic and mitotic DNA replication in budding yeast. Although the mechanism of origin selection and activation appears to be conserved during the meiotic cell cycle, we find that a subset of potential origins are regulated by the meiotic transcriptional program. We found that HU inhibits meiotic entry in a Cln3-dependent manner. Deletion of *CLN3* enabled the mapping of early replicating origins in HU-treated meiotically dividing cells. The comparison of both early replicating origins in HU treated cells and S phase replication profiles from meiotic and mitotically dividing cells revealed differences in the time of initiation of DNA replication at a number of origins. In particular, the average time of replication initiation was delayed for the majority of origins. We propose that the slower S phase in meiotic yeast cells is due to both fewer early origins of replication in meiosis and slower relative fork rates.

Transcription regulates pre-RC assembly at a subset of origins

Although the majority of potential origins were selected in both mitotic and meiotic cell cycles, we identified a subset of sites that show differential pre-RC association. At most of these sites, the differences in pre-RC formation were associated with changes in the transcriptional activity of the locus. Previous reports indicated that transcription through an origin is deleterious to replication complex assembly and replication initiation. Driving transcription through an

origin of replication with a strong promoter causes origin inactivation (Snyder, Sapolsky et al. 1988; Tanaka, Halter et al. 1994). Mori and Shirahige demonstrated that ARS605 is inactivated by meiosis-specific transcription of the overlapping gene *MSH4*. Activation of *MSH4* transcription was associated with the loss of ORC association (Mori and Shirahige 2007). We did not identify ARS605 as a meiosis-specific origin in this study because we detected a small amount of MCM binding, although the levels of MCM association were significantly lower during pre-meiotic G1 than during pre-mitotic G1 (Supplemental Figure 1). It is possible that we observed residual MCM association at ARS605 because we collected samples for Mcm2-7 analysis relatively early in the meiotic cell cycle, when *MSH4* transcription was not yet fully activated. However, we identified 17 additional potential origins that are regulated by transcription of the locus during the meiotic cell cycle.

Normally, pre-RCs are formed as cells exit mitosis, and we have observed pre-RCs at multiple origins in G1 before cells were inoculated into sporulation medium (data not shown). At some loci that did not show Mcm2-7 association in pre-meiotic G1, transcription could have been induced in acetate-based medium prior to meiotic entry, such that they never formed pre-RCs. At other loci, such as *MSH4* and *SPO22*, transcription was induced after cells entered meiosis. Therefore, origins that have already formed pre-RCs are still susceptible to transcriptional inactivation, probably because replication complexes are removed by the transcriptional machinery. We noted that none of the meiosis-specific origins were novel. Either ARS activity or Mcm2-7 binding was detected in previous studies using mitotically dividing cells (www.oridb.org). However, none of them were shown to initiate DNA replication in the chromosome in mitotic studies, suggesting they do not function in their normal context

Only ~5% of potential origins are located within transcribed regions, presumably due to the incompatibility of transcription and replication. Most of the transcriptionally regulated origins identified in this study were located close to another pre-RC binding site; the average distance of the next closest origin was 15 kb, versus an average inter-origin distance of 28kb for all potential origins. Therefore, under conditions that inactive the origin, the region can be replicated by forks from the next closest origin. We did not measure replication initiation at transcriptionally regulated origins in this study because in many cases it was not possible to unambiguously assign initiation events indicated as peaks in the replication timing profiles to a specific potential origin. This was expected, as the broad peaks we observe in the replication profiles do not provide sufficient resolution to distinguish initiation events from potential origins that are located close to each other on the chromosome.

HU inhibits meiotic entry in a Cln3 dependent manner

We observed that wild-type cells sporulated in the presence of 200mM HU arrested in the absence of any significant DNA replication. This finding was surprising, given that the described checkpoint response of mitotically dividing cells grown in 200mM HU depends on the presence of replication forks. Therefore, a substantial amount of replication in all cells would be expected to produce an arrest in the entire population. Instead, we propose that sporulating cells exposed to HU arrest in G1 prior to meiotic entry. This idea is consistent with the impaired induction of early meiotic transcripts described here and by others (Lamb and Mitchell 2001). Deletion of CLN3 allowed cells to enter pre-meiotic S phase in the presence of HU and urea, providing further evidence that the mechanism of inhibition is metabolic.

It was previously reported that the intra-S phase checkpoint function to preserve viability in sporulating cells exposed to low and high concentrations of HU (Stuart and Wittenberg 1998). It will be interesting to reinvestigate the role of the intra-S phase checkpoint in budding yeast in *cln3Δ* cells. In fission yeast, the intra-S phase checkpoint ensures full replication prior to initiation of meiotic recombination (Tonami, Murakami et al. 2005). Initiation of recombination involves the introduction of hundreds of double-strand breaks into the genome, and if this occurred during DNA replication, it would be severely deleterious to the cell. Studies of a version of chromosome III that has delayed replication of a single arm due to deletion of several origins demonstrated that recombination was also delayed in response to late DNA replication (Borde, Goldman et al. 2000). Therefore it has been hypothesized that there is a signal that inhibits local DSB formation until replication has been completed (Hochwagen and Amon 2006). Because the intra-S phase checkpoint ensures full replication prior to mitotic cell cycle progression, it may also prevent the initiation of recombination during pre-meiotic S phase.

Fewer early replicating origins during pre-meiotic S phase

Analysis of *cln3Δ* cells sporulated in the presence of HU revealed that both the number and identity of early replicating origins differ in the meiotic and mitotic cell cycles. These data indicate that the regulation of replication initiation is altered in meiosis. We excluded a role for the Rec8 and Spo11 proteins in regulation of replication initiation, as elimination of these proteins did not significantly alter the profile of early pre-meiotic replication in HU. Additionally, we did not detect any differences in replication timing at DSB sites between the meiotic and mitotic cell cycles, indicated that chromatin changes prior to DSB formation also do not affect replication timing. Therefore we conclude that meiosis-specific cohesion and the

initiation of recombination do not regulate the altered replication timing program that we observed in pre-meiotic S phase. While it is clear that replication timing affects the time of local DSB formation (Borde, Goldman et al. 2000; Murakami, Borde et al. 2003), we suggest that the coordination of these two processes functions only to regulate the timing of recombination, but not DNA replication.

Pre-meiotic and pre-mitotic DNA replication kinetics differ

This study reveals significant differences between the pre-meiotic and pre-mitotic temporal replication programs. First, we observe that, although a similar number of origins are active in each cell cycle, there are fewer early origins of replication. Therefore, the average time of initiation is delayed at the majority of origins during pre-meiotic S phase. This could be due to differences in time of replication initiation or because of less efficient origin activation in meiosis. If pre-meiotic DNA replication initiation occurred later in S phase for most origins, but with similar efficiency, the relative relationship between the replication time of origins and the other genomic loci should remain the same as in mitotically dividing cells, that is that origins would be enriched in the earlier part of S phase. Alternatively, an origin that initiated replication in less than 100% of cells would often be passively replicated later in S phase by forks from neighboring origins, so it would have a later average replication time. Additionally, when the origin is passively replicated, it does not replicate earlier in S phase than neighboring loci, so it would not be enriched in early S phase. We observed that in the meiotic cell cycle the replication time of origins was more similar to the replication time of the genome, which was different from the trend observed for mitotic cells (Figure 2C). This result is consistent with a model of less efficient origin activation in pre-meiotic S phase.

Consistent with the model that origin activation is less efficient in the meiotic cell cycle, we observed that the replication profiles in meiosis were always far less distinct than during the mitotic cell cycle. One possible explanation is that the lower signal to noise ratio is due to non-replicating cells in the population. However, even in our most synchronous sporulations, the meiotic replication profiles exhibited lower signal to noise ratios than mitotic profiles. The observed "noise" is consistent with a model of less efficient origin firing in meiosis. If origin firing were less efficient and stochastic, there could be significant non-uniformity between cells in the population. According to this model, a given site could be replicated by forks from different origins and at different times during S phase in each cell. Additionally, if the origins were on the opposite sides of that site, the replication fork would travel in opposite directions in different cells. Thus, the replication time and relative kinetics of replication of neighboring sequences would differ in each cell, and would produce a less distinct and uniform composite replication profile. This model would also predict a slower average rate of replication, since at some loci forks traveling in opposite directions in different cells. Comparison of the pre-meiotic and pre-mitotic replication profiles revealed similar slopes, although given that pre-meiotic S phase is twice as long, this indicates that forks traveled slower during pre-meiotic S phase.

One explanation for the less efficient replication initiation observed in meiotically dividing cells is that there is a limiting initiation factor in meiotic cells. One candidate is the level of CDK activity, which is absolutely required for replication initiation. Removal of Clb5 in mitotic cells causes a reduction in late origin activation, but the presence of Clb6 substitutes to drive pre-mitotic S phase. In meiotic cells, *CLB5* deletion has an even more severe phenotype, with very delayed and inefficient replication (Stuart and Wittenberg 1998), suggesting residual

Clb6/CDK activity is lower than in mitotic cells. Thus, we hypothesize that the overall levels of CDK activity may be limited during sporulation.

A second and non-exclusive model for slow pre-meiotic DNA replication is that the levels of dNTPs are lower in meiosis, due to the starvation conditions necessary to induce sporulation. Because yeast must be starved to induce sporulation, dNTPs are produced through the degradation of RNA. Previous studies indicated that sporulating yeast may contain low levels of nucleotide precursors (Sando and Miyake 1971). We postulate that lowered levels of nucleotides could lead to the observed decrease in both initiation efficiency and fork progression rates. This idea is reminiscent of mitotic studies in the presence of HU. Growth of cells in HU leads to both a decrease in efficiency of late origin activation and slower fork rates, which results in a protracted S phase (Alvino, Collingwood et al. 2007). The observation that meiotic cells arrest more tightly in response to HU is also consistent with a model of reduced dNTP levels. To test this idea, we attempted to artificially increase nucleotide levels by deleting *SML1*, an inhibitor of RNR (Chabes, Domkin et al. 1999). We observed that *sml1Δ* cells had a severe delay in meiotic entry (data not shown), suggesting that nucleotide levels themselves may play a role regulating meiotic entry. Thus, due to the intrinsic metabolic regulation of sporulation, it may not be possible to genetically dissect the role of nucleotide levels in the regulation of meiotic DNA replication.

Why a slow S phase?

We put forward the model that the slow pre-meiotic S phase is due to less efficient origin activation and slower replication progression than during mitotic cell divisions. A slow S phase would be detrimental to mitotic cells grown under competitive conditions because it would decrease their cell cycle length and growth rate. In contrast, the meiotic program is a form of terminal differentiation and cells are not prepared to divide again immediately following meiotic exit. In meiotically dividing cells, it may be advantageous to proceed slowly through the cell cycle, but do so in an accurate manner. If nucleotide levels are lower in sporulating cells, fast DNA replication could lead to increased rates of errors, which would then be passed on to progeny. In higher eukaryotes, meiosis takes place only in germ cells, which differentiate within special organs in response to specific developmental cues. Although these germ cells are not limited by nutrient availability, there may be other advantages to slower DNA replication in meiosis, such as increased fidelity. Alternatively, although we could find no evidence that meiosis specific cohesin or homologous recombination regulate the rate of DNA replication, the slower pre-meiotic S phase itself may promote the accurate establishment of cohesin or recombination structures. Following pre-meiotic DNA replication, in meiotic G2/prophase, chromosomes undergo large changes in structure and nuclear localization, which eventually result in their compaction and organization necessary for homologous recombination. It is possible that the length of pre-meiotic S phase is modulated to accommodate the factors necessary to accomplish this chromosome reorganization.

Materials and Methods

Strains and Growth Conditions

Strains used in this study are isogenic to SK1 and are listed in Supplemental Table 1. Gene disruptions were carried out using a PCR based protocol. FLO8 was deleted in some strains to reduce flocculation. To induce synchronous meiosis, strains were pre-inoculated at OD_{600} = 0.3 in YPA medium (1% yeast extract, 2% bactopeptone, 1% potassium acetate), grown for 16 hours at 30°C, washed twice, and resuspended at OD_{600} = 1.9 in SPO medium (0.3% potassium acetate, 0.02% raffinose). Specific growth conditions are described in figure legends.

Chromatin immuno-precipitation

For pre-meiotic Mc2-7 analysis, 20 mls of cells were harvested after 1 hours in sporulation media. For pre-mitotic Mcm2-7 analysis, cells were arrested with μg/ml alpha factor and 50 ml of culture at OD_{600} = 0.8 was collected. Mcm2-7 chromatin immunoprecipitation was performed as described (Aparicio, Weinstein et al. 1997). $1/10^{th}$ of the lysate was removed as an input sample. Mcm2-7 were immunoprecipitated using UM185 anti-MCM polyclonal Ab for 16 hours at 4 degrees.

Fluorescent labeling and microarray hybridization

For ChIP experiments, 1/2 of the immunoprecipitated DNA and $1/10^{th}$ of the input DNA were labeled. For pooled S-phase and HU replication profiles, ~5 μg of DNA from replicating or G1 arrest cells were labeled. Samples were labeled with Cy3-dUTP and Cy5-dUTP by random priming using 4 μg random nonamer oligo (IDT) and 10 units of Klenow (New England Biolabs, Beverly, MA). Unincorporated dye was removed using microcon columns (30-kDa MW cutoff, Millipore, Bedford, MA), and samples were co-hybridized to custom Agilent arrays (Wilmington, DE) using a standard protocol.

Microarray data analysis

For each co-hybridization, Cy3 and Cy5 levels were calculated using Agilent Feature Extractor CGH software. Background normalization, $\log_2$ ratios for each experiment and scale normalizations across each set of duplicated experiments were calculated using the sma package (Yang, Dudoit et al. 2001) in R, a computer language and environment for statistical computing (v2.1.0, http://www.r-project.org).

Significant Mcm2-7 binding sites were defined as sites that were significantly enriched ($P<0.05$) in all of 3 individual experiments. Sites within 500 bp of each other were merged into a single binding site. Mcm2-7 binging sites were assigned to a previously characterized origin if they overlapped the defined region (www.oridb.org). Meiosis- and mitosis-specific origins were confirmed by visual inspection of the ChIP data. Clear Mcm2-7 peaks were detected at some sites that did not make the statistical cutoff, however, they were manually included in the list of binding sites if they corresponded to a known origin and had a significantly enriched counterpart in the second data set. For analysis of replication timing, Mcm2-7 sites were defined as the midpoint of the defined origin region. The replication time of each Mcm2-7 binding site was

determined for each experiment by assigning it to the time of the closest point on the smoothed and predicted replication timing curve.

For pooled S-phase and HU DNA samples, DNA replication profiles were smoothed and predicted every 50 bp using the loess smoothing spline with a span=0.025 and a spar=0.45.

Analysis of the replication time for Spo11 binding sited and ssDNA enriched sites was perfomed as for the Mcm2-7 binding sites.

RNA isolation and RT-PCR

2 ml of cells at OD_{600} = 1.8 were collected. RNA was isolated and RT-PCR was performed as previously described (Lau, Blitzblau et al. 2002). For each PCR reaction, cDNA synthesized from 2.5 ng RNA was amplified with 25 pmol each gene specific primer for 26 cycles with Taq polymerase. Primer sequences are available upon request.

Supplemental Table 1: Strains

Name	Genotype	Reference
YHB65	*MATa, ho::LYS2, lys2, ura3, leu2::hisG, his3::hisG, trp1::hisG, flo8::KanMX*	This study
YHB95	*MATa/alpha, ho::LYS2/ ho::LYS2, lys2/lys2, ura3/ura3, leu2::hisG/leu2::hisG, his3::hisG/his3::hisG,trp1::hisG/trp1::hisG, flo8::KanMX/flo8::KanMX*	This study
KBY518	*MATa/alpha, ho::hisG/ho::hisG, lys2/lys2, ura3/ura3, leu2::hisG/leu2::hisG,trp1::hisG/trp1::hisG, his3-11/his3-11,15,ime2-as1-myc::TRP1(M146G)/ime2-as1-myc::TRP1(M146G)*	Benjamin et al.
YHB150	*MATa/alpha, ho::LYS2/ ho::LYS2, lys2/lys2, ura3/ura3, leu2::hisG/leu2::hisG, his3::hisG/his3::hisG,trp1::hisG/trp1::hisG, flo8::KanMX/flo8::KanMX,cln3::LEU/cln3::LEU2, spo11::URA3,spo11::URA3*	This study
YHB153	*MATa/alpha, ho::LYS2/ ho::LYS2, lys2/lys2, ura3/ura3, leu2::hisG/leu2::hisG, his3::hisG/his3::hisG,trp1::hisG/trp1::hisG, flo8::KanMX/flo8::KanMX, cln3::LEU2/cln3::LEU2, rec8::URA3,rec8::URA3*	This study
YAA4224	*MATa/alpha, ho::LYS2/ho::LYS2, lys2/lys2, his4x/HIS4, leu2::hisG/leu2::hisG, ura3/ura3, trp1::hisG/TRP1, cln3::LEU2/cln3::LEU2*	Reference?
YAH2487	*MATa/alpha, ho::LYS2/ho::LYS2, lys2/lys2, ura3/ura3, leu2::hisG/leu2::hisG, his3::hisG/his3::hisG, rad50S::URA3/rad50S::URA3, SPO11-18MYC::TRP1/SPO11-18MYC::TRP1*	This study
NKY1551	*MATa/a, ho::LYS2/ho::LYS2, lys2/lys2, ura3/ura3, leu2::hisG/leu2::hisG, arg4-nsp/arg4-bgl, his4XLEU2-URA3/his4BLEU2, dmc1::ARG4/dmc1::ARG4*	Bishop et al. 1992

Supplemental Figures

Supplemental Figure 1

As in Figure 1A, MCM localization is shown for all chromosomes. MCM enrichment is plotted versus chromosome position each chromosome as indicated for meiotic cells (red, enrichment is upwards) and mitotic cells (blue, enrichment is downwards). Inverted triangles indicated significant MCM binding sites.

Supplemental Figure 2

As in Figure 2A, DNA replication profiles are shown for all chromosomes. Replication profiles are plotted versus chromosome position each chromosome as indicated for pre-meiotic S phase (red) and pre-mitotic S phsae (blue).

Supplemental Figure 3

As in Figure 4, replication profiles for *cln3Δ* in sporulation rich media supplemented with 200mM HU are shown for all chromosomes. Replication profiles are plotted versus chromosome position each chromosome as indicated for pre-meiotic S phase (red) and pre-mitotic S phase (blue).

Supplemental Figure 4

As in Figure 5, HU replication profiles for cells sporulated in the presence of 200mM HU are shown for *cln3Δ* (red), *cln3Δ rec8Δ* (purple) and *cln3Δ spo11Δ* (brown) cells. Asterisks indicate the position of origins that are considered replicated in each strain.

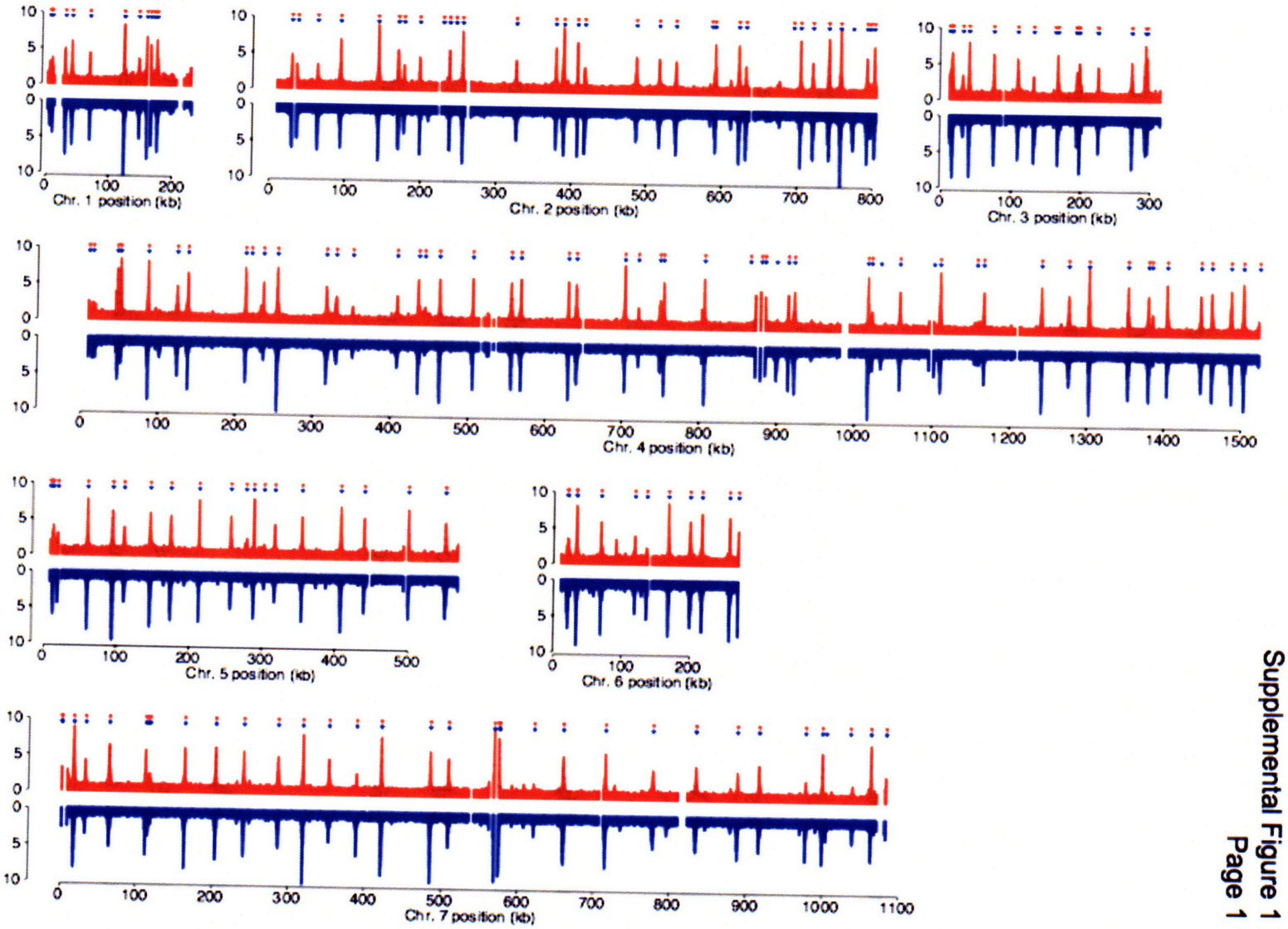

Supplemental Figure 1
Page 1

Supplemental Figure 1
Page 2

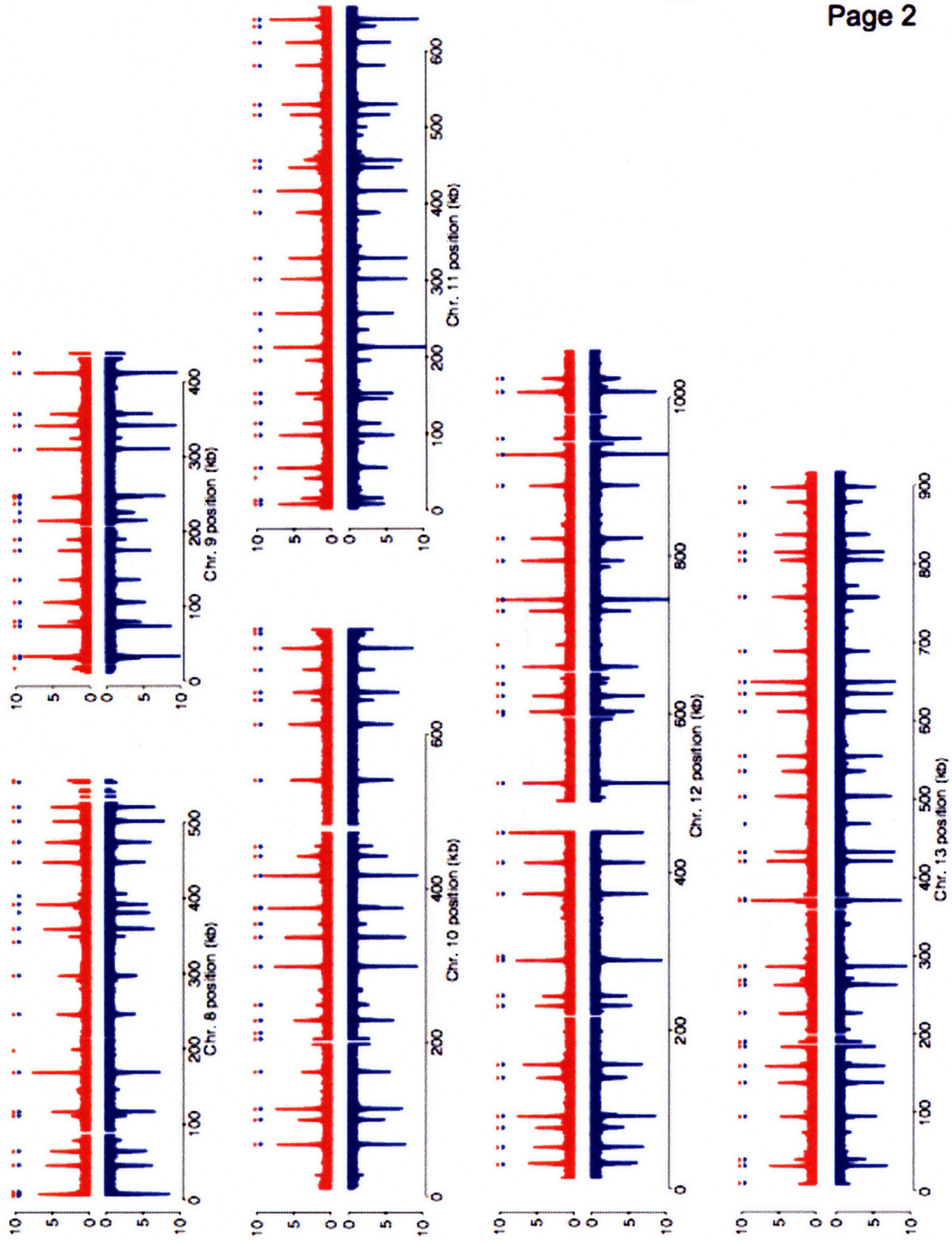

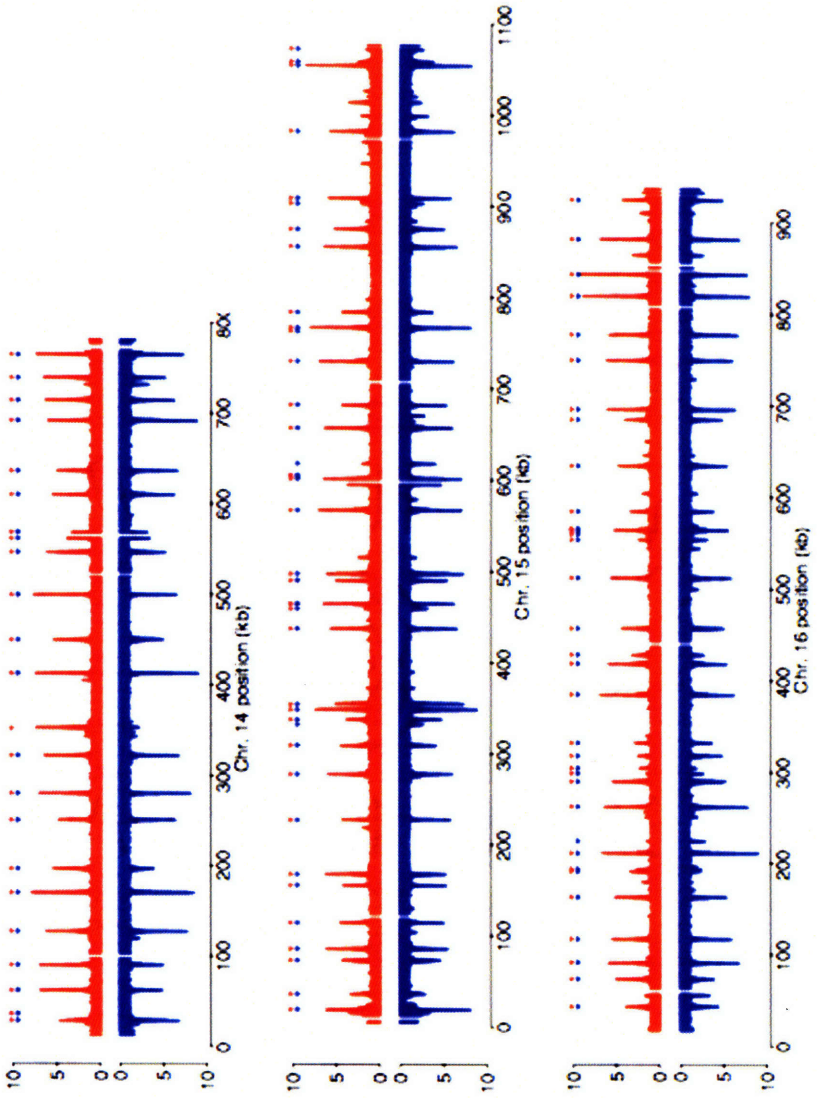
Chr. 14 position (kb)
Chr. 15 position (kb)
Chr. 16 position (kb)

Supplemental Figure 2
Page 1

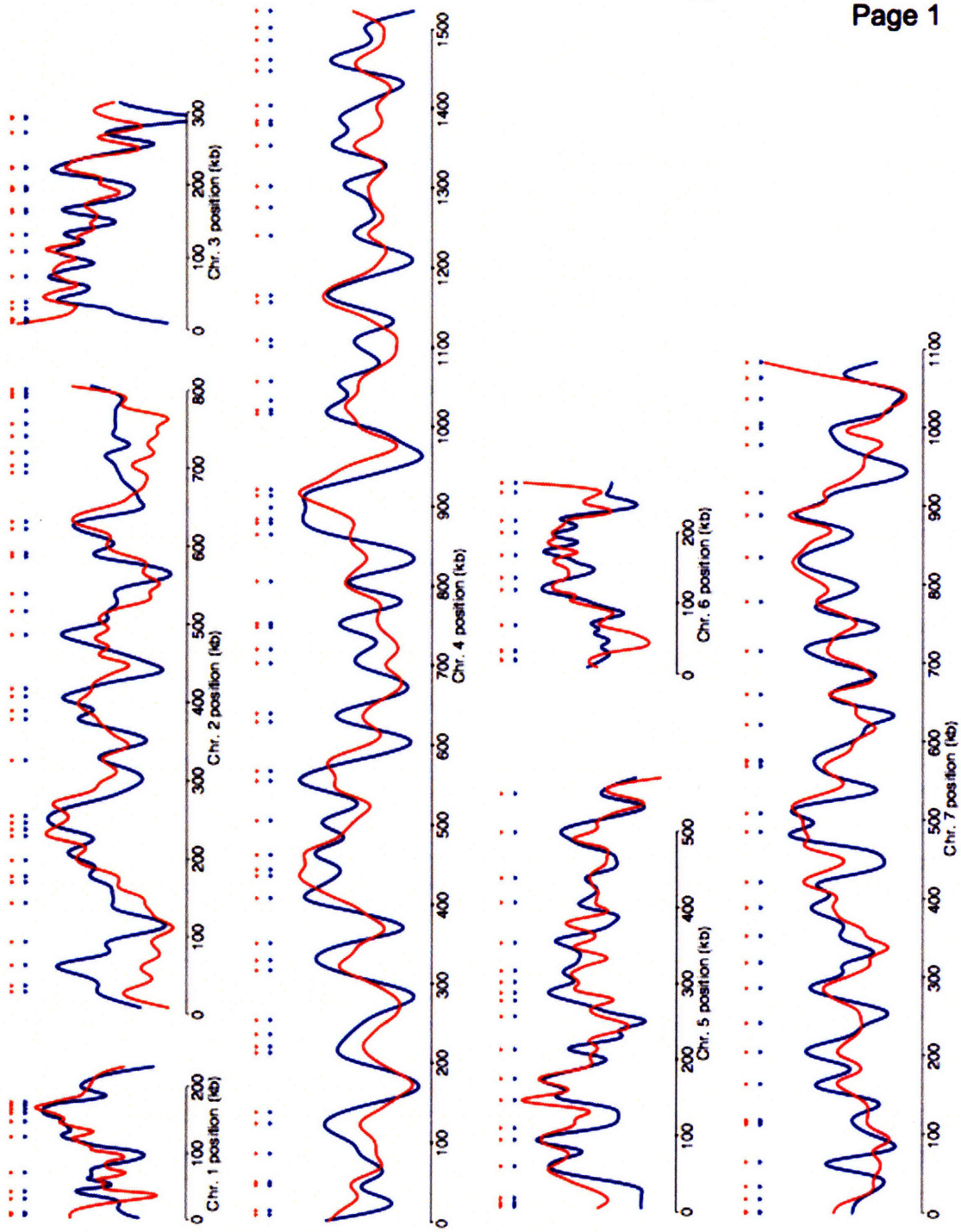

Supplemental Figure 2
Page 2

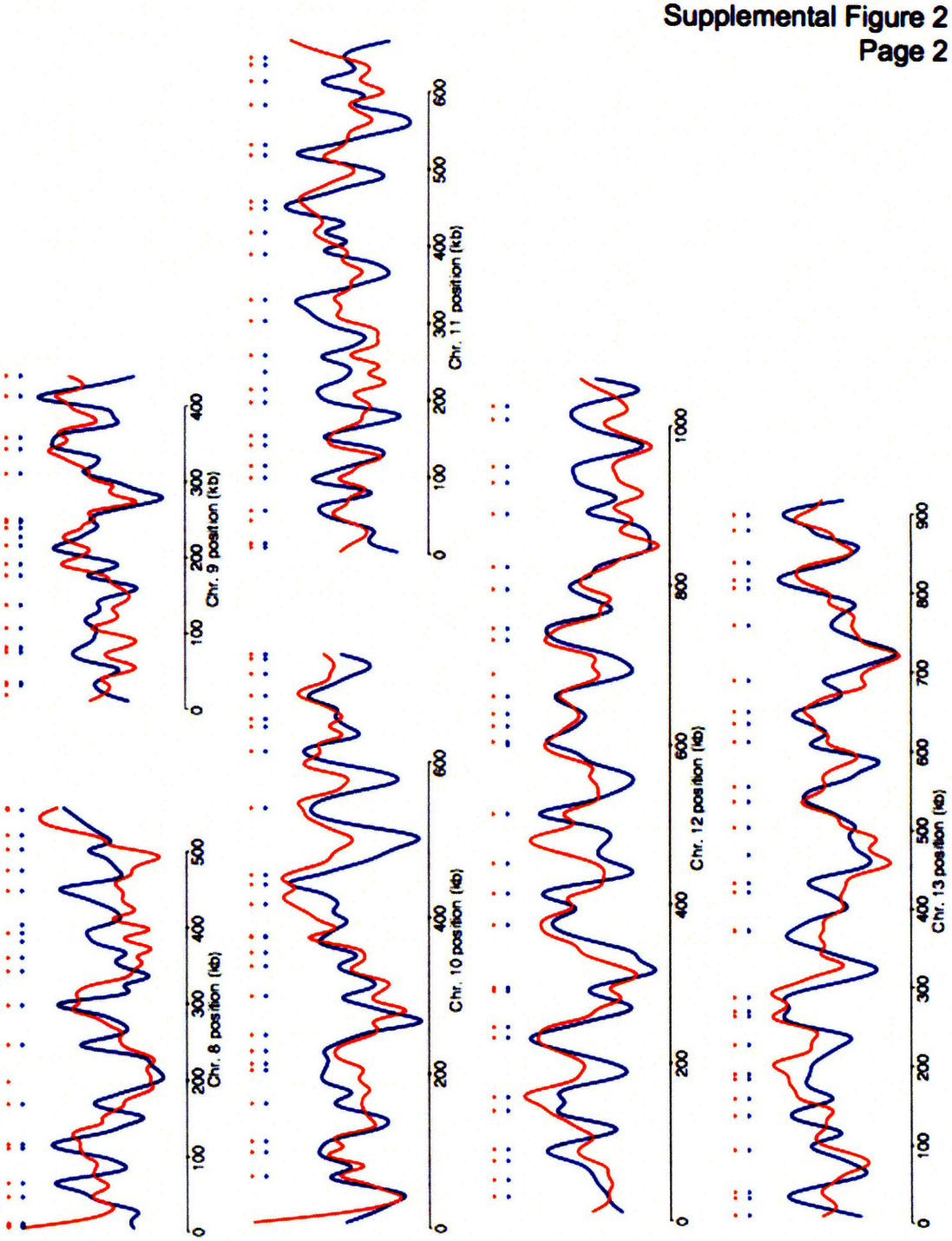

Supplemental Figure 2
Page 3

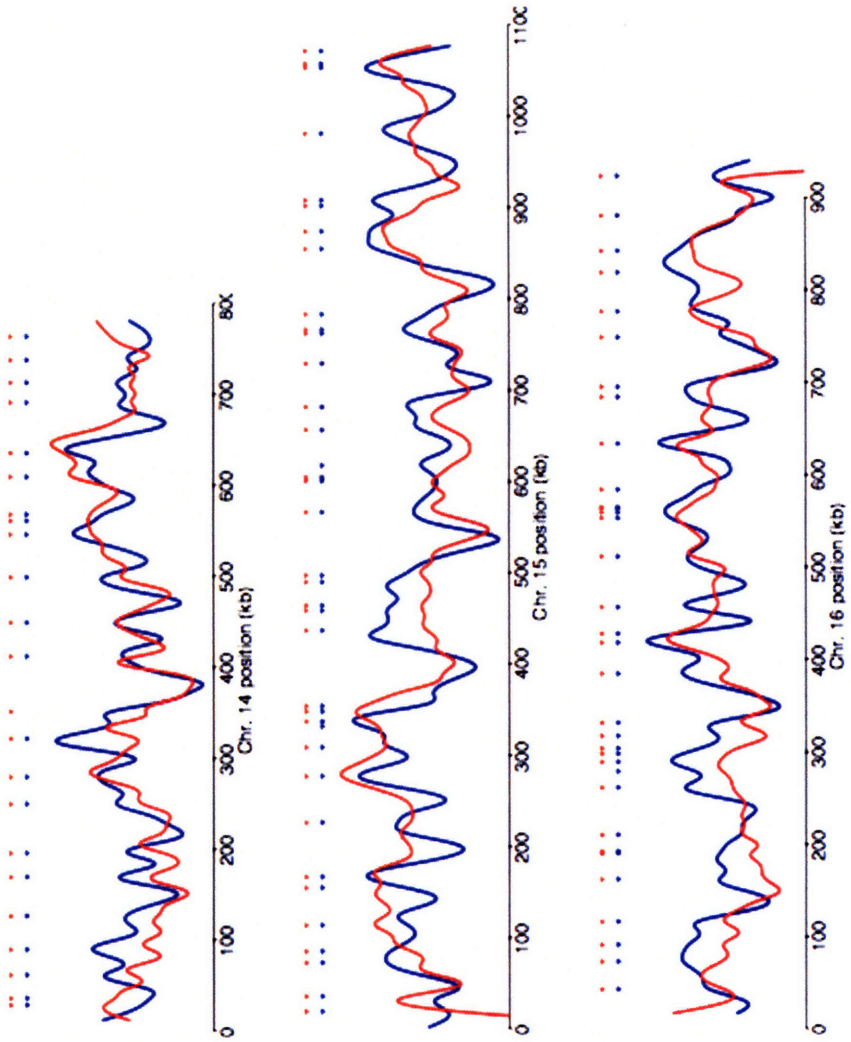

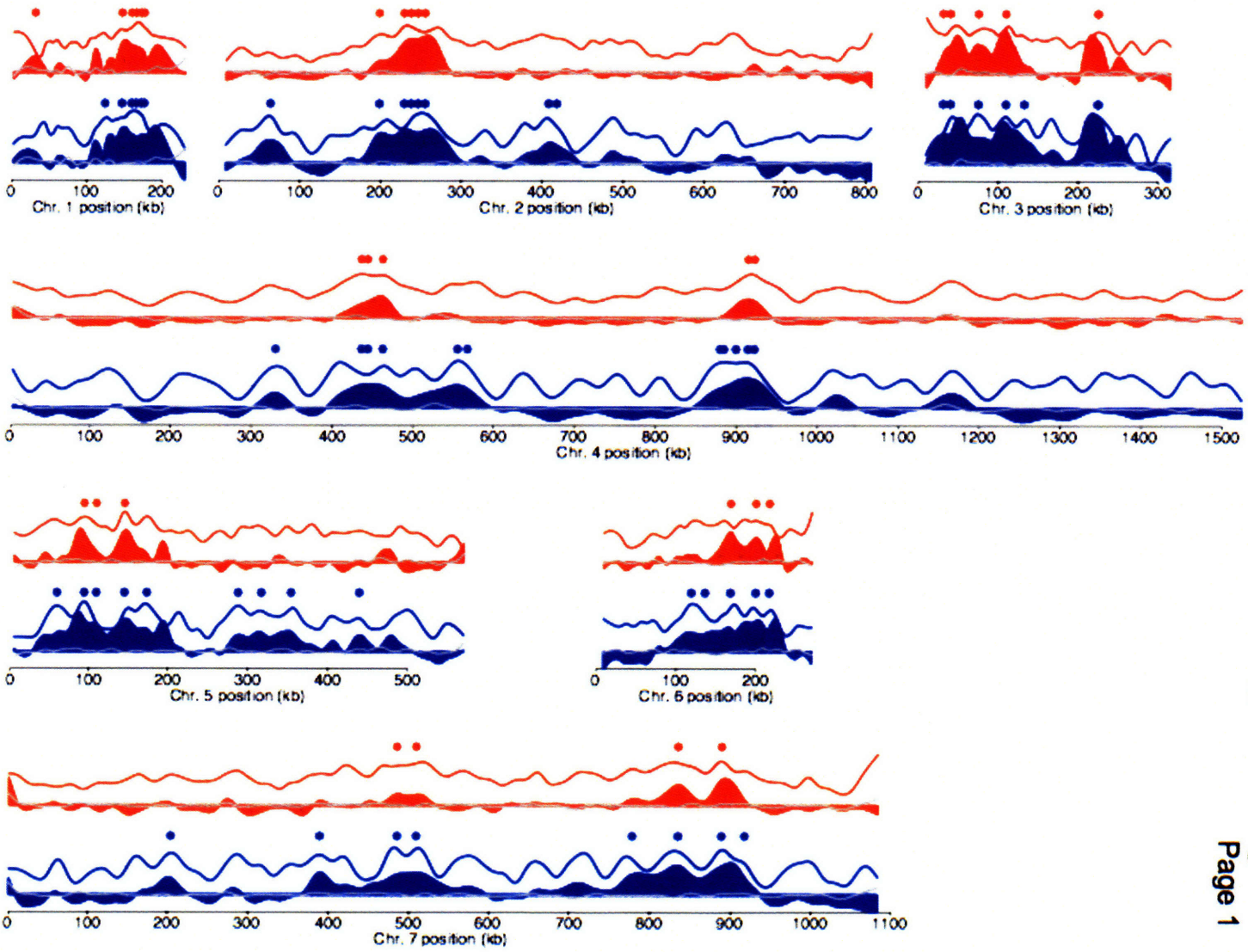

Supplemental Figure 3
Page 1

Supplemental Figure 3
Page 2

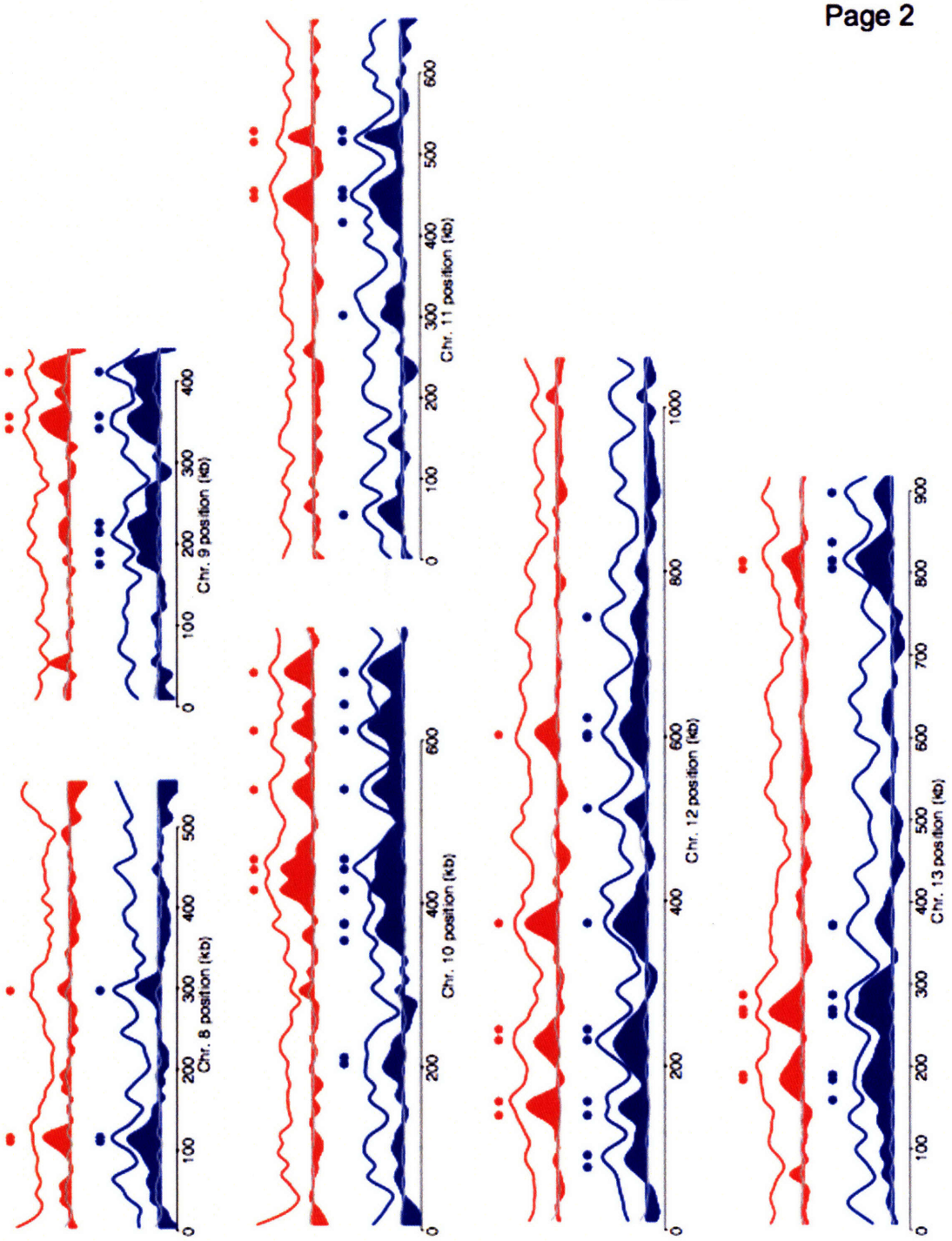

Supplemental Figure 3
Page 3

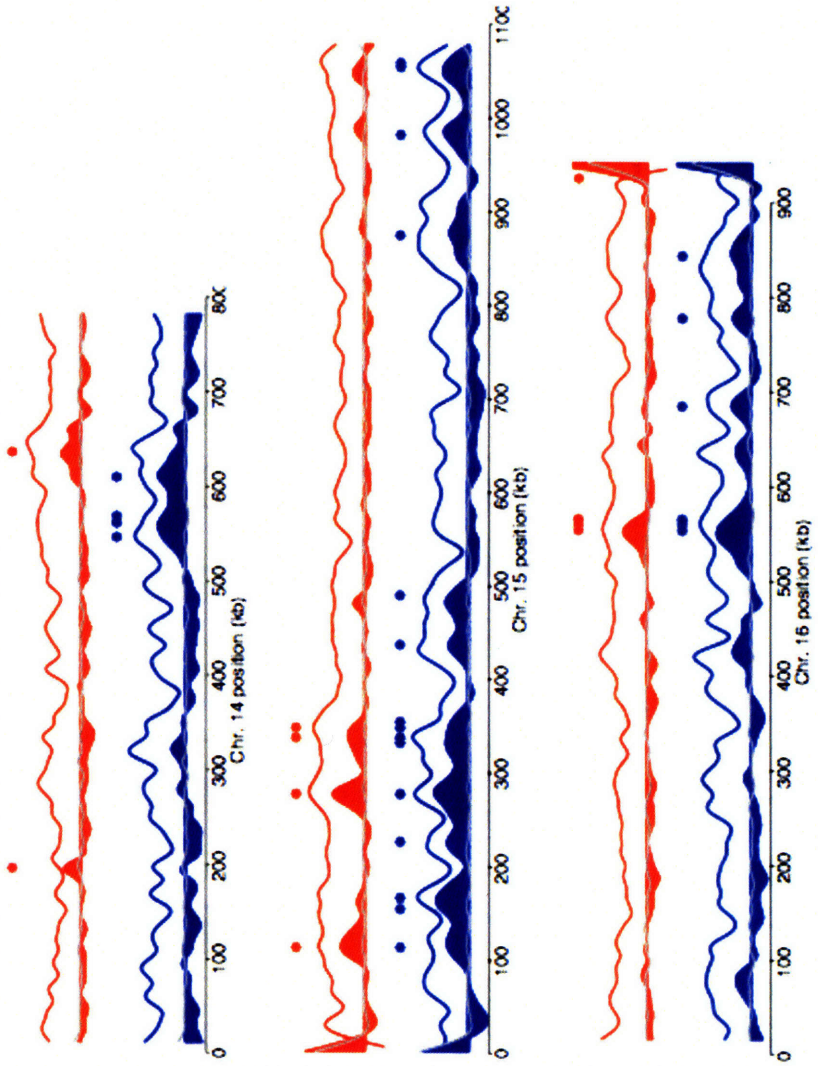

0 100 200
Chr. 1 position (kb)
0 100 200 300 400 500 600 700 800
Chr. 2 position (kb)
0 100 200 300
Chr. 3 position (kb)
0 100 200 300 400 500 600 700 800 900 1000 1100 1200 1300 1400 1500
Chr. 4 position (kb)
0 100 200 300 400 500
Chr. 5 position (kb)
0 100 200
Chr. 6 position (kb)
0 100 200 300 400 500 600 700 800 900 1000 1100
Chr. 7 position (kb)

Supplemental Figure 4
Page 2

Supplemental Figure 4
Page 3

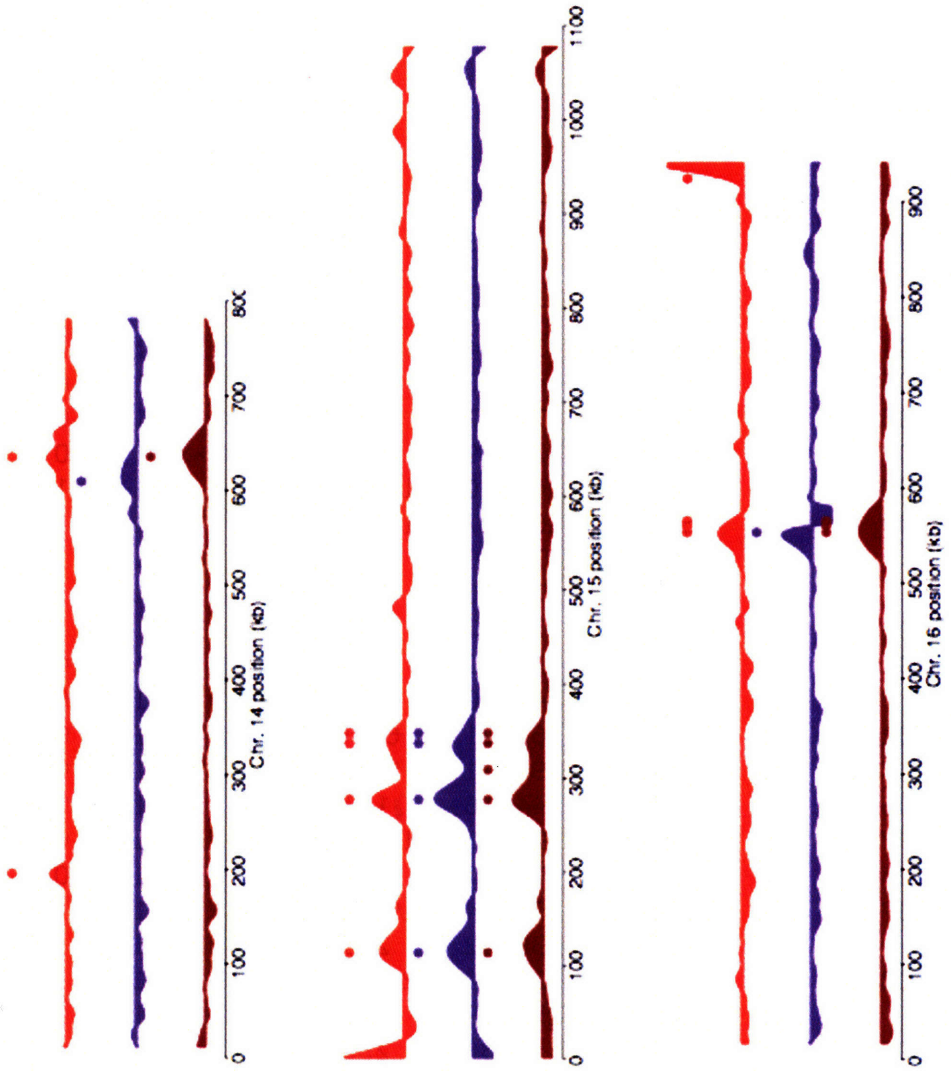

Supplemental Table 1

All potential origins identified in this study. The number, systematic name, chromosome and positions are indicated. MIT = identified by Mcm2-7 localization in pre-mitotic G1. MEI = identified by Mcm2-7 localization in pre-meiotic G1. mei HU = identified in *cln3Δ* cells in sporulated with HU, mit HU = identified in *cln3Δ* cells in rich media with HU after 4 hours, *rec8Δ* HU = identified in *rec8Δ* cells sporulated with HU, *spo11Δ* HU = identified in *spo11Δ* cells sporulated with HU.

ID	Name	Chr	Start	End	Position	MIT	MEI	mei HU	mit HU	*rec8Δ* HU	*spo11Δ* HU
1	ARS102.5	1	6136	7136	6636	1	1	0	0	0	0
2	ARS103	1	7998	8548	8273	1	1	0	0	0	0
3		1	8775	10656	9715.5	1	1	0	0	0	0
4	ARS104	1	30946	31184	31065	1	1	1	0	0	0
5	ARS105	1	40716	43300	42008	1	1	0	0	0	0
6	ARS106	1	70258	70491	70374.5	1	1	0	0	0	0
7	ARS107	1	124350	124599	124474.5	1	1	0	1	1	1
8	ARS108	1	146703	147690	147196.5	1	1	1	1	1	1
9	ARS109	1	159906	160127	160016.5	1	1	1	1	1	1
10	NA	1	162000	170000	166000	1	1	1	1	1	1
11	NA	1	168000	176000	172000	1	1	1	1	1	1
12	ARS110	1	176154	176402	176278	1	1	1	1	1	1
13	ARS201.5	2	28933	29152	29042.5	1	1	0	0	0	0
14	NA	2	33000	41000	37000	1	1	0	0	0	0
15	ARS202	2	63186	63421	63303.5	1	1	0	1	0	0
16	ARS203	2	93410	93811	93610.5	1	1	0	0	0	0
17	ARS206	2	142868	144016	143442	1	1	0	0	0	0
18	ARS207	2	170049	170298	170173.5	1	1	0	0	0	0
19	ARS207.1	2	177529	177877	177703	1	1	0	0	0	0
20	ARS207.5	2	198193	198434	198313.5	1	1	1	1	0	0
21	NA	2	221842	236842	229342	1	1	1	1	1	1
22	ARS208	2	237644	237879	237761.5	1	1	1	1	1	1
23	NA	2	238849	253849	246349	1	1	1	1	1	1
24	ARS209	2	254890	255136	255013	1	1	1	1	1	1
25	ARS211	2	326099	326335	326217	1	1	0	0	0	0
26	ARS212	2	378434	379194	378814	1	1	0	0	0	0
27	ARS213	2	389245	390368	389806.5	1	1	0	0	0	0
28	ARS214	2	407831	408064	407947.5	1	1	0	1	0	0
29	ARS215	2	417739	418035	417887	1	1	0	1	0	0
30	ARS216	2	486661	486909	486785	1	1	0	0	0	0
31	ARS217	2	516805	517805	517305	1	1	0	0	0	0
32	ARS218	2	539137	539699	539418	1	1	0	0	0	0

33	NA	2	583000	591000	587000	1	1	0	0	0	0
34	ARS219	2	591424	591713	591568.5	1	1	0	0	0	0
35	ARS220	2	622625	622894	622759.5	1	1	0	0	0	0
36	ARS221	2	631934	632246	632090	1	1	0	0	0	0
37	NA	2	687531	702531	695031	1	1	0	0	0	0
38	ARS222	2	704250	704521	704385.5	1	1	0	0	0	0
39	ARS223	2	720601	721038	720819.5	1	1	0	0	0	0
40	ARS224	2	741512	741802	741657	1	1	0	0	0	0
41	ARS225	2	757390	757621	757505.5	1	1	0	0	0	0
42	ARS227	2	773918	774348	774133	1	0	0	0	0	0
43	ARS228	2	792116	792340	792228	1	1	0	0	0	0
44	ARS228.5	2	796259	797162	796710.5	1	1	0	0	0	0
45	ARS229	2	801930	802617	802273.5	1	1	0	0	0	0
46	ARS301	3	11145	11401	11273	1	1	0	0	1	0
47	ARS302	3	14574	14849	14711.5	1	1	0	0	1	0
48	ARS303	3	14870	15213	15041.5	1	1	0	0	1	0
49	ARS320	3	15213	16274	15743.5	1	1	0	0	1	0
50	ARS304	3	30199	30657	30428	1	1	1	1	1	1
51	ARS305	3	39158	39706	39432	1	1	1	1	1	1
52	ARS306	3	74457	74677	74567	1	1	1	1	1	1
53	ARS307	3	108775	109291	109033	1	1	1	1	1	1
54	ARS309	3	131978	132322	132150	1	1	0	1	1	1
55	NA	3	159363	166363	162863	1	1	0	0	0	0
56	ARS310	3	166494	167340	166917	1	1	0	0	0	0
57	NA	3	192527	193643	193085	1	1	0	0	0	0
58	ARS313	3	194256	194505	194380.5	1	1	0	0	0	0
59	ARS314	3	197369	197601	197485	1	1	0	0	0	0
60	NA	3	222963	224792	223877.5	1	1	1	1	1	1
61	ARS315	3	224807	225053	224930	1	1	1	1	1	1
62	ARS316	3	272844	273088	272966	1	1	0	0	0	0
63	ARS317	3	292524	292826	292675	1	1	0	0	0	0
64	ARS318	3	294396	295027	294711.5	1	1	0	0	0	0
65	NA	4	7596	11052	9324	1	1	0	0	0	0
66		4	14180	15179	14679.5	1	1	0	0	0	0
67	ARS404	4	46181	46237	46209	1	1	0	0	0	0
68		4	48974	51657	50315.5	1	1	0	0	0	0
69	ARS405	4	85945	86177	86061	1	1	0	0	0	0
70	ARS406	4	123617	123902	123759.5	1	1	0	0	0	0
71	NA	4	137003	138437	137720	1	1	0	0	0	0
72	ARS409	4	212420	212669	212544.5	1	1	0	0	0	0
73	NA	4	212806	227806	220306	1	1	0	0	0	0
74	NA	4	235363	236487	235925	1	1	0	0	0	0
75	ARS410	4	253789	254038	253913.5	1	1	0	0	0	0
76	NA	4	315773	318097	316935	1	1	0	0	0	0
77	ARS413	4	329564	329813	329688.5	1	1	0	1	0	0
78	ARS413.5	4	350835	351804	351319.5	1	1	0	0	0	0
79	ARS414	4	408070	408312	408191	1	1	0	0	0	0
80	NA	4	434223	437917	436070	1	1	1	1	1	1
81	NA	4	443318	444447	443882.5	1	1	1	1	1	1

82	ARS416	4	462430	462700	462565	1	1	1	1	1	1
83	ARS417.5	4	505336	505578	505457	1	1	0	0	0	0
84	ARS418	4	555224	555461	555342.5	1	1	0	1	0	0
85	ARS419	4	567490	567737	567613.5	1	1	0	1	0	0
86	NA	4	628203	630547	629375	1	1	0	0	0	0
87	ARS421	4	639859	640108	639983.5	1	1	0	0	0	0
88	ARS422	4	702879	703125	703002	1	1	0	0	0	0
89	NA	4	719873	721227	720550	1	1	0	0	0	0
90	ARS422.5	4	748384	748630	748507	1	1	0	0	0	0
91	ARS423	4	753159	753391	753275	1	1	0	0	0	0
92	ARS425	4	806044	806270	806157	1	1	0	0	0	0
93	NA	4	857472	872472	864972	1	1	0	0	0	0
94	NA	4	875791	882791	879291	1	1	0	1	0	0
95		4	883722	884721	884221.5	1	1	0	1	0	0
96	NA	4	898253	899887	899070	1	0	0	1	0	0
97	ARS428	4	913780	914029	913904.5	1	1	1	1	1	1
98	ARS429	4	921682	921930	921806	1	1	1	1	1	1
99	ARS430	4	1016624	1016922	1016773	1	1	0	0	0	0
100		4	1021249	1022434	1021841.5	1	1	0	0	0	0
101	ARS430.5	4	1033069	1034182	1033625.5	1	0	0	0	0	0
102	ARS431	4	1057828	1058076	1057952	1	1	0	0	0	0
103		4	1101254	1102796	1102025	1	0	0	0	0	0
104	ARS431.5	4	1109955	1110196	1110075.5	1	1	0	0	0	0
105		4	1157088	1158087	1157587.5	1	1	0	0	0	0
106	ARS432.5	4	1165998	1166221	1166109.5	1	1	0	0	0	0
107	ARS433	4	1240869	1241098	1240983.5	1	1	0	0	0	0
108	ARS434	4	1276212	1276440	1276326	1	1	0	0	0	0
109	ARS435	4	1302579	1302819	1302699	1	1	0	0	0	0
110	ARS437	4	1353494	1353667	1353580.5	1	1	0	0	0	0
111	NA	4	1379198	1380752	1379975	1	1	0	0	0	0
112	NA	4	1381291	1388291	1384791	1	1	0	0	0	0
113	ARS440	4	1404277	1404512	1404394.5	1	1	0	0	0	0
114	ARS441	4	1447298	1448928	1448113	1	1	0	0	0	0
115	ARS442	4	1461849	1462161	1462005	1	1	0	0	0	0
116	ARS446	4	1486905	1487149	1487027	1	1	0	0	0	0
117	NA	4	1501448	1504702	1503075	1	1	0	0	0	0
118	NA	4	1522298	1526152	1524225	1	1	0	0	0	0
119	ARS503	5	6464	7230	6847	1	1	0	0	0	0
120	ARS504	5	8786	10019	9402.5	1	1	0	0	0	0
121	NA	5	10425	12929	11677	1	1	0	0	0	0
122	NA	5	17067	19023	18045	1	1	0	0	0	0
123	ARS507	5	59282	59516	59399	1	1	0	1	0	0
124	ARS508	5	93977	94218	94097.5	1	1	1	1	1	1
125	NA	5	108553	110467	109510	1	1	1	1	1	1
126	ARS510	5	145539	145782	145660.5	1	1	1	1	1	1
127	ARS511	5	173636	173874	173755	1	1	0	1	1	1
128	ARS512	5	212381	212630	212505.5	1	1	0	0	0	0
129	NA	5	255623	256957	256290	1	1	0	0	0	0
130	NA	5	275573	278877	277225	1	1	0	0	0	0

131	ARS514	5	287504	287750	287627	1	1	0	1	0	0
132	NA	5	301213	302387	301800	1	1	0	0	0	0
133	NA	5	316043	317307	316675	1	1	0	1	0	0
134	ARS516	5	353504	353751	353627.5	1	1	0	1	0	0
135	ARS517	5	406747	406949	406848	1	1	0	0	0	0
136	ARS518	5	438929	439178	439053.5	1	1	0	1	0	0
137	ARS520	5	498417	499343	498880	1	1	0	0	0	0
138	ARS522	5	549560	549809	549684.5	1	1	0	0	0	0
139	ARS600.3	6	18682	19864	19273	1	1	0	0	0	0
140	ARS600.4	6	19669	20826	20247.5	1	1	0	0	0	0
141	ARS601	6	32472	32995	32733.5	1	1	0	0	0	0
142	ARS602	6	32666	33247	32956.5	1	1	0	0	0	0
143	ARS603	6	68690	68869	68779.5	1	1	0	0	0	0
144	ARS603.5	6	118631	118952	118791.5	1	1	0	1	0	0
145	ARS605	6	135979	136080	136029.5	1	1	0	1	0	0
146	ARS606	6	167606	168041	167823.5	1	1	1	1	1	1
147	ARS607	6	199382	199493	199437.5	1	1	1	1	1	1
148	ARS608	6	216344	216692	216518	1	1	1	1	1	1
149	ARS609	6	256263	256418	256340.5	1	1	0	0	0	0
150	ARS610	6	269404	270022	269713	1	1	0	0	1	0
151	NA	7	23	778	400.5	1	1	0	0	0	0
152		7	875	1874	1374.5	1	1	0	0	0	0
153	NA	7	15327	19624	17475.5	1	1	0	0	0	0
154	NA	7	31980	34434	33207	1	1	0	0	0	0
155	ARS702	7	64279	64528	64403.5	1	1	0	0	0	0
156	ARS704	7	112080	112319	112199.5	1	1	0	0	0	0
157	NA	7	114771	115990	115380.5	1	1	0	0	0	0
158	ARS706	7	117471	117955	117713	1	1	0	0	0	0
159	ARS707	7	163180	163447	163313.5	1	1	0	0	0	0
160	ARS710	7	203917	204159	204038	1	1	0	1	0	0
161	NA	7	240393	242127	241260	1	1	0	0	0	0
162	ARS714	7	285951	286246	286098.5	1	1	0	0	0	0
163		7	317412	319774	318593	1	1	0	0	0	0
164	ARS716	7	352695	352917	352806	1	1	0	0	0	0
165	ARS717	7	388658	388892	388775	1	1	0	1	0	0
166	ARS718	7	421093	421342	421217.5	1	1	0	0	0	0
167	ARS719	7	484932	485160	485046	1	1	1	1	1	1
168	ARS720	7	508729	508978	508853.5	1	1	1	1	1	1
169	ARS721	7	568490	568738	568614	1	1	0	0	0	0
170	ARS722	7	574622	574916	574769	1	1	0	0	0	0
171	NA	7	574978	576840	575909	1	1	0	0	0	0
172	NA	7	620243	622517	621380	1	1	0	0	0	0
173	ARS727	7	659809	660054	659931.5	1	1	0	0	0	0
174	ARS728	7	715273	715556	715414.5	1	1	0	0	0	0
175	ARS729	7	777967	778216	778091.5	1	1	0	1	0	0
176	ARS731	7	834492	834736	834614	1	1	1	1	1	1
177	ARS731.5	7	888350	888599	888474.5	1	1	1	1	1	1
178	NA	7	916233	917857	917045	1	1	0	1	0	0
179	ARS733	7	977730	977979	977854.5	1	1	0	0	0	0

180	ARS734	7	999448	999695	999571.5	1	1	0	0	0	0
181	NA	7	1004198	1006102	1005150	1	0	0	0	0	0
182	NA	7	1033147	1040147	1036647	1	1	0	0	0	0
183	NA	7	1061998	1064852	1063425	1	1	0	0	0	0
184	ARS131a	7	1082959	1084336	1083647.5	1	1	0	0	0	0
185	ARS131n	8	5158	6168	5663	1	1	0	0	0	0
186	ARS802	8	7534	7782	7658	1	1	0	0	0	0
187	NA	8	9711	11566	10638.5	1	1	0	0	0	0
188	NA	8	45113	47112	46112.5	1	1	0	0	0	0
189	ARS805	8	64255	64489	64372	1	1	0	0	0	1
190	NA	8	110423	112247	111335	1	1	1	1	1	1
191	NA	8	115683	117257	116470	1	1	1	1	1	1
192	ARS809	8	168531	168773	168652	1	1	0	0	0	0
193	NA	8	190417	205417	197917	0	1	0	0	0	0
194	ARS813	8	245719	245968	245843.5	1	1	0	0	0	0
195	NA	8	296233	298222	297227.5	1	1	1	1	1	0
196	NA	8	334538	349538	342038	1	1	0	0	0	0
197	NA	8	358953	360647	359800	1	1	0	0	0	0
198	NA	8	380153	382157	381155	1	0	0	0	0	0
199	ARS818	8	392148	392391	392269.5	1	1	0	0	0	0
200	NA	8	395590	410590	403090	1	0	0	0	0	0
201	ARS820	8	447619	447853	447736	1	1	0	0	0	0
202	NA	8	474023	475267	474645	1	1	0	0	0	0
203	ARS822	8	501751	501992	501871.5	1	1	0	0	0	0
204	NA	8	519478	521607	520542.5	1	1	0	0	0	0
205		8	553040	554039	553539.5	1	1	0	0	1	0
206	ARS824	8	555996	556327	556161.5	0	1	0	0	1	0
207	NA	9	15901	19066	17483.5	0	1	0	0	0	1
208	NA	9	30065	31646	30855.5	1	1	0	0	0	0
209	NA	9	32509	34859	33684	1	1	0	0	0	0
210	NA	9	72923	75194	74058.5	1	1	0	0	0	0
211	NA	9	79786	81344	80565	1	1	0	0	0	0
212	ARS909	9	105821	106048	105934.5	1	1	0	0	0	0
213	ARS911	9	136094	136335	136214.5	1	1	0	0	0	0
214	ARS912	9	175034	175355	175194.5	1	1	0	1	0	0
215	NA	9	189523	190747	190135	1	1	0	1	0	0
216	ARS913	9	214675	214826	214750.5	1	1	0	1	1	1
217	NA	9	224943	227297	226120	1	0	0	1	0	0
218	NA	9	230258	245258	237758	1	1	0	0	0	0
219	ARS913.5	9	245694	245932	245813	1	1	0	0	0	0
220	ARS914	9	247579	247800	247689.5	1	1	0	0	0	0
221	NA	9	247893	249347	248620	1	1	0	0	0	0
222	NA	9	308193	311477	309835	1	1	0	0	0	0
223	ARS919	9	341853	342096	341974.5	1	1	1	1	1	1
224	ARS920	9	357156	357393	357274.5	1	1	1	1	1	1
225	ARS922	9	411817	412053	411935	1	1	1	1	1	1
226	NA	9	437553	439847	438700	1	1	0	0	0	0
227	ARS1005	10	67467	67949	67708	1	1	0	0	0	0
228	ARS1006	10	99359	99796	99577.5	1	1	0	0	0	0

229	ARS1007	10	113226	113828	113527	1	1	0	0	0	0
230	ARS1007.5	10	161435	161860	161647.5	1	1	0	0	0	0
231	ARS1008	10	203729	204614	204171.5	1	1	0	1	0	0
232	NA	10	204755	219755	212255	1	1	0	1	0	0
233	ARS1009	10	228248	228740	228494	1	1	0	0	0	0
234	ARS1009.5	10	248600	249300	248950	1	1	0	0	0	0
235	ARS1010	10	298471	298952	298711.5	1	1	0	0	0	0
236	ARS1011	10	336976	337225	337100.5	1	1	0	0	0	0
237	NA	10	353463	355722	354592.5	1	1	0	1	0	0
238	ARS1012	10	374575	374818	374696.5	1	1	0	1	0	0
239	ARS1013	10	375401	375923	375662	1	1	0	1	0	0
240	ARS1014	10	416888	417134	417011	1	1	1	1	1	1
241	ARS1015	10	442248	442658	442453	1	1	1	1	1	1
242	ARS1016	10	454276	455248	454762	1	1	1	1	1	1
243	ARS1018	10	540239	540474	540356.5	1	1	1	1	1	1
244	ARS1019	10	612542	612975	612758.5	1	1	1	1	1	1
245	NA	10	643813	644767	644290	1	1	0	1	0	0
246	ARS1020	10	654069	654309	654189	1	1	0	0	0	0
247	ARS1021	10	683328	683817	683572.5	1	1	1	1	1	1
248	ARS1022	10	711590	711837	711713.5	1	1	0	0	0	0
249		10	730341	731340	730840.5	1	1	0	0	0	0
250	ARS1024	10	736728	736970	736849	1	1	0	0	0	0
251	NA	11	7397	9007	8202	1	1	0	0	0	0
252	NA	11	10002	17002	13502	1	1	0	0	0	0
253	NA	11	39000	47000	43000	0	1	0	0	0	0
254	ARS1103	11	55670	55917	55793.5	1	1	0	1	0	0
255	ARS1104.5	11	98329	98568	98448.5	1	1	0	0	0	0
256	NA	11	113073	115127	114100	1	1	0	0	0	0
257	NA	11	133321	148321	140821	1	1	0	0	0	0
258	ARS1106	11	152934	153173	153053.5	1	1	0	0	0	0
259	ARS1106.3	11	196038	196284	196161	1	1	0	0	0	0
260	ARS1106.7	11	213080	213385	213232.5	1	1	0	0	0	0
261	NA	11	235293	236577	235935	1	0	0	0	0	0
262	NA	11	256478	258327	257402.5	1	1	0	0	0	0
263	NA	11	301463	303017	302240	1	1	0	1	0	0
264	ARS1109	11	329322	329571	329446.5	1	1	0	0	0	0
265	ARS1112	11	388607	388902	388754.5	1	1	0	0	0	0
266	ARS1113	11	416822	417055	416938.5	1	1	0	1	0	0
267	ARS1114	11	447657	447892	447774.5	1	1	1	1	1	1
268	ARS1114.5	11	454453	459197	456825	1	1	1	1	1	1
269	ARS1116	11	516653	516902	516777.5	1	1	1	1	0	0
270	NA	11	528843	531477	530160	1	1	1	1	0	0
271	ARS1118	11	581468	581706	581587	1	1	0	0	0	0
272	ARS1120	11	611874	612107	611990.5	1	1	0	0	0	0
273	NA	11	632003	634377	633190	1	1	0	0	0	0
274	ARS1123	11	642355	642602	642478.5	1	1	0	0	0	0
275	NA	12	28749	32505	30627	1	1	0	0	0	0
276	NA	12	51239	52929	52084	1	1	0	0	0	0
277	NA	12	75896	77618	76757	1	1	0	1	0	0

278	ARS1206	12	91417	91659	91538	1	1	0	1	0	0
279	NA	12	139293	140447	139870	1	1	1	1	0	1
280	ARS1209	12	156646	156883	156764.5	1	1	1	1	1	1
281	ARS1211	12	231179	231422	231300.5	1	1	1	1	1	1
282	NA	12	242693	246032	244362.5	1	1	1	1	1	1
283	ARS1212	12	289220	289469	289344.5	1	1	0	0	0	0
284	NA	12	290304	297304	293804	1	1	0	0	0	0
285	ARS1213	12	373156	373400	373278	1	1	1	1	1	1
286	ARS1215	12	412668	412897	412782.5	1	1	0	0	0	0
287	ARS1216	12	450485	450726	450605.5	1	1	0	0	0	0
288	ARS1217	12	512868	513117	512992.5	1	1	0	1	0	0
289	NA	12	595804	602804	599304	1	0	0	1	0	0
290	ARS1218	12	602938	603155	603046.5	1	1	1	1	1	1
291	NA	12	622103	623937	623020	1	1	0	1	0	0
292	NA	12	637013	639757	638385	1	1	0	0	0	0
293	ARS1220	12	659823	660072	659947.5	1	1	0	0	0	0
294	NA	12	684000	692000	688000	0	1	0	0	0	0
295	NA	12	729123	732237	730680	1	1	0	0	0	0
296	ARS1223	12	744942	745179	745060.5	1	1	0	1	0	0
297	ARS1226	12	794020	794269	794144.5	1	1	0	0	0	0
298	NA	12	821403	823002	822202.5	1	1	0	0	0	0
299	ARS1227.5	12	888569	888810	888689.5	1	1	0	0	0	0
300	NA	12	927043	929292	928167.5	1	1	0	0	0	0
301	NA	12	947123	949407	948265	1	1	0	0	0	0
302	ARS1232	12	1007180	1007470	1007325	1	1	0	0	0	0
303	ARS1234	12	1023967	1024207	1024087	1	1	0	0	0	0
304	NA	13	8791	10699	9745	1	1	0	0	0	0
305	ARS1303	13	31687	31935	31811	1	1	0	0	0	0
306	NA	13	38724	40444	39584	1	1	0	0	0	0
307	ARS1305	13	94216	94463	94339.5	1	1	0	0	0	0
308	ARS1307	13	137299	137548	137423.5	1	1	0	0	0	0
309	NA	13	158563	159797	159180	1	1	0	1	0	0
310	ARS1308	13	183793	184037	183915	1	1	1	1	1	1
311		13	189593	190592	190092.5	1	1	1	1	1	1
312	NA	13	227023	227487	227255	1	1	0	0	0	0
313	ARS1309	13	263062	263296	263179	1	1	1	1	1	1
314	NA	13	268223	269987	269105	1	1	1	1	1	1
315	ARS1310	13	286782	287067	286924.5	1	1	1	1	1	1
316	ARS1312	13	370976	371221	371098.5	1	1	0	1	0	0
317	NA	13	372017	373196	372606.5	1	1	0	1	0	0
318	NA	13	420160	421983	421071.5	1	1	0	0	0	0
319	NA	13	431453	433827	432640	1	1	0	0	0	0
320	ARS1316	13	468177	468468	468322.5	1	0	0	0	0	0
321	NA	13	502233	504197	503215	1	1	0	0	0	0
322	ARS1320	13	535595	535843	535719	1	1	0	0	0	0
323	NA	13	553563	556237	554900	1	1	0	0	0	0
324	ARS1323	13	611273	611488	611380.5	1	1	0	0	0	0
325	ARS1324	13	634479	634714	634596.5	1	1	0	0	0	0
326	ARS1325	13	649307	649551	649429	1	1	0	0	0	0

327	NA	13	687903	689917	688910	1	1	0	0	0	0
328	ARS1327	13	758222	758470	758346	1	1	0	0	0	0
329	ARS1329	13	805116	805338	805227	1	1	1	1	1	1
330	ARS1330	13	815341	815567	815454	1	1	1	1	1	1
331	NA	13	836823	838167	837495	1	1	0	1	0	0
332	NA	13	877553	879907	878730	1	1	0	0	0	0
333	ARS1332	13	897804	898040	897922	1	1	0	1	0	0
334	ARS1405	14	28467	28699	28583	1	1	0	0	0	0
335	NA	14	28756	43756	36256	1	1	0	0	0	0
336	ARS1406	14	61597	61894	61745.5	1	1	0	0	0	0
337	ARS1407	14	89528	89802	89665	1	1	0	0	0	0
338	NA	14	125623	127807	126715	1	1	0	0	0	0
339	ARS1411	14	169566	169804	169685	1	1	0	0	0	0
340	ARS1412	14	196055	196291	196173	1	1	1	0	0	0
341	ARS1413	14	250259	250506	250382.5	1	1	0	0	0	0
342	ARS1414	14	279875	280108	279991.5	1	1	0	0	0	0
343	ARS1415	14	321917	322210	322063.5	1	1	0	0	0	0
344	NA	14	348469	355469	351969	0	1	0	0	0	0
345	ARS1417	14	412263	412493	412378	1	1	0	0	0	0
346	ARS1419	14	449343	449588	449465.5	1	1	0	0	0	0
347	ARS1420	14	498987	499232	499109.5	1	1	0	0	0	0
348	ARS1421	14	545966	546201	546083.5	1	1	0	1	0	0
349	ARS1422	14	561106	561384	561245	1	1	0	1	0	0
350	NA	14	567715	569020	568367.5	1	1	0	1	0	0
351	ARS1424	14	609458	609706	609582	1	1	0	1	1	0
352	ARS1426	14	635660	635901	635780.5	1	1	1	0	0	1
353	ARS1427	14	691482	691727	691604.5	1	1	0	0	0	0
354	NA	14	712633	714697	713665	1	1	0	0	0	0
355	NA	14	737003	740237	738620	1	1	0	0	0	0
356	NA	14	763353	765237	764295	1	1	0	0	0	0
357	NA	15	18367	20227	19297	1	1	0	0	0	0
358	ARS1506.5	15	35667	35903	35785	1	1	0	0	0	0
359	ARS1507	15	72636	72872	72754	1	1	0	0	0	0
360	ARS1508	15	85195	85444	85319.5	1	1	0	0	0	0
361	ARS1509	15	113843	114084	113963.5	1	1	1	1	1	1
362	ARS1509.5	15	154972	155462	155217	1	1	0	1	0	0
363	ARS1510	15	166974	167220	167097	1	1	0	1	0	0
364	NA	15	223471	230471	226971	1	1	0	1	0	0
365	ARS1511	15	277529	277778	277653.5	1	1	1	1	1	1
366	NA	15	308463	310157	309310	1	1	0	0	0	1
367	NA	15	331493	332707	332100	1	0	0	1	0	0
368	ARS1513	15	337279	337528	337403.5	1	1	1	1	1	1
369	NA	15	347633	348862	348247.5	1	1	1	1	1	1
370	NA	15	353743	354887	354315	1	1	0	1	0	0
371	ARS1513.5	15	436732	436966	436849	1	1	0	1	0	0
372	NA	15	458023	459327	458675	1	1	0	0	0	0
373	NA	15	463698	464877	464287.5	1	1	0	0	0	0
374	ARS1514	15	489645	490129	489887	1	1	0	1	0	0
375	NA	15	496203	498207	497205	1	1	0	0	0	0

376	ARS1516	15	566409	566643	566526	1	1	0	0	0	0
377	ARS1517	15	600885	600960	600922.5	1	1	0	0	0	0
378	NA	15	601221	608221	604721	1	1	0	0	0	0
379	NA	15	616913	618427	617670	1	0	0	0	0	0
380	ARS1519	15	656632	656876	656754	1	1	0	0	0	0
381	NA	15	680823	683197	682010	1	1	0	0	0	0
382	ARS1521	15	729739	729969	729854	1	1	0	0	0	0
383	NA	15	759221	766221	762721	1	1	0	0	0	0
384	ARS1523	15	766617	766862	766739.5	1	1	0	0	0	0
385	ARS1524	15	783344	783563	783453.5	1	1	0	0	0	0
386	NA	15	854173	856027	855100	1	1	0	0	0	0
387	ARS1526	15	874190	874434	874312	1	1	0	1	0	0
388	NA	15	901383	903147	902265	1	1	0	0	0	0
389	ARS1528	15	908288	908537	908412.5	1	1	0	0	0	0
390	ARS1529	15	981454	981690	981572	1	1	0	1	0	0
391	ARS1529.5	15	1053490	1053901	1053695.5	1	1	0	1	0	0
392	NA	15	1056048	1059952	1058000	1	1	0	1	0	0
393	NA	15	1071098	1072802	1071950	1	1	0	0	0	0
394	ARS1604	16	42976	43212	43094	1	1	0	0	0	0
395	ARS1605	16	73038	73283	73160.5	1	1	0	0	0	0
396	NA	16	89758	92975	91366.5	1	1	0	0	0	0
397	ARS1607	16	116505	116765	116635	1	1	0	0	0	0
398	NA	16	161693	163447	162570	1	1	0	0	0	0
399	NA	16	189963	191457	190710	1	1	0	0	0	0
400		16	192489	193755	193122	1	1	0	0	0	0
401	NA	16	210143	211437	210790	1	1	0	0	0	0
402		16	223605	225070	224337.5	1	0	0	0	0	0
403	NA	16	261168	262687	261927.5	1	1	0	0	0	0
404	ARS1614	16	289483	289704	289593.5	1	1	0	0	0	0
405	NA	16	297813	299287	298550	1	1	0	0	0	0
406	NA	16	303433	305027	304230	1	1	0	0	0	0
407	NA	16	316743	318397	317570	1	1	0	0	0	0
408	NA	16	331043	332607	331825	1	1	0	0	0	0
409	ARS1618	16	384536	384784	384660	1	1	0	0	0	0
410	ARS1619	16	418132	418359	418245.5	1	1	0	0	0	0
411	NA	16	427273	428757	428015	1	1	0	0	0	0
412	ARS1620.5	16	456557	456805	456681	1	1	0	0	0	0
413	ARS1621	16	511619	511940	511779.5	1	1	0	0	0	0
414	NA	16	552403	554287	553345	1	1	1	1	1	1
415	NA	16	556133	563133	559633	1	1	1	1	0	1
416	ARS1622	16	563822	564061	563941.5	1	1	1	1	0	1
417	ARS1622.5	16	565046	565289	565167.5	1	1	1	1	0	1
418	NA	16	583493	585147	584320	1	1	0	0	0	0
419	ARS1623	16	633868	634117	633992.5	1	1	0	0	0	0
420	ARS1624	16	684383	684632	684507.5	1	1	0	1	0	0
421	ARS1625	16	695432	695681	695556.5	1	1	0	0	0	0
422	ARS1626	16	749094	749341	749217.5	1	1	0	0	0	0
423	ARS1626.5	16	776921	777152	777036.5	1	1	0	1	0	0
424	ARS1627	16	819153	819393	819273	1	1	0	0	0	0

425	ARS1628	16	842646	842894	842770	1	1	0	1	0	0
426	ARS1630	16	880854	881102	880978	1	1	0	0	0	0
427		16	923117	924882	923999.5	1	1	1	0	0	0

References

Alvino, G. M., D. Collingwood, et al. (2007). "Replication in Hydroxyurea: It's a matter of time." Mol Cell Biol.

Aparicio, O. M., D. M. Weinstein, et al. (1997). "Components and dynamics of DNA replication complexes in S. cerevisiae: redistribution of MCM proteins and Cdc45p during S phase." Cell **91**(1): 59-69.

Benjamin, K. R., C. Zhang, et al. (2003). "Control of landmark events in meiosis by the CDK Cdc28 and the meiosis-specific kinase Ime2." Genes Dev **17**(12): 1524-39.

Borde, V., A. S. Goldman, et al. (2000). "Direct coupling between meiotic DNA replication and recombination initiation." Science **290**(5492): 806-9.

Bowers, J. L., J. C. Randell, et al. (2004). "ATP hydrolysis by ORC catalyzes reiterative Mcm2-7 assembly at a defined origin of replication." Mol Cell **16**(6): 967-78.

Cha, R. S., B. M. Weiner, et al. (2000). "Progression of meiotic DNA replication is modulated by interchromosomal interaction proteins, negatively by Spo11p and positively by Rec8p." Genes Dev **14**(4): 493-503.

Chabes, A., V. Domkin, et al. (1999). "Yeast Sml1, a protein inhibitor of ribonucleotide reductase." J Biol Chem **274**(51): 36679-83.

Chu, S., J. DeRisi, et al. (1998). "The transcriptional program of sporulation in budding yeast." Science **282**(5389): 699-705.

Collins, I. and C. S. Newlon (1994). "Chromosomal DNA replication initiates at the same origins in meiosis and mitosis." Mol Cell Biol **14**(5): 3524-34.

Colomina, N., E. Gari, et al. (1999). "G1 cyclins block the Ime1 pathway to make mitosis and meiosis incompatible in budding yeast." Embo J **18**(2): 320-9.

Coverley, D. and R. A. Laskey (1994). "Regulation of eukaryotic DNA replication." Annu Rev Biochem **63**: 745-76.

DePamphilis, M. L. (2003). "The 'ORC cycle': a novel pathway for regulating eukaryotic DNA replication." Gene **310**: 1-15.

Diffley, J. F. (2004). "Regulation of early events in chromosome replication." Curr Biol **14**(18): R778-86.

Dirick, L., L. Goetsch, et al. (1998). "Regulation of meiotic S phase by Ime2 and a Clb5,6-associated kinase in Saccharomyces cerevisiae." Science **281**(5384): 1854-7.

Donaldson, A. D., M. K. Raghuraman, et al. (1998). "CLB5-dependent activation of late replication origins in S. cerevisiae." Mol Cell **2**(2): 173-82.

Feng, W., D. Collingwood, et al. (2006). "Genomic mapping of single-stranded DNA in hydroxyurea-challenged yeasts identifies origins of replication." Nat Cell Biol **8**(2): 148-55.

Hochwagen, A. and A. Amon (2006). "Checking your breaks: surveillance mechanisms of meiotic recombination." Curr Biol **16**(6): R217-28.

Hyrien, O., C. Maric, et al. (1995). "Transition in specification of embryonic metazoan DNA replication origins." Science **270**(5238): 994-7.

Klein, F., P. Mahr, et al. (1999). "A Central Role for Cohesins in Sister Chromatid Cohesion, Formation of Axial Elements and Recombination during Yeast Meiosis." Cell **98**: 91-103.

Lamb, T. M. and A. P. Mitchell (2001). "Coupling of Saccharomyces cerevisiae early meiotic gene expression to DNA replication depends upon RPD3 and SIN3." Genetics **157**(2): 545-56.

Lau, A., H. Blitzblau, et al. (2002). "Cell-cycle control of the establishment of mating-type silencing in S. cerevisiae." Genes Dev **16**(22): 2935-45.
Lei, M. and B. K. Tye (2001). "Initiating DNA synthesis: from recruiting to activating the MCM complex." J Cell Sci **114**(Pt 8): 1447-54.
Mendez, J. and B. Stillman (2003). "Perpetuating the double helix: molecular machines at eukaryotic DNA replication origins." Bioessays **25**(12): 1158-67.
Mori, S. and K. Shirahige (2007). "Perturbation of the activity of replication origin by meiosis-specific transcription." J Biol Chem **282**(7): 4447-52.
Murakami, H., V. Borde, et al. (2003). "Correlation between premeiotic DNA replication and chromatin transition at yeast recombination initiation sites." Nucleic Acids Res **31**(14): 4085-90.
Nieduszynski, C. A., Y. Knox, et al. (2006). "Genome-wide identification of replication origins in yeast by comparative genomics." Genes Dev **20**(14): 1874-9.
Padmore, R., L. Cao, et al. (1991). "Temporal comparison of recombination and synaptonemal complex formation during meiosis in S. cerevisiae." Cell **66**(6): 1239-56.
Primig, M., R. M. Williams, et al. (2000). "The Core Meiotic Transcriptome in Budding Yeasts." Nat. Genet. **26**: 415-423.
Raghuraman, M. K., E. A. Winzeler, et al. (2001). "Replication dynamics of the yeast genome." Science **294**(5540): 115-21.
Sando, N. and S. Miyake (1971). "Biochemical changes in yeast during sporulation. I. Fate of nucleic acids and related compounds." Dev Growth Differ **12**(4): 273-83.
Santocanale, C. and J. F. Diffley (1998). "A Mec1- and Rad53-dependent checkpoint controls late-firing origins of DNA replication." Nature **395**(6702): 615-8.
Shirahige, K., Y. Hori, et al. (1998). "Regulation of DNA-replication origins during cell-cycle progression." Nature **395**(6702): 618-21.
Snyder, M., R. J. Sapolsky, et al. (1988). "Transcription interferes with elements important for chromosome maintenance in Saccharomyces cerevisiae." Mol Cell Biol **8**(5): 2184-94.
Stuart, D. and C. Wittenberg (1998). "CLB5 and CLB6 Are Required for Premeiotic DNA Replication and Activation of the Meiotic S/M Checkpoint." Genes Dev **12**: 2698-2710.
Tanaka, S., D. Halter, et al. (1994). "Transcription through the yeast origin of replication ARS1 ends at the ABFI bind

ing site and affects extrachromosomal maintenance of minichromosomes." Nucleic Acids Res **22**(19): 3904-10.
Tonami, Y., H. Murakami, et al. (2005). "A checkpoint control linking meiotic S phase and recombination initiation in fission yeast." Proc Natl Acad Sci U S A **102**(16): 5797-801.
Williamson, D. H., L. H. Johnston, et al. (1983). "The timing of the S phase and other nuclear events in yeast meiosis." Exp Cell Res **145**(1): 209-17.
Wyrick, J. J., J. G. Aparicio, et al. (2001). "Genome-wide distribution of ORC and MCM proteins in S. cerevisiae: high-resolution mapping of replication origins." Science **294**(5550): 2357-60.
Xu, W., J. G. Aparicio, et al. (2006). "Genome-wide mapping of ORC and Mcm2p binding sites on tiling arrays and identification of essential ARS consensus sequences in S. cerevisiae." BMC Genomics **7**: 276.
Yabuki, N., H. Terashima, et al. (2002). "Mapping of early firing origins on a replication profile of budding yeast." Genes Cells **7**(8): 781-9.

Yang, Y. H., S. Dudoit, et al. (2001). Normalization of cDNA microarray data. SPIE BiOS 2001, San Jose, CA.
Zickler, D. and N. Kleckner (1999). "Meiotic chromosomes: integrating structure and function." Annu Rev Genet **33**: 603-754.

Chapter III

Mapping of meiotic single-stranded DNA reveals double-strand break hotspots near centromeres and telomeres

Summary

BACKGROUND

Every chromosome requires at least one crossover to be faithfully segregated during meiosis. At least two levels of regulation govern crossover distribution; where the initiating DNA double-strand breaks (DSBs) occur and whether those DSBs are repaired as crossovers.

RESULTS

We mapped meiotic DSBs in budding yeast by identifying sites of DSB-associated single-stranded DNA (ssDNA) accumulation. These analyses revealed substantial DSB activity in regions close to centromeres, where crossover formation is largely absent. Our data suggest that centromeric suppression of recombination occurs at the level of break repair rather than DSB formation. Additionally, we found an enrichment of DSBs within a ~100-kb region near the ends of all chromosomes. Introduction of new telomeres was sufficient to induce large ectopic regions of increased DSB formation, revealing a remarkable long-range effect of telomeres on DSB formation. The concentration of DSBs close to chromosome ends increases the relative DSB density on small chromosomes, providing an interference-independent mechanism to ensure that all chromosomes receive at least one crossover per homolog pair.

CONCLUSIONS

Together, our results indicate that selective DSB repair accounts for crossover suppression near centromeres, and suggest a simple telomere-guided mechanism to ensure sufficient DSB activity on all chromosomes.

Introduction

During gametogenesis, a diploid progenitor cell undergoes two distinct nuclear divisions to produce four haploid gametes; in meiosis I homologous chromosomes are segregated and in meiosis II sister chromatids are partitioned. The proper segregation of homologous chromosomes requires the establishment of a physical connection between each homolog pair. In most organisms, this linkage takes the form of a crossover, a reciprocal exchange of DNA strands between homologs (Petronczki, Siomos et al. 2003; Bishop and Zickler 2004). Failure to form stable crossovers results in chromosome non-disjunction, infertility and birth defects.

Crossovers are the product of homolog-directed repair of meiotic DSBs. Breaks are formed by the topoisomerase-related enzyme Spo11 (Bergerat, de Massy et al. 1997; Keeney, Giroux et al. 1997), which becomes covalently linked to the DNA during the reaction. Removal of Spo11 from DNA ends allows 5'-strand resection (Sun, Treco et al. 1991). The resulting ssDNA forms the substrate for subsequent strand invasion, which is catalyzed by the two recA homologs, Rad51 and Dmc1. Approximately half of the strand-invasion reactions are further processed into double Holliday junctions and crossovers (Allers and Lichten 2001; Hunter and Kleckner 2001).

The limiting number of crossovers per meiosis requires strict regulation of crossover formation and distribution. Two mechanisms are thought to ensure that even small chromosomes receive at least one crossover (Lichten and Goldman 1995; Petes 2001). First, small chromosomes have a higher DSB density than large chromosomes, thereby increasing the chances that one DSB will be repaired as a crossover (Gerton, DeRisi et al. 2000). Secondly, a

phenomenon called crossover interference prevents the formation of new crossovers near existing crossovers to ensure optimally spaced crossover distribution along chromosomes (Bishop and Zickler 2004). In addition, crossovers are prevented in regions where they would be deleterious to the cell. Crossovers are suppressed near centromeres, where they would interfere with meiotic chromosome segregation (Lamb, Sherman et al. 2005; Rockmill, Voelkel-Meiman et al. 2006). Similarly, crossovers are reduced in the vicinity of the repetitive DNA at the telomeres (Su, Barton et al. 2000) and in the rDNA (Petes and Botstein 1977), where they could lead to interactions between non-homologous chromosomes and loss of rDNA repeats, respectively.

Crossover distribution is governed to a large extent by the initial placement of DSBs (Lichten and Goldman 1995; Petes 2001). In budding yeast, much of our understanding of where DSBs form stems from the analysis of *rad50S*-type mutants (*rad50S*, *mre11S*, and *com1/sae2Δ*), in which meiotic DSBs do not get repaired and Spo11 remains covalently attached to the DNA ends (Keeney, Giroux et al. 1997). Studies of individual loci showed that DSBs form preferentially at so-called hotspots, the majority of which are located in intergenic regions containing promoters (Wu and Lichten 1994; Baudat and Nicolas 1997). In addition, genome-wide analysis of Spo11 localization revealed hot and cold regions of DSB formation, and showed specific depletion of DSB hotspots near telomeres, centromeres, and the rDNA (Baudat and Nicolas 1997; Gerton, DeRisi et al. 2000; Borde, Lin et al. 2004; Mieczkowski, Dominska et al. 2006; Robine, Uematsu et al. 2007). However, because *rad50S*-type mutations have been shown to change the rate of DSB formation at some loci (Conrad, Dominguez et al. 1997; Borde,

Goldman et al. 2000; Blat, Protacio et al. 2002), existing DSB maps might not accurately reflect the distribution of DSBs in wild-type cells.

We have developed an alternative method to localize DSB hotpots by detecting the ssDNA intermediate that surrounds each DSB site. Analysis of sites of ssDNA accumulation in meiosis confirmed that DSBs occur predominantly in promoters and are enriched near highly expressed genes. In addition, consistent with genetic data, high levels of DSBs could be detected to within ~20 kb of chromosome ends. Remarkably, we discovered strong DSB hotspots close to centromeres, indicating that the repression of recombination in these regions must occur at the level of DSB repair. Finally, we found that telomeres induce ~100-kb regions of increased DSB formation close to the ends of all chromosomes, suggesting a simple mechanism to distribute DSB activity to chromosomes of all sizes.

Results

Labeling of ssDNA reveals DSB sites.

We mapped meiotic DSB hotspots by detection of ssDNA (Figure 1A). ssDNA is a direct metabolite of meiotic DSBs (Cao, Alani et al. 1990; Sun, Treco et al. 1991) that, due to its distinct chemical properties, can be specifically purified and labeled for microarray analysis (Feng, Collingwood et al. 2006). Approximately 600 nucleotides of ssDNA are typically exposed on either side of a meiotic DSB in wild-type cells (Sun, Treco et al. 1991). This number is increased in *dmc1* mutant cells, which are unable to repair DSBs and arrest with long tracts of ssDNA (Bishop, Park et al. 1992). Therefore, for our initial analysis we chose a wild-type SK1 strain, as well as an isogenic *dmc1Δ* mutant strain. Both strains were induced to undergo

synchronous meiosis and total genomic DNA was isolated. ssDNA was enriched and fluorescently labeled. Labeled probes from cells in meiotic prophase and a control population that had not begun DSB formation were co-hybridized to a high-density tiled microarray (~300 bp between array features). Plotting the meiotic ssDNA signal versus chromosomal position revealed a reproducible profile of ssDNA enrichment at specific chromosomal loci in both wild-type and *dmc1Δ* strains (Figure 1B and Supplemental Figure 1). To ensure that the ssDNA signal we detected was due to DSBs induced by Spo11, and not the result of DNA replication or spontaneous DNA damage repair, we performed the same experiment using a catalytic mutant of *SPO11* (*spo11-Y135F*) that is unable to form meiotic DSBs (Bergerat, de Massy et al. 1997). We observed no sites of significant ssDNA enrichment in the *spo11Y135F* strain (Figure 1B and Supplemental Figure 1). Therefore, this method specifically detects Spo11-dependent meiotic DSBs.

Consistent with a large body of genetic data, we observed DSBs across most of the genome. We used several approaches to validate the DSB sites predicted by our method. First, ssDNA arrays faithfully reproduced the overall DSB profile of chromosome III as detected by pulsed-field gel electrophoresis and Southern blot (Figure 1C). We observed that peak height corresponded to signal intensity of hotspots on the Southern blot, indicating that ssDNA signal reflects hotspot activity. Second, we detected all of the well-characterized hotspots that have previously been confirmed by Southern blot, including *ARG4*, *DED81*, *CYS3*, *HIS2*, *YCR047C*, *CDC19*, and *HIS4LEU2* (Lichten and Goldman 1995), as well as the majority of hotspots and cold regions directly tested in other genome-wide studies (Gerton, DeRisi et al. 2000; Borde, Lin et al. 2004). To further support our results, we analyzed several predicted pericentromeric and

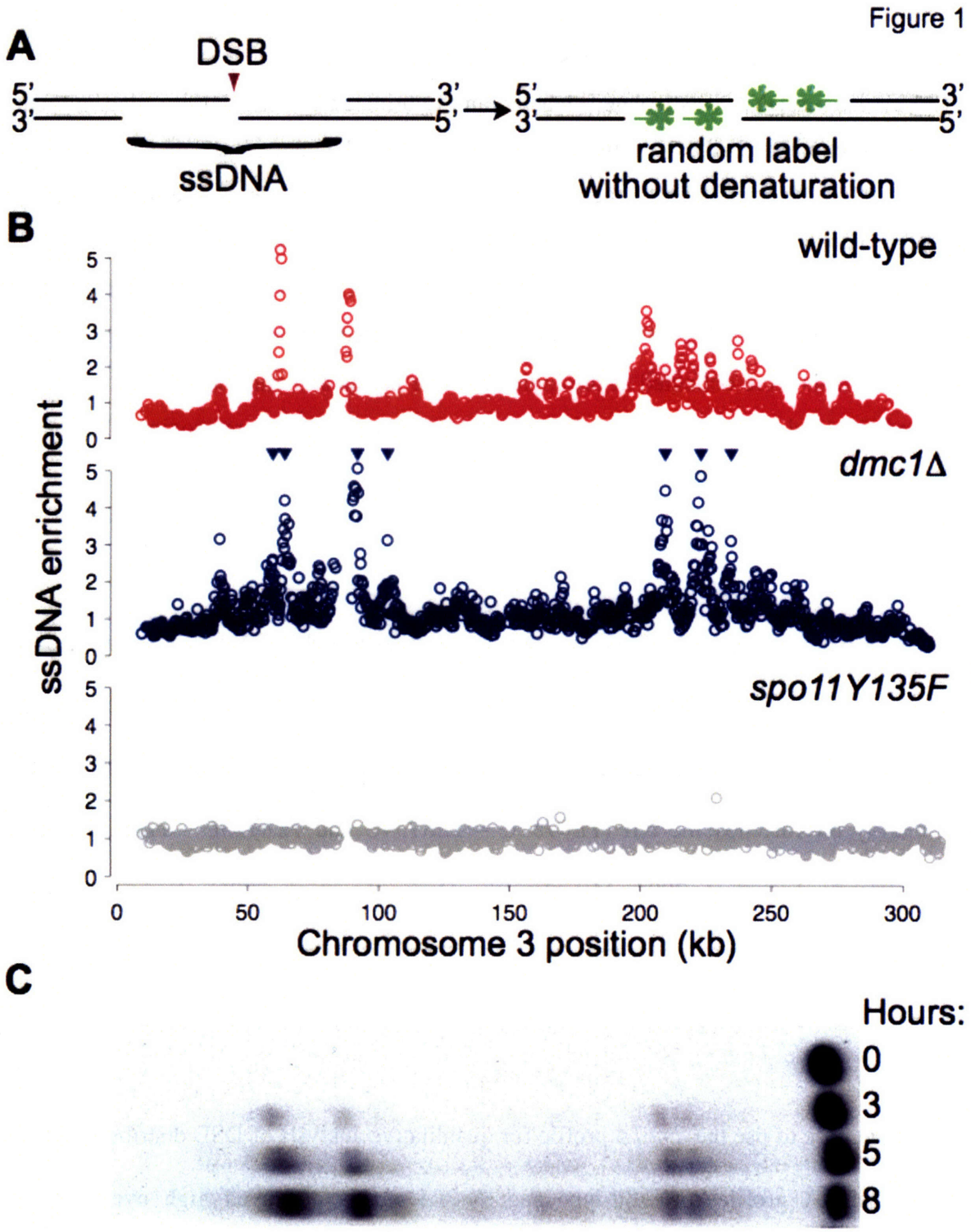

Figure 1: Meiotic ssDNA profiles.

Wild-type (NKY1551), *dmc1Δ* (NKY1455), and *spo11-Y135F* (A10914) cultures were induced to undergo synchronous meiosis. (A) ssDNA, produced by 5' to 3' strand resection at DSBs, was

specifically labeled by random priming without a denaturation step. (B) Premeiotic control samples were harvested at 0h, meiotic samples were harvested after 3h (NKY1551, A10914) or 5h (NKY1455). ssDNA was isolated, labeled and hybridized to high-density tiled microarrays. The fold enrichment of ssDNA in the meiotic sample over the control sample was calculated for each feature on the array. The average signal from the two independent experiments was plotted versus chromosome position for each feature on chromosome III for wild-type (red), *dmc1Δ* (blue), and *spo11-Y135F* (grey) strains (all chromosomes are shown in Supplemental Figure 1). Statistically significant DSB sites for *dmc1Δ* are indicated by inverted triangles. (C) *dmc1Δ* (NKY1455) cells were collected at the indicated time points and chromosome III was analyzed by pulsed-field gel electrophoresis and Southern blot using the telomere proximal *YCL60c* probe (Baudat and Nicolas 1997).

---

telomere proximal hotspots by Southern blot. In all cases tested, ssDNA profiles were excellent predictors of DSB sites in both wild-type and *dmc1Δ* cells (see below and data not shown). We also confirmed the absence of any measurable hotspot signal in the cold regions surrounding the rDNA array on chromosome XII (*YLR151C – YLR154C* and *YLR163C - YLR176C*; data not shown) (Borde, Lin et al. 2004; Mieczkowski, Dominska et al. 2006). A similar method of ssDNA enrichment was independently developed by Buhler et al. and comparable results were observed (M. Lichten, personal communication).

We chose to use the *dmc1Δ* profile for quantitative analysis of DSB distribution, because, although ssDNA profiles of wild-type and *dmc1Δ* strains displayed high overall similarity (Figure1 and Supplemental Figure 1), the *dmc1Δ* profile exhibited a substantially better signal-to-noise ratio. We believe that this difference in signal is largely a consequence of ongoing repair in wild-type cells. Due to the limited synchrony of meiotic cultures, as well as overlap in the

timing of meiotic DSB formation and repair (Hunter and Kleckner 2001), some DSBs may already be repaired in wild-type cells while others have yet to form. By contrast, no repair occurs in *dmc1Δ* mutant cells (Schwacha and Kleckner 1997). Furthermore, other recombinases did not contribute *DMC1*-independent repair activity, because profiles of *dmc1Δ rad51Δ* and *rad52Δ* mutants were nearly identical to those of *dmc1Δ* (data not shown). Thus, unlike wild-type cells, the *dmc1Δ* mutation likely permits quantitative detection of cumulative DSB formation across the genome.

To search for determinants of hotspot activity, we focused on the most active DSB hotspots, as both ssDNA profiles and Southern analysis indicated that the majority of DSB activity occurs at these sites. Multiple contiguous points were enriched above background at each peak, consistent with the density of our array and length of ssDNA exposed in the *dmc1Δ* mutant cells. Therefore, we defined a hotspot as a cluster of >3 adjacent sites that were significantly enriched in at least two individual experiments. By these criteria, we identified 258 hotspots in the *dmc1Δ* strain that we used for subsequent study (blue triangles; Figure 1A, Supplemental Figure 1 and Supplemental Table 2).

Hotspots mapped by ssDNA versus Spo11 localization.

We initially compared the hotspots identified by our ssDNA profiles to hotspots mapped by Spo11 localization analysis (ChIP) in *rad50S* or *sae2Δ* mutants (Gerton, DeRisi et al. 2000; Borde, Lin et al. 2004). Of the 258 hotspots detected by ssDNA enrichment in the *dmc1Δ* strain, we found that only 89 overlapped with the 177 DSB sites described by Gerton, et al. (Gerton, DeRisi et al. 2000) and 130 overlapped with the 585 described by Borde, et al. (Borde, Lin et al.

2004). To eliminate many of the experimental variables that could account for these discrepancies, we mapped sites of Spo11 binding in a *rad50S* SK1 strain on high-density arrays by directly labeling the immunoprecipitated chromatin without amplification (Supplemental Figure 1). Using the same criteria for hotspot identification as in our ssDNA analysis, we identified 232 significant sites of Spo11 attachment across the genome. Comparison of the DSBs identified by ssDNA enrichment and Spo11 binding in this study revealed 123 loci (~50%) present in both data sets. In addition, we noted that the relative peak heights varied greatly at hotspots that were identified by both ssDNA and Spo11 ChIP. This suggests that the incomplete correspondence between hotspots identified by ssDNA enrichment and Spo11 ChIP was largely not a consequence of strain background, array densities, or data analysis.

Previous reports suggested that *rad50S*-type mutations alter DSB frequencies in some parts of the genome (Dresser, Ewing et al. 1997; Borde, Goldman et al. 2000; Blat, Protacio et al. 2002). To test whether the observed differences between DSB hotspots mapped by ssDNA enrichment and Spo11 ChIP are a consequence of altered DSB distribution between *dmc1Δ* and *rad50S* mutants, we selected several hotspots and analyzed DSB formation in both mutants by Southern blot. The well-characterized *YCR047C* hotspot was detected by ssDNA mapping and Spo11 ChIP and was equally active in *dmc1Δ* and *rad50S* mutants (Figure 2A). In contrast, several other hotspots close to the telomere of chromosome XVI (*YPL274W* and *YPL221W*; Figure 2A), and in pericentromeric regions (*CEN2*, *CEN4*, and *CEN15*; see below) displayed markedly reduced or undetectable activity in *rad50S* mutants. Altered DSB activity was also apparent by pulsed-field gel electrophoresis and Southern blot of chromosomes VIII (Figure 2B) and III (Supplemental Figure 2). Finally, in *rad50S* mutants a higher fraction of chromosomes

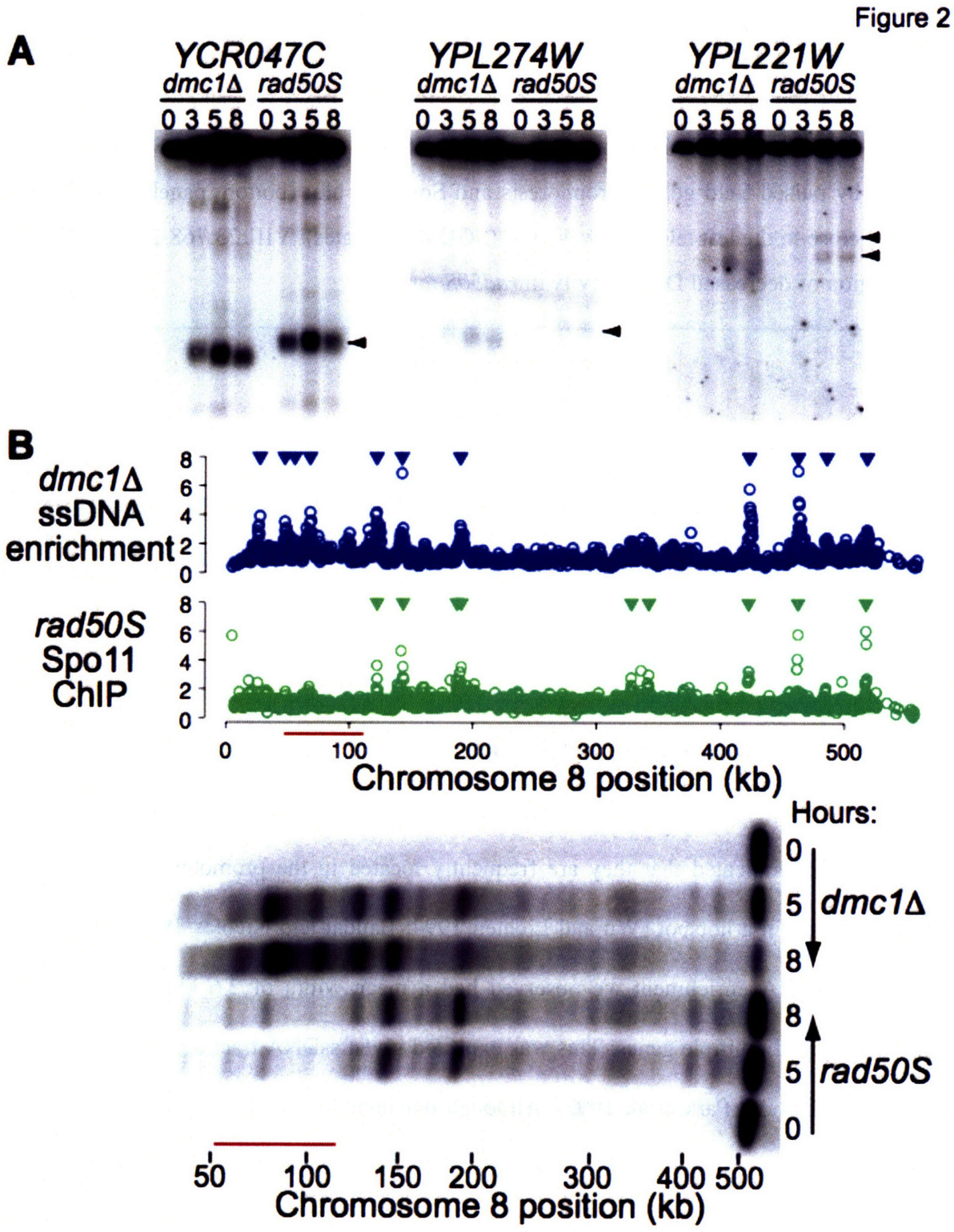

Figure 2: DSB hotspots in *dmc1Δ* and *rad50S*.

dmc1Δ (NKY1455) and *rad50S* (A11675) cells were induced to undergo meiosis and samples were collected at the indicated time points. (A) Genomic DNA was digested and analyzed by

Southern blot. The following restriction enzymes and probes (SGD coordinates) were used: *YCR047C*, HindIII, III:209,361-210,030 (Hunter and Kleckner 2001); *YPL274W*, PstI/XhoI, XVI:20,281-21,012; *YPL221W*, XbaI, XVI:128,661-129,550. Black arrowheads indicate major DSB sites. (B) Hotspot distribution on chromosome VIII as determined by ssDNA analysis (top panels) and by pulsed-field gel electrophoresis and Southern blot (bottom panel). For Southern blot a probe close to the left telomere was used (SGD coordinates): VIII:23,768-25,407. Red line indicates region of decreased DSB activity in *rad50S* mutant.

---

remained unbroken, suggesting that overall levels of DSB formation may be reduced (Figure 2B and Supplemental Figure 2). Similar data were obtained by Buhler et al. (M. Lichten, personal communication). We conclude that DSB hotspots are utilized differently in *rad50S* and *dmc1Δ* strains.

DSBs are enriched in promoters of active genes.

We next examined where breaks occurred with regard to gene-coding regions. Fine-scale mapping of DSBs indicated that they are frequently located in the promoters of one or more adjacent genes within a hotspot (Wu and Lichten 1994; Baudat and Nicolas 1997; Petes 2001). The peaks of ssDNA enrichment we observed had a mean width of 2.6 kb per hotspot, and typically overlapped multiple genes. This was expected given ssDNA tract lengths of >1 kb in a *dmc1Δ* mutant (Bishop, Park et al. 1992). Although our method does not have the resolution to detect individual break points within a hotspot, we employed multiple statistical approaches to reveal trends in DSB site selection. First, assuming that the peak of ssDNA enrichment at each hotspot was located close to the most common break site, we confirmed that DSBs occurred preferentially in promoters. In particular, peaks were located in divergent promoters three times

more frequently than expected, whereas they were underrepresented at sites of convergent transcription and in coding regions (Figure 3A). To further refine the positions of break sites relative to genes, we calculated the composite ssDNA enrichment profile for all 1105 genes overlapping a DSB hotspot. Consistent with the results above, the composite profile showed the highest ssDNA signal in the promoter region (Figure 3B). To resolve the position of break sites at individual genes, we plotted the relative ssDNA enrichment across the largest 226 hotspot-associated genes (Figure 3C). We found that ~80% of genes exhibited higher ssDNA signal in their promoters and 5' ends relative to the rest of the coding or downstream regions. Moreover, the vast majority (44/47) of the 3' regions that exhibited elevated ssDNA enrichment contained a promoter for the adjacent gene. Together, these findings are consistent with the model that the majority of DSBs occur in intergenic regions containing promoters.

Because the activity of a number of hotspots requires the binding of transcription factors (Petes 2001; Mieczkowski, Dominska et al. 2006), we investigated the connection between transcription and DSB hotspots. Using published meiotic gene expression data (Primig, Williams et al. 2000), we found that the average expression level of genes at peaks of DSB hotspots was 30% higher than the mean expression level in the genome (Student's t-test, $p<0.0009$; Figure 3D). However, we observed no enrichment of meiotically regulated genes within hotspots (Supplemental Table 2). Similarly, there was no difference between expression levels of genes surrounding DSB hotspots from meiosis-competent MATa/α cells or meiosis-incompetent MATα/α cells (Figure 3D)(Primig, Williams et al. 2000). These data imply that DSBs occur preferentially in the promoters of active, but not necessarily meiosis-specific, genes.

Figure 4

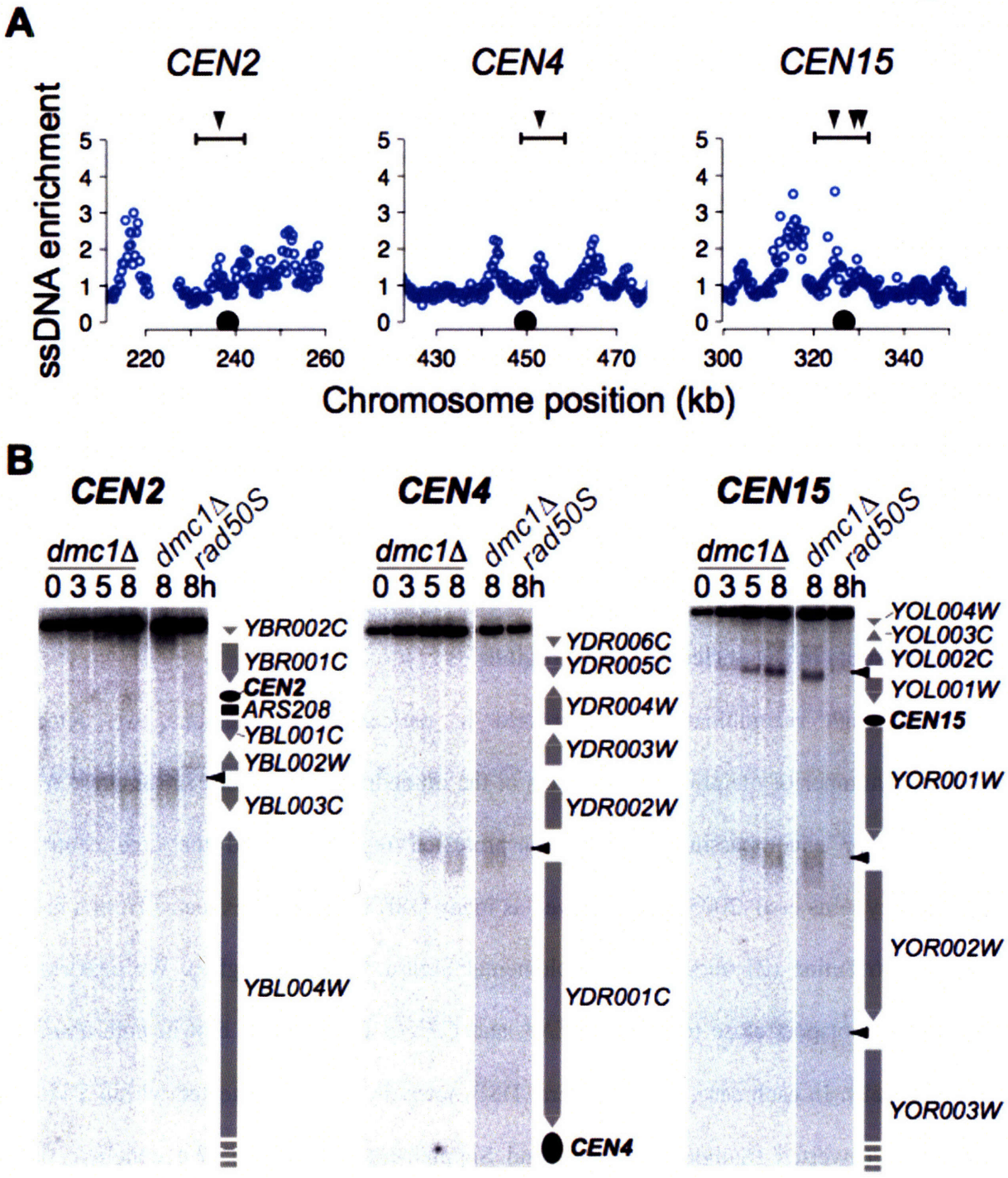

Figure 4: Hotspots near centromeres.

(A) ssDNA enrichment versus chromosome position is plotted for a window of +/- 25 kb for *CEN2*, *CEN4* and *CEN15*. Black dots indicate the centromere position. Black bars indicate

between tandem, divergent or convergent transcripts. These data deviated significantly from those expected by a random distribution of the 258 hotspots in single copy genomic sequence (χ^2, p=7.4E-9). (B) Composite ssDNA enrichment profile. Array features associated with each gene were assigned to one of 10 open reading frame (ORF) bins or 5 upstream or downstream intergenic bins based on their relative position within each region. The profile represents the mean $\log_2$ ratios calculated for each bin. (C) Heat map representing scaled $\log_2$ ratios of ssDNA enrichment for the upstream, coding and downstream regions of each of the 226 largest genes coinciding with DSB sites in the *dmc1Δ* strain (NKY1455). To compare across genes, mean $\log_2$ ratios for all features associated with each gene were adjusted to 0. (D) The average expression level after 2 hours in sporulation media is shown for all genes (yellow bars) and the genes coinciding with DSB sites in the *dmc1Δ* strain (blue bars) for sporulating a/α and control non-sporulating α/α cells (Primig, Williams et al. 2000).

Strong hotspots in the pericentromeric regions.

Although recombination is repressed in pericentromeric regions, we detected a substantial number of meiotic DSB hotspots in the immediate vicinity of centromeres. Within a 50-kb window encompassing the cohesion-protected regions around the core centromeres (Kiburz, Reynolds et al. 2005), we observed as many DSB hotspots as expected from a model of random distribution (21 versus 17, Supplemental Figure 3, blue triangles). We confirmed the existence of hotspots close to *CEN2*, *CEN4*, and *CEN15* by Southern blot in both *dmc1Δ* and wild-type cells. In each case, one or several DSB hotspots could be detected within 5 kb of the centromere (inverted triangles, Figure 4 and Supplemental Figure 4). We conclude that the pericentromeric regions are not protected from meiotic DSB formation.

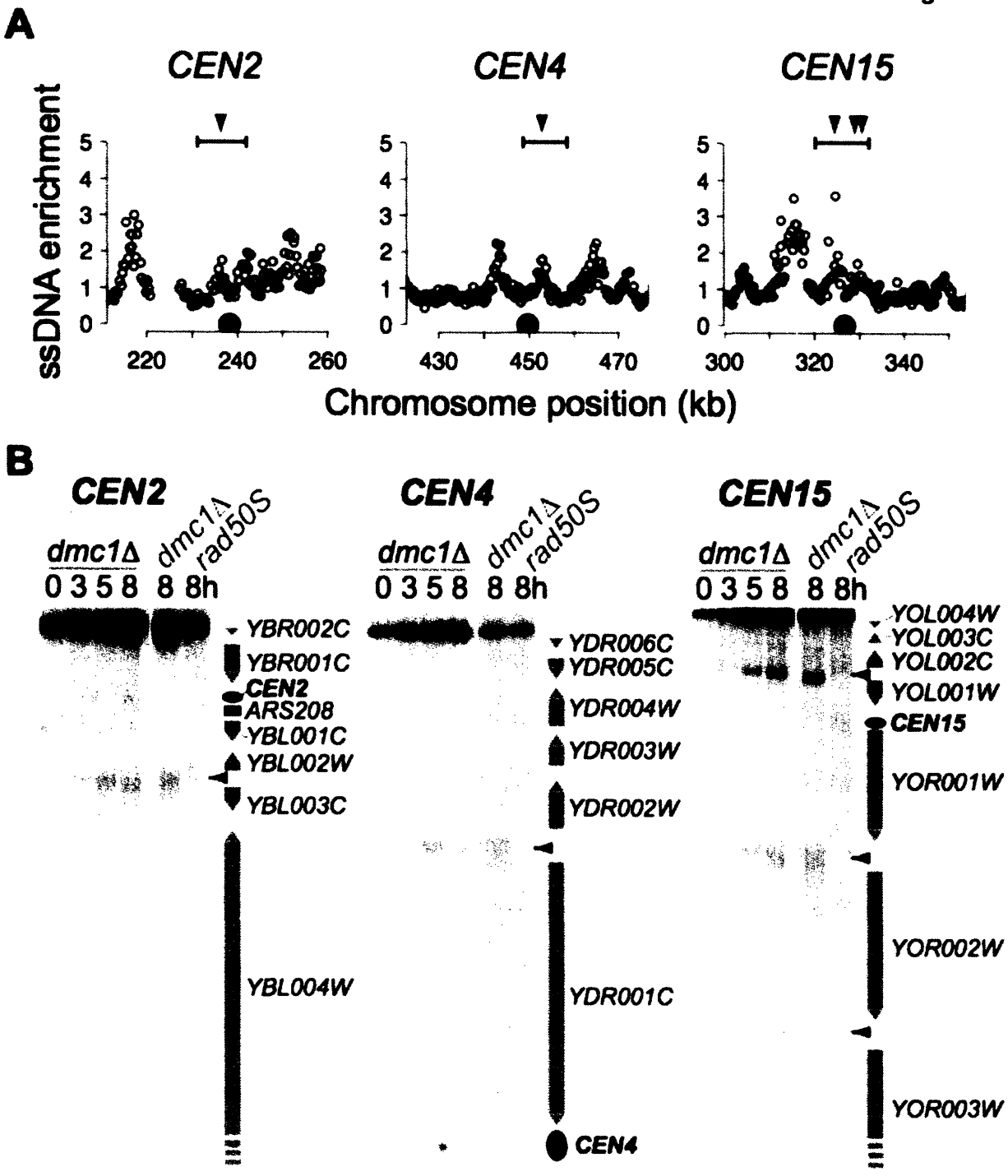

Figure 4: Hotspots near centromeres.

(A) ssDNA enrichment versus chromosome position is plotted for a window of +/- 25 kb for *CEN2*, *CEN4* and *CEN15*. Black dots indicate the centromere position. Black bars indicate

positions of restriction fragments detected by Southern blot and inverted triangles indicate confirmed DSB sites (see panel B). (B) *dmc1Δ* (NKY1455) and *rad50S* cells (A11675) were induced to undergo synchronous meiosis. At the indicated time points, samples were collected and DNA analyzed by Southern blot. The following restriction enzymes and probes (SGD coordinates) were used: *CEN2*, SacI, II:231,552-232,350; *CEN4*, SpeI, IV:449,212-449,721; *CEN15*, SphI/NheI, XV:331,713-332,402. Grey arrows indicate the positions of open reading frames, black ovals indicate centromeres, black arrowheads indicate major DSB sites.

Hotspots distribution near the rDNA and telomeres.

We next analyzed DSB formation around the rDNA and near telomeres, genomic regions that were previously reported to exhibit a significantly lower than average number of DSB hotspots (Gerton, DeRisi et al. 2000; Borde, Lin et al. 2004; Mieczkowski, Dominska et al. 2006; Mieczkowski, Dominska et al. 2007; Robine, Uematsu et al. 2007). Recombination within the 100-200 copies of the rDNA can lead to unequal exchange and rDNA loss, which is lethal to cells. ssDNA analysis confirmed an absence of strong hotspots within 100 kb of the rDNA (Supplemental Figure 1). Recombination within the rDNA array is prevented, at least in part, by Pch2, a meiosis specific ATPase that localizes to the nucleolus and plays a poorly defined role in the recombination checkpoint (San-Segundo and Roeder 1999). ssDNA analysis in a *pch2Δ dmc1Δ* mutant revealed strong DSB signal in the rDNA proximal regions (Figure 5A), indicating the Pch2 prevents DSB formation in the single copy sequence surrounding the rDNA. These results were confirmed by Southern blot analysis (Figure 5B). Nucleolar localization of Pch2 is dependent on the Sir2 protein (San-Segundo and Roeder 1999), and therefore we tested whether the silencing of DSBs close to the rDNA was also dependent on Sir2. Contrary to the *pch2Δ dmc1Δ* strain, a *sir2Δ dmc1*Δ strain lacked strong DSB hotspots close to the rDNA (Figure 5A).

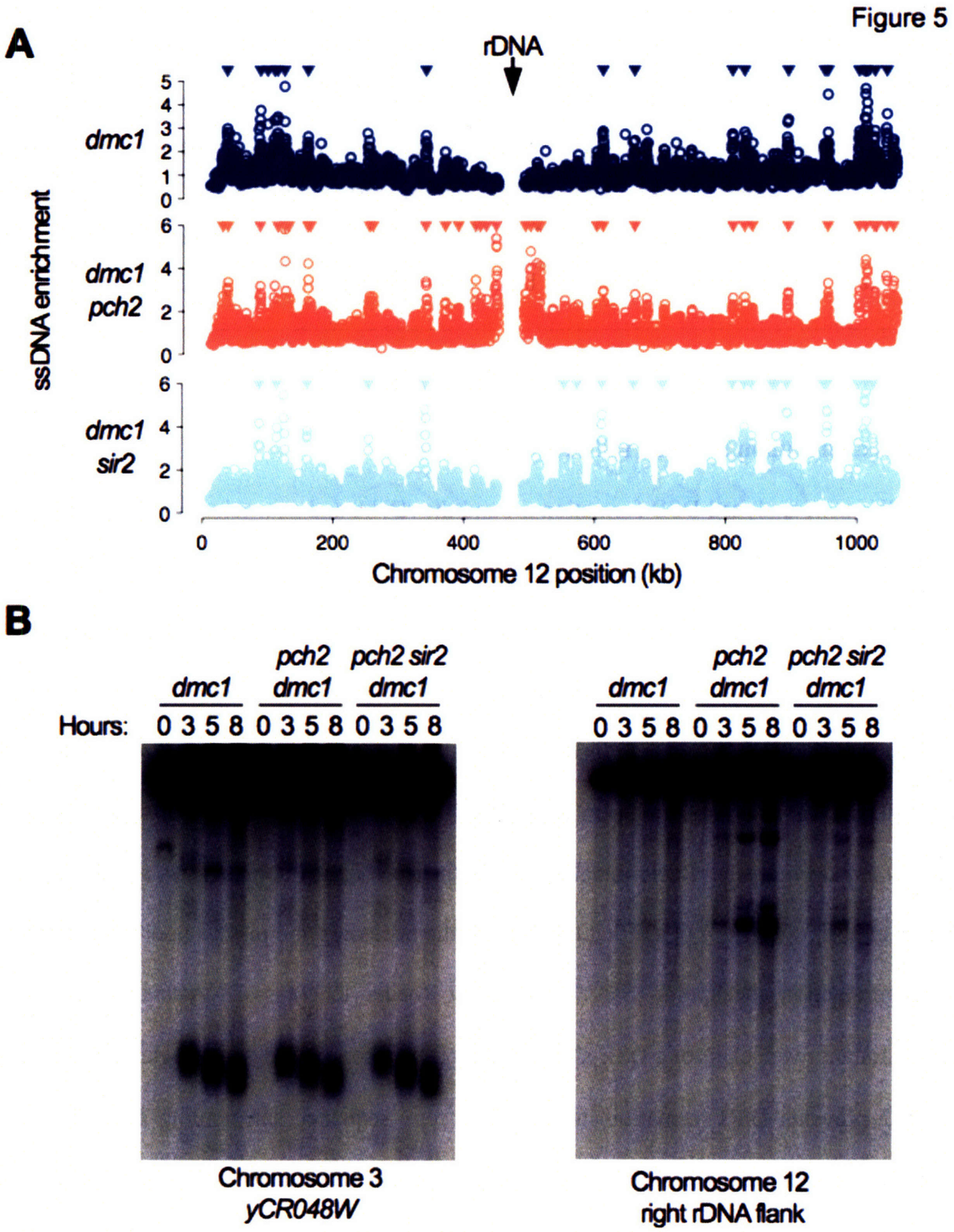

Figure 5: Pch2 silences DSBs near the rDNA

dmc1Δ (NKY1455), *pch2Δ* (YAH2629) and *sir2Δ* (YAH2593) cultures were induced to undergo synchronous meiosis. (A) ssDNA enrichment versus chromosome position was plotted

for chromosome XII for each strain indicated. The position of the rDNA is marked. Inverted triangles indicate statistically significant DSB hotspots.
(B) DNA samples were collected for the indicated strains at the specified timepoints. Probes for *YCR048W* (left panel) and the right rDNA flank (right panel) were used for
Southern blot analysis.

Epistasis analysis by Southern blot revealed that a *pch2Δ sir2Δ dmc1Δ* strain lacked strong DSB activity near to the rDNA (Figure 5B). It is possible that the presence of Sir2 at the rDNA increases DSB activity close to the rDNA, requiring an additional Pch2-dependent mechanism to silence those breaks to prevent recombination within the rDNA.

Recombination at chromosome ends is also prevented, both because the repetitive nature of the sequences at the ends of chromosomes does not favor interhomolog interaction, as well as because cohesin distal to the crossover site is required to hold chromosomes together at meiosis I. We observed a depletion of hotspots within 20 kb of telomeres, where we detected only half, where we detected only half the number of DSB hotspots expected from a random distribution (6 versus 14, Figure 6A), and the mean distance from a telomere to the closest hotspot was 40 kb. Furthermore, when we plotted ssDNA enrichment versus distance from telomere for all data points, we observed a noticeable decrease in overall ssDNA enrichment in the first 20 kb from the telomere (Figure 6B). The 20-kb zone of DSB depletion is much more limited than that of previous studies using *rad50S* or *sae2Δ* mutations that observed depletion of hotspots within 40-100 kb of telomeres (Gerton, DeRisi et al. 2000; Borde, Lin et al. 2004; Mieczkowski, Dominska et al. 2007; Robine, Uematsu et al. 2007). In our analysis of Spo11 binding sites, DSB hotspots were depleted within 40 kb of telomeres, and the mean distance from the telomere to the closest hotspot was 100 kb. We believe that the bias against telomere proximal hotspots in the Spo11

Figure 6

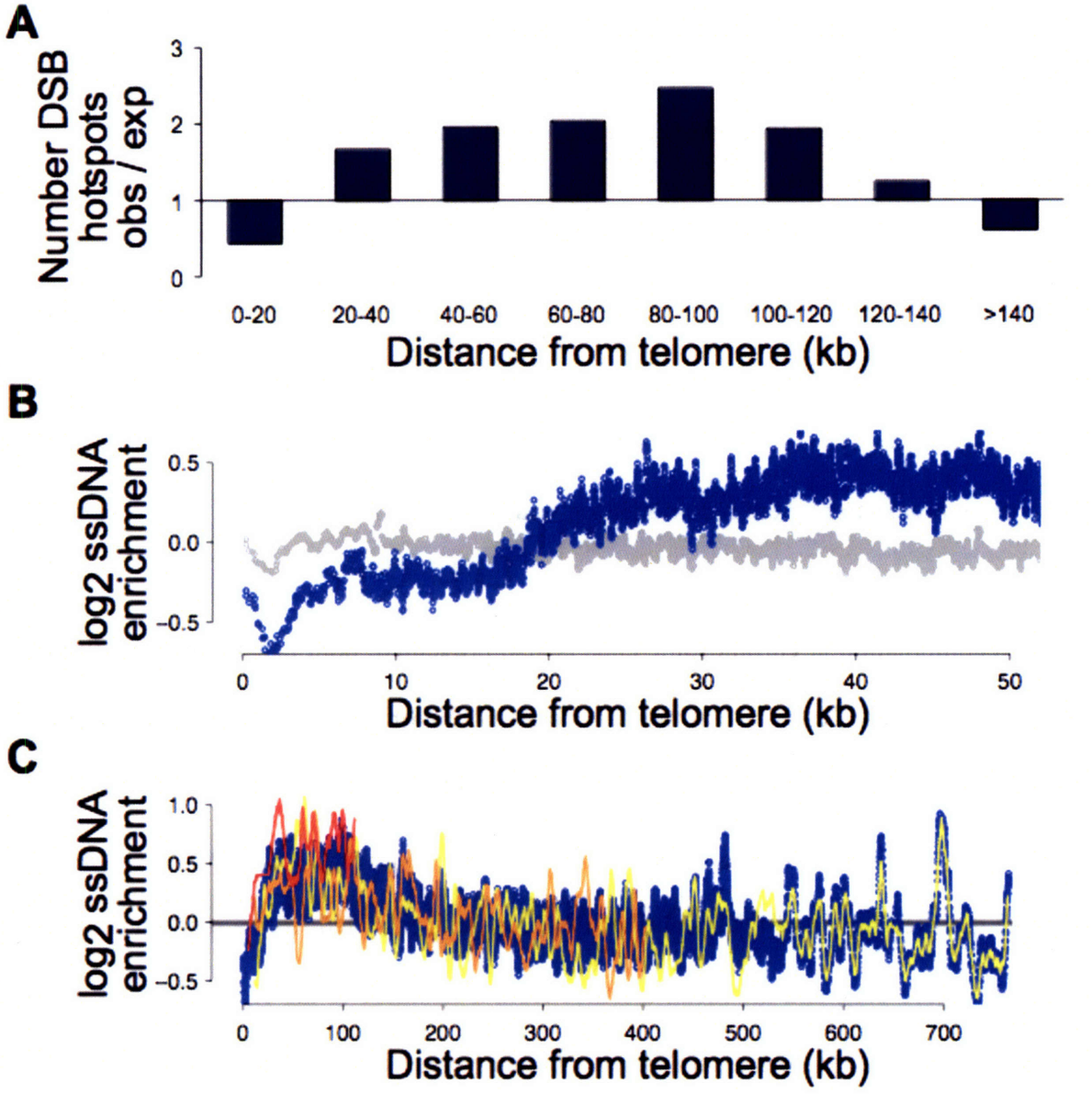

Figure 6: Levels of DSB formation in telomere proximal regions.

(A) The ratio of observed to expected number of DSB hotspot peaks in *dmc1Δ* (NKY1455) is plotted as a function of their distance from the telomere. These data deviated significantly from those expected by a random distribution of the 258 hotspots in the single copy genomic sequence (χ^2, p=1.4E-19). Distance from telomere was defined from the start of annotated single-copy sequence at chromosome ends (SGD; www.yeastgenome.org). (B) The $\log_2$ ratio of ssDNA enrichment signal from all 32 subtelomeric regions was plotted as a function of distance from the telomere; *dmc1Δ* (NKY1455; blue), *spo11-Y135F* (A10914; grey). Data were smoothed by

applying a moving average over 20 consecutive points. (C) As in panel B, except the entire data set for all distances from telomere is shown for *dmc1Δ* (NKY1455; blue). The data points for the individual chromosomes 1 (red line), 2 (orange line) and 4 (yellow line), smoothed by applying a moving average over 40 consecutive points, are overlaid on the total data profile.

ChIP experiments is due to the use of the *rad50S* background. Pulsed-field gel analysis revealed a selective reduction of DSBs near the left telomere of chromosome VIII in *rad50S* mutants (Figure 2B), and similar reduction was also observed for telomere proximal hotspots on chromosome III (Borde, Goldman et al. 2000). The limited 20-kb zone of DSB depletion is supported by both genetic and microarray data that demonstrate a strong reduction of crossover recombination within 25 - 30 kb of telomeres (Su, Barton et al. 2000) (J. Fung, personal communication).

Strikingly, in the region 20-120 kb from a telomere, hotpots mapped using ssDNA analysis were twice as prevalent as expected under a random distribution model (137 versus 68). Southern blot analysis confirmed the existence of telomere proximal hotspots on the left arm of chromosome XVI and on the right arm of chromosome III (*YPL274W*, *YPL255W*, *YPL221W*, *YCR024C-A*; Figure 2A, and data not shown). By contrast, hotspots were underrepresented at regions >120 kb from a telomere, where we detected 115 hotspots instead of the expected 176. A similar trend of telomere proximal enrichment and internal depletion of ssDNA was also observed when we plotted the total ssDNA signal versus distance from telomere for all data points (Figure 6C; blue points). The existence of elevated break levels close to the ends of

chromosomes is supported by recent genetic data in yeast (D. Kaback, J. Fung, personal communications).

The telomere proximal enrichment of ssDNA may underlie a well-known and widely conserved meiotic phenomenon. Work from a number of organisms has shown that small chromosomes receive more crossovers per unit length than large chromosomes (Kaback, Guacci et al. 1992; Copenhaver, Browne et al. 1998; Kong, Gudbjartsson et al. 2002), which may ensure that small chromosomes receive at least one crossover and are thus faithfully segregated during meiosis I. It has been suggested that this size bias is controlled, at least partially, at the level of DSBs, because analysis of Spo11 distribution indicated that small chromosomes had more hotspots per unit length and that these hotspots were "hotter" (Gerton, DeRisi et al. 2000). ssDNA enrichment analysis similarly revealed that the average amount of ssDNA was higher for the smallest chromosomes (Figure 7A). Additionally, the two smallest chromosomes had far more hotspots per unit length as compared to the larger chromosomes (11 and 15 hotspots each, versus the expected 5 and 6, respectively), although this bias did not extend to the other small chromosomes. Remarkably, when we plotted ssDNA enrichment for individual chromosomes, large and small chromosomes alike followed the same pattern of increased levels of DSBs within a 100-kb region near the chromosome ends (Figure 6C, lines). The 20-120 kb window size of increased ssDNA signal was constant for all chromosomes and is almost exactly half the size of the smallest chromosome (230 kb). Thus, the telomere proximal enrichment of ssDNA likely accounts for the increased average ssDNA signal of small chromosomes (Figure 7C), and may ensure that all chromosomes receive sufficient DSBs, regardless of their size.

Figure 7

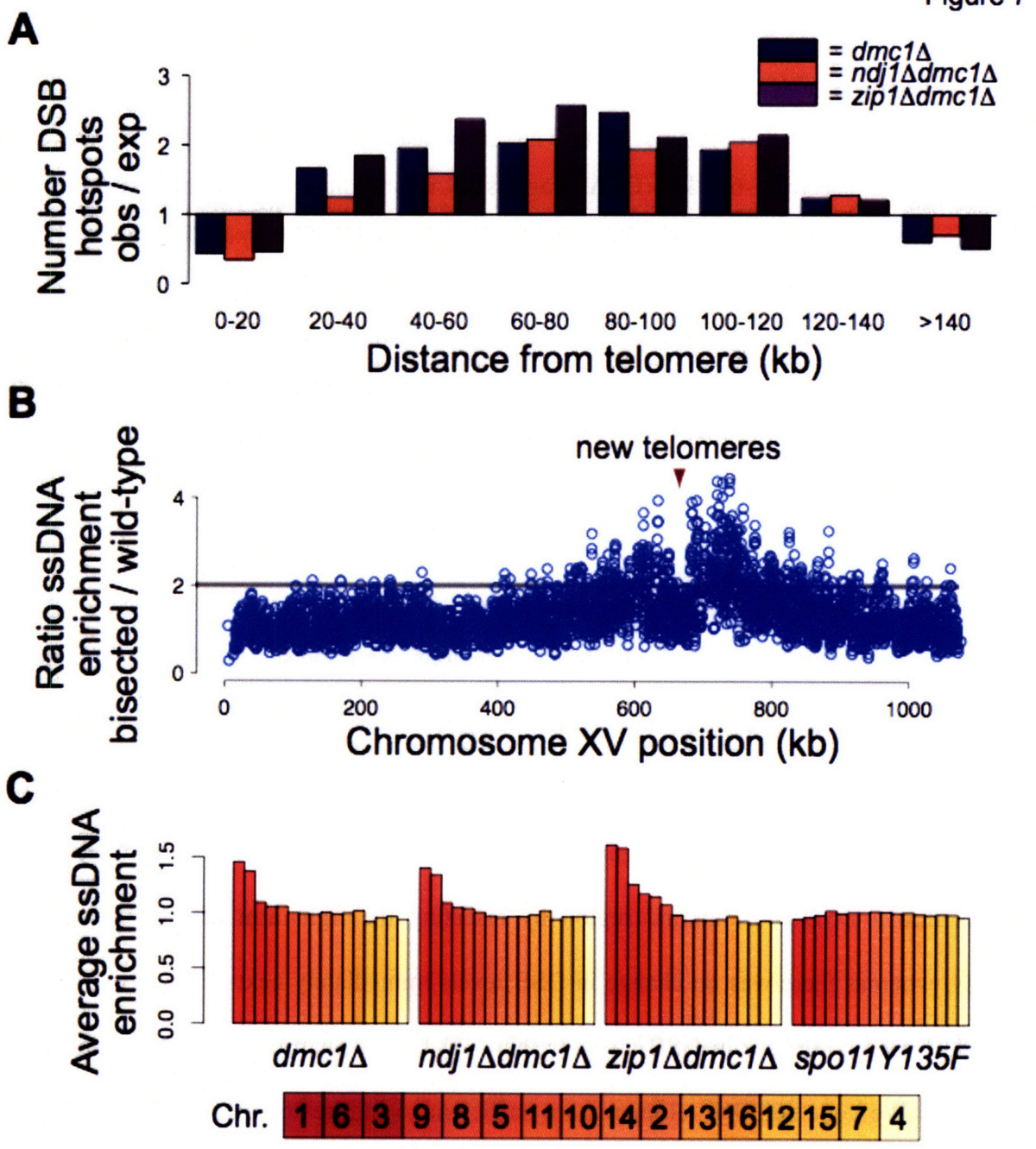

Figure 7: Effects of telomeres on DSB levels.

(A) The ratio of observed to expected number of DSB hotspot peaks is plotted as a function of their distance from the telomere for *dmc1Δ* (NKY1455; blue), *ndj1Δ dmc1Δ* (YAH2626; orange), *zip1Δ dmc1Δ* (YAH2650; purple). These data deviated significantly from those expected by a random distribution of the 258 hotspots in the single copy genomic sequence (χ^2, p=1.4E-19, 4.0E-13 and 2.0E-31, respectively). (B) The ratio of ssDNA enrichment was

calculated for a *dmc1Δ* strain containing a bisected chromosome XV (YAH3112) relative to the wild-type chromosome XV *dmc1Δ* strain (NKY1455). The ratio of ssDNA enrichment (YAH3112/NKY1455) was plotted for chromosome XV. The average ratio of ssDNA enrichment ratio of the two strains is 1. The arrowhead indicates the position where the chromosome was bisected, ~674 kb. (C) Average ssDNA enrichment per chromosome in *dmc1Δ* (NKY1455), *ndj1Δ dmc1Δ* (YAH2626), *zip1Δ dmc1Δ* (YAH2650), *spo11-Y135F* (A10914) cells. Mean ssDNA enrichment signal relative to the mean signal for the entire data set was calculated for all features on each chromosome. For chromosome XII, only the non-rDNA sequences were included in the analysis. Bars representing the normalized average ssDNA enrichment for each chromosome were sorted by chromosome length. Gradient colors correlate with chromosome length.

The observation that the DSB-enriched regions were present near the ends of all chromosomes raised the possibility that the proximity to telomeres induced higher DSB levels in these regions. Alternatively, subtle differences in local DNA sequence composition could lead to elevated DSB formation. To distinguish between these possibilities, we introduced new telomeres into a DSB-poor internal region by bisecting the right arm of chromosome XV. Strikingly, whereas there was no change in DSB levels immediately next to the new telomeres, we found a marked increase in DSB levels within ~20-120 kb from the new chromosome ends (Figure 7B). We conclude that telomeres are sufficient to induce the 100-kb domain of DSB enrichment near chromosome ends.

Chromosomes undergo major structural changes during meiosis that may directly influence large-scale DSB distribution. Around the time of DSB formation, meiotic telomeres congress into a loose cluster conformation known as the bouquet (Scherthan 2001). The bouquet

later disperses and chromosomes become associated with the highly structured protein lattice of the synaptonemal complex (SC) (Zickler 2006). To test whether bouquet formation or the SC affect large-scale DSB distribution, we analyzed the requirement for two factors, *NDJ1*, a telomeric protein necessary for bouquet formation (Chua and Roeder 1997; Conrad, Dominguez et al. 1997; Trelles-Sticken, Dresser et al. 2000), and *ZIP1*, a central component of the SC that also plays a role in maintaining crossover interference (Sym, Engebrecht et al. 1993; Sym and Roeder 1994; Bishop and Zickler 2004). Disruption of *NDJ1* had no apparent effect on DSB hotspot distribution (Supplemental Figure 1). Like *dmc1Δ* cells, *ndj1Δ dmc1Δ* mutants demonstrated a biased hotspot distribution, with depletion in a 20-kb window near telomeres and enrichment outside that zone (Figure 7A). Furthermore, small chromosomes still exhibited increased ssDNA signal in *ndj1Δ dmc1Δ* mutants (Figure 7C). Similarly, deletion of *ZIP1* had no clear effect on hotspot distribution or the depletion of DSBs within 20 kb of telomeres (Supplemental Figure 1 and Figure 7A), although we did notice a slight increase in the DSB signal of small chromosomes in *zip1Δ dmc1Δ* mutants (Figure 7C). We conclude that the telomere proximal distribution of DSBs is largely independent of bouquet formation and the SC.

Discussion

In this study we present a method for detecting DSB-associated ssDNA that can reliably predict DSB hotspots in both wild-type and mutant cells. Remarkably, we observed substantial DSBs formation within the pericentromeric regions. Because interhomolog repair is suppressed around centromeres, our findings indicate a specialized mode of DSB repair in those regions. In addition, analysis of ssDNA profiles revealed that telomeres induce elevated levels of DSBs

within a broad zone from 20-120 kb from chromosome ends. This distribution of DSBs suggests a mechanism to ensure that chromosomes of all sizes receive a minimum number of DSBs.

ssDNA derived hotspot profiles differ noticeably from the profiles obtained by mapping Spo11-associated DNA. We believe that this difference is a consequence of the *rad50S*-type mutations used to trap Spo11 at DSB sites, which alters the pattern of meiotic DSB formation (Dresser, Ewing et al. 1997; Borde, Goldman et al. 2000; Blat, Protacio et al. 2002). Although not all hotspots are affected, we demonstrate that many DSB hotspots close to telomeres and centromeres are substantially less active in *rad50S* mutants. At this point it is unclear why only some hotspots are sensitive to *rad50S*-type mutations. The fact that *rad50S* is epistatic to *dmc1Δ* with respect DSB distribution argues against the possibility that DSBs at *rad50S*-sensitive hotspots are turned over more rapidly (Dresser, Ewing et al. 1997). Rather, it appears that these breaks never form. It is possible that feedback mechanisms halt DSB formation as aberrant DSBs accumulate in *rad50S* mutants. Alternatively, there could be limiting levels of factors that are not recycled when Spo11 is not released. In either case one would predict that *rad50S*-sensitive hotspots form DSBs later than hotspots not affected by this mutation.

Remarkably, we found that DSB levels around centromeres are much higher than predicted from the low rates of meiotic recombination in these regions. For example, quantification of the Southern signal at the *YDR001C* hotspot (Figure 4B, middle panel), indicated that 7.8±1.8% of chromosomes receive a DSB at this site. *YDR001C* lies between *CEN4* and the well-characterized centromere-linked marker *TRP1* (*YDR007W*). Assuming that *YDR001C* is the only major hotspot between these two markers, we would expect a genetic

distance between *CEN4* and *TRP1* of ~7.5 cM (see Methods), substantially more than the 0.3-0.5 cM observed in mapping studies (www.yeastgenome.org). Therefore, crossover repair can only account for about 5% of repair at *YDR001C*. Interestingly, repair from the homolog without strand exchange (non-crossover repair) is thought to be similarly reduced in pericentromeric regions (Lambie and Roeder 1988). These data strongly suggest that centromeric DSBs are less frequently repaired by homolog-directed DSB repair than breaks in other parts of the genome.

Our results indicate that an alternate pathway governs DSB repair around centromeres. The fact that centromeric DSBs accumulate in the absence of the Dmc1 recombinase, argues that these breaks are not repaired by non-homologous end joining, but rather by homologous recombination. Because Dmc1 is required for both meiotic inter-homolog and inter-sister repair (Schwacha and Kleckner 1997), we favor the possibility that pericentromeric DSBs are repaired using the sister chromatid as the preferred repair template. Inter-sister repair normally accounts for only ~20% of the DSB repair events during meiotic recombination (Haber, Thorburn et al. 1984; Schwacha and Kleckner 1997). However, meiotic DSBs within the repetitive rDNA array are almost exclusively repaired from the sister chromatid (Petes and Pukkila 1995). A similar meiotic inter-sister repair bias may exist around centromeres. Interestingly, the abundance of Red1, a lateral element component that prevents meiotic inter-sister repair, is selectively reduced near *CEN3* (Blat, Protacio et al. 2002). It is tempting to speculate that local depletion of Red1 allows inter-sister repair around centromeres. Alternatively, the high concentration of cohesin complexes at centromeres and/or a distinct subunit composition of centromeric cohesin complexes, as observed in *S. pombe* (Kitajima, Yokobayashi et al. 2003), could also influence DSB repair in the pericentromeric regions.

The distribution of meiotic DSB hotspots is regulated on multiple levels. Locally, DSBs are known to occur almost exclusively in intergenic regions containing promoters, although not all promoter regions receive DSBs (Wu and Lichten 1994; Baudat and Nicolas 1997; Petes 2001). Our results point to a role of transcriptional activation in promoting DSB formation, because we observed an enrichment of highly expressed genes at hotspots. However, studies of the *HIS4* associated hotspot suggest it may not be transcription of these genes *per se* that is necessary for hotspot activity (White, Dominska et al. 1993). Instead, transcription factors and histone modifications associated with transcriptional activation may contribute to a chromatin environment that provides accessibility to DSB factors (Petes 2001; Maleki and Keeney 2004). High GC content was also implicated in the regulation of DSB formation (Gerton, DeRisi et al. 2000; Birdsell 2002; Mieczkowski, Dominska et al. 2006). We found that the GC content of intergenic regions containing DSB hotspots was higher than average (37.87% versus 35.35%, Student's t-test, p=2.2x10E-16). However, this correlation could be driven, at least in part, by the fact that DSB hotspots are overrepresented in promoter-containing and larger intergenic regions, both of which have higher than average GC content.

In addition to local regulation, DSBs formation is also controlled regionally, in particular near chromosome ends. We observed two very defined regions near telomeres; the distal-most ~20 kb of single-copy sequence were largely devoid of hotspots, whereas the next ~100 kb exhibited higher levels of DSB formation than in the rest of the genome. How might this DSB distribution be regulated? The depletion of DSBs within 20 kb of telomeres may be, at least partially, a *cis* effect of the repeat-rich DNA sequences found in immediate proximity of yeast

subtelomeric regions, because DSB formation remains low when these sequences are moved to more internal positions (Barton, Su et al. 2003). By contrast, we could induce DSB-rich 100-kb regions ectopically on chromosome XV by introducing new telomeres. This effect argues against a role of the local DNA sequence in establishing the 100-kb regions, and would be consistent with the spreading of a trans-acting factor from chromosome ends. Sir-dependent heterochromatin has been reported to affect 4-16 kb of single copy sequence at chromosome ends (Renauld, Aparicio et al. 1993) and may control DSB formation. Interestingly, deletion of the *SIR2* gene not only leads to an increase in DSBs near telomeres, but also to a decrease in DSB formation in the region 10 – 120 kb from the telomeres (Mieczkowski, Dominska et al. 2007), which is very similar to the domain in which we observe increased DSB activity. It may be worth reinvestigating the role of telomeric heterochromatin in regulating DSB activity using ssDNA enrichment, since this method provides increased sensitivity in detection of telomere proximal DSBs. Finally, although we have excluded a role for bouquet formation or the SC, it remains a possibility that other aspects of nuclear architecture such as chromosomal position with respect to the nuclear periphery or the nucleolus may influence the regional distribution of DSBs.

Small chromosomes exhibit higher relative levels of crossover formation than large chromosomes (Kaback, Guacci et al. 1992; Copenhaver, Browne et al. 1998; Kong, Gudbjartsson et al. 2002). We propose that this effect is driven, at least in part, by the telomere-induced increase in DSB formation near chromosome ends, which has a proportionally stronger influence on small chromosomes. A localized increase in DSB formation can also explain why a recent report analyzing genetic recombination on translocated chromosomes failed to find a

chromosome-size effect. The analyzed telomere proximal intervals did not change their position with respect to the 100-kb domains (Turney, de Los Santos et al. 2004). Theoretical work has suggested the existence of two pathways that control crossover distribution (Stahl, Foss et al. 2004). The major pathway is under the control of crossover interference, a chromosome-size dependent mechanism that functions to distribute crossovers evenly along chromosomes. In addition, a minor interference-independent pathway was postulated that leads to roughly equal amounts of crossovers on all chromosomes, independent of their size (Stahl, Foss et al. 2004). Because the telomere proximal domains lead to a chromosome-size independent increase in DSB formation, we speculate that these domains function in such an interference-independent pathway of crossover formation. In this respect, our observation that *zip1Δ dmc1Δ* mutants exhibit somewhat increased levels of DSB formation on small chromosomes is interesting, because disruption of *MSH4*, which acts in the same epistasis group as *ZIP1* (Borner, Kleckner et al. 2004), leads to an increase in crossover recombination specifically on small chromosomes (Stahl, Foss et al. 2004). This observation raises the possibility that the increase in recombination in *msh4* mutants occurs at the level of DSB formation and supports the idea that the DSB-enriched domains near telomeres function in the interference-independent pathway of crossover formation.

In humans, average recombination rates of small chromosomes are about twice as high as those of large chromosomes (Kong, Gudbjartsson et al. 2002). It is possible that similar regions of increased DSB formation exist near the ends of human chromosomes. Because ssDNA is thought to be a universal intermediate of homologous recombination, adaptations of the method presented here should permit the mapping and analysis of meiotic DSB hotspots in other eukaryotes, including mice and humans.

Acknowledgments

This work was carried out in equal collaboration with Andreas Hochwagen. We are grateful to N. Kleckner, A. Amon and F. Klein for providing strains. We thank J. Falk for technical assistance, and M. de Vries, A. Amon, and T. Orr-Weaver for helpful discussions and critical reading of the manuscript. We are indebted to M. Lichten, J. Fung, and D. Kaback for sharing data prior to publication.

Materials and Methods

Strains and Growth Conditions

Strains used in this study are isogenic to SK1 and are listed in Supplemental Table 1. *dmc1::ARG4*, *zip1::LYS*, *spo11-Y135F-HA::URA3*, and *SPO11-18MYC* were described previously (Bishop, Park et al. 1992; Sym, Engebrecht et al. 1993; Cha, Weiner et al. 2000; Prieler, Penkner et al. 2005). *ndj1::KanMX* and *pch2::KanMX* were transferred from the EUROSCARF deletion collection into SK1 using a PCR-based approach. *sir2::TRP1* was created using plasmid SPB841 (L. Guarente, unpublished). Diploid *sir2::TRP1/sir2::TRP1* were made using a covering plasmid containing SIR2 and URA3, which was subsequently removed by growth on FOA. To induce synchronous meiosis, strains were pre-inoculated at OD_{600} = 0.3 in BYTA medium (50mM potassium phthalate, 1% yeast extract, 2% bactotryptone, 1% potassium acetate), grown for 16 hours at 30°C, washed twice, and resuspended at OD_{600} = 1.9 in SPO medium (0.3% potassium acetate).

ssDNA Isolation

ssDNA isolation was based on a method described in (MacAlpine, Perlman et al. 1998). For each time point, ~10^9 cells were fixed in 70% ethanol at –20°C. Cells were spheroplasted in sorbitol buffer (1M sorbitol, 1% beta-mercaptoethanol, 0.2 mg/ml zymolyase 100T, 0.1M EDTA, pH 7.4). Spheroplasts were lysed in NDS (0.6% SDS, 300mM EDTA, 10mM Tris.HCl, pH 9.5) and DNA deproteinated with proteinase K (0.25mg/ml; Roche) at 50°C. DNA was twice purified by extraction with phenol:chloroform:isoamylalcohol, precipitated with isopropanol, treated with RNase A, and stored in TE (1mM EDTA, 10mM Tris.HCl, pH 7.5) at 4°C. Vortexing was avoided at all points to limit shearing of DNA. 25 μg DNA were digested to completion using EcoRI (New England Biolabs). ssDNA was enriched by batch absorption to BND cellulose (Huberman, Spotila et al. 1987).

Microarray detection of ssDNA

1.5 μg each of 0 hr and 3 or 5 hr ssDNA samples were labeled with Cy3-dUTP or Cy5-dUTP (Amersham Biosciences, Piscataway, NJ; GE Healthcare) by random priming without denaturation using 4 μg random nonamer oligo (IDT) and 10 units of Klenow (New England Biolabs, Beverly, MA). Unincorporated dye was removed using microcon columns (30-kDa MW cutoff, Millipore, Bedford, MA), and samples were co-hybridized to custom Agilent arrays (Wilmington, DE) using a standard protocol. See NCBI GEO for a complete description of arrays. For each set of experiments a dye swap was performed on experimental replicates.

Spo11 localization

20 mls of cells were harvested after 5 hours in sporulation media. Spo11 chromatin immunoprecipitation was performed as described (Aparicio, Weinstein et al. 1997), except without cross-linking in formaldehyde. $1/10^{th}$ of the lysate was removed as an input sample. Spo11-myc was immunoprecipitated using 2 μg 9E11 (Abcam) for 16 hours at 4 degrees. 1/2 of the immunoprecipitated DNA and $1/10^{th}$ of the input DNA were labeled with Cy3-dUTP and

Cy5-dUTP by random priming as described above for ssDNA, except that the DNA was denatured for 5 minutes at 95 degrees prior to the extension reaction. Unincorporated dye was removed as above. For each experiment, a dye swap was performed on experimental replicates.

Microarray data analysis

For each cohybridization, Cy3 and Cy5 levels were calculated using Agilent Feature Extractor CGH software. Background normalization, $\log_2$ ratios for each experiment and scale normalizations across each set of duplicated experiments were calculated using the sma package (Yang, Dudoit et al. 2001) in R, a computer language and environment for statistical computing (v2.1.0, http://www.r-project.org). All data sets in this chapter have been deposited in the NCBI Gene Expression Omnibus (http://www.ncbi.nlm.nih.gov/geo/), and are accessible through GEO Series accession number GSE9503.

DSB sites were defined as >3 proximal points on the chromosome with p-values<0.125 (using pnorm function in R) in each of 2 independent experiments. The DSB site was defined as a merged region from the start to end of all significant data points, while the peak was plotted at the location of the maximum ssDNA signal after smoothing by applying a moving average across 5 consecutive chromosomal features. For peak comparisons within high-density data sets, DSB sites were defined as the same if any of the enriched points were identical. For comparison to data sets by Gerton, et al. and Borde, et al. (Gerton, DeRisi et al. 2000; Borde, Lin et al. 2004), DSB sites were defined as the same if the ssDNA DSB region was within 2 kb of the detected Spo11 site.

Metagene analysis was conducted similarly to previous reports (Pokholok, Harbison et al. 2005). To align data for individual genes, all features in the upstream, coding or downstream regions genes overlapping any portion of a significant peak in the *dmc1Δ* dataset were assigned to a bin representing relative position. To compare across genes, *dmc1Δ* ssDNA enrichment $\log_2$ ratios for all features associated with each gene were mean-normalized, hierarchically clustered and displayed as a heatmap using Java TreeView. The mean enrichment ratio was calculated for each bin to produce the composite ssDNA enrichment profile.

To assess %GC content while controlling for sequence length, %GC content was calculated for each 100bp windows for all genomic intergenic regions. The average %GC content and the total distribution of %GC content for all 100bp windows was calculated for all intergenics and for all intergenics containing a DSB hotspot peak.

Other Techniques

Southern analysis was performed as described in (Hunter and Kleckner 2001). DNA fragments were separated in 0.6% agarose/1X TBE gels and blotted onto Hybond-XL membranes (GE Healthcare) using alkaline transfer. Southern signals were quantified using a Fujifilm BAS-2500 image reader V1.8 and Multi Gauge V2.2 software. Pulsed field gel electrophoresis and Southern analysis of chromosome III were performed as described in (Baudat and Nicolas 1997).

Supplemental Table 1: Strains

Name	Genotype	Reference
NKY1551	*MATa/α, ho::LYS2/ho::LYS2, lys2/lys2, ura3/ura3, leu2::hisG/leu2::hisG, arg4-nsp/arg4-bgl, his4X-LEU2-URA3/his4B-LEU2*	(Storlazzi, Xu et al. 1995)
NKY1455	Same as NKY1551, but *dmc1::ARG4/dmc1::ARG4*	(Bishop, Park et al. 1992)
A10914	Same as NKY1551, but *spo11-Y135F-HA::URA3/ spo11-Y135F-HA::URA3*	This study
A11675	Same as NKY1551, but *rad50S::URA3/rad50S::URA3*	(Hochwagen, Tham et al. 2005)
YAH2487	*MATa/α, ho::LYS2/ho::LYS2, lys2/lys2, ura3/ura3, leu2::hisG/leu2::hisG, his3::hisG/his3::hisG, rad50S::URA3/rad50S::URA3, SPO11-18MYC::TRP1/SPO11-18MYC::TRP1*	This study
YAH2626	Same as NKY1455, but *ndj1::KanMX/ndj1::KanMX*	This study
YAH2650	Same as NKY1455, but *zip1::LYS2/zip1::LYS2*	This study
YAH3112	*MATa/α, ho::LYS2/ho::LYS2, lys2/lys2, ura3/ura3, leu2::hisG/leu2::hisG, arg4-nsp/arg4-bgl, his4B-LEU2/his4B-LEU2, Chr15(673,979)::URA3::TEL/ Chr15(673,979)::URA3::TEL, TEL::CEN4::Chr15(674,000)/ TEL::CEN4::Chr15(674,000)*	This study

Supplemental Figure 1: Meiotic ssDNA profiles for all chromosomes

As in Figure 1, the average ssDNA enrichment for wild-type (NKY1551), *dmc1Δ* (NKY1455), *ndj1Δ dmc1Δ* (YAH2626), *zip1Δ dmc1Δ* (YAH2650) and *spo11-Y135F* (A10914) strains and the average Spo11 enrichment from chromatin-immunoprecipitaiton for *SPO11-18myc rad50S* (YAH2487) were plotted versus chromosome position for each chromosome. For each experiment, the features for which the p value <0.125 in two independent experiments are indicated by colored symbols. Statistically significant DSB sites (see materials and methods) are indicated by inverted triangles.

Supplemental Figure 2: Hotspots on chromosome III in *dmc1Δ* and *rad50S* mutants.

As in Figure 2B, hotspot distribution on chromosome III was determined by pulsed-field gel electrophoresis and Southern blot. The same probe was used as in Figure 1C.

Supplemental Figure 3: Centromere proximal DSB hotspots

As in Figure 3A, the average ssDNA enrichment for *dmc1Δ* (NKY1455) cells is plotted versus chromosome position +/- 25 kb from each centromere. Statistically significant DSB sites are indicated by inverted triangles and black dots indicate the centromere position.

Supplemental Figure 4: Centromere proximal DSB hotspots in WT cells

Analysis was carried out identically to Figure 3, but in wild-type (NKY1551) cells. (A) The average ssDNA enrichment for is plotted versus chromosome position for the window of +/- 25 kb for *CEN2*. *CEN4* and *CEN15*. Black dots indicate the centromere position and inverted triangles indicate DSB sites confirmed by Southern blot. (B) Southern blot analysis for *CEN2*, *CEN4* and *CEN15* was conducted as described in Figure 3B.

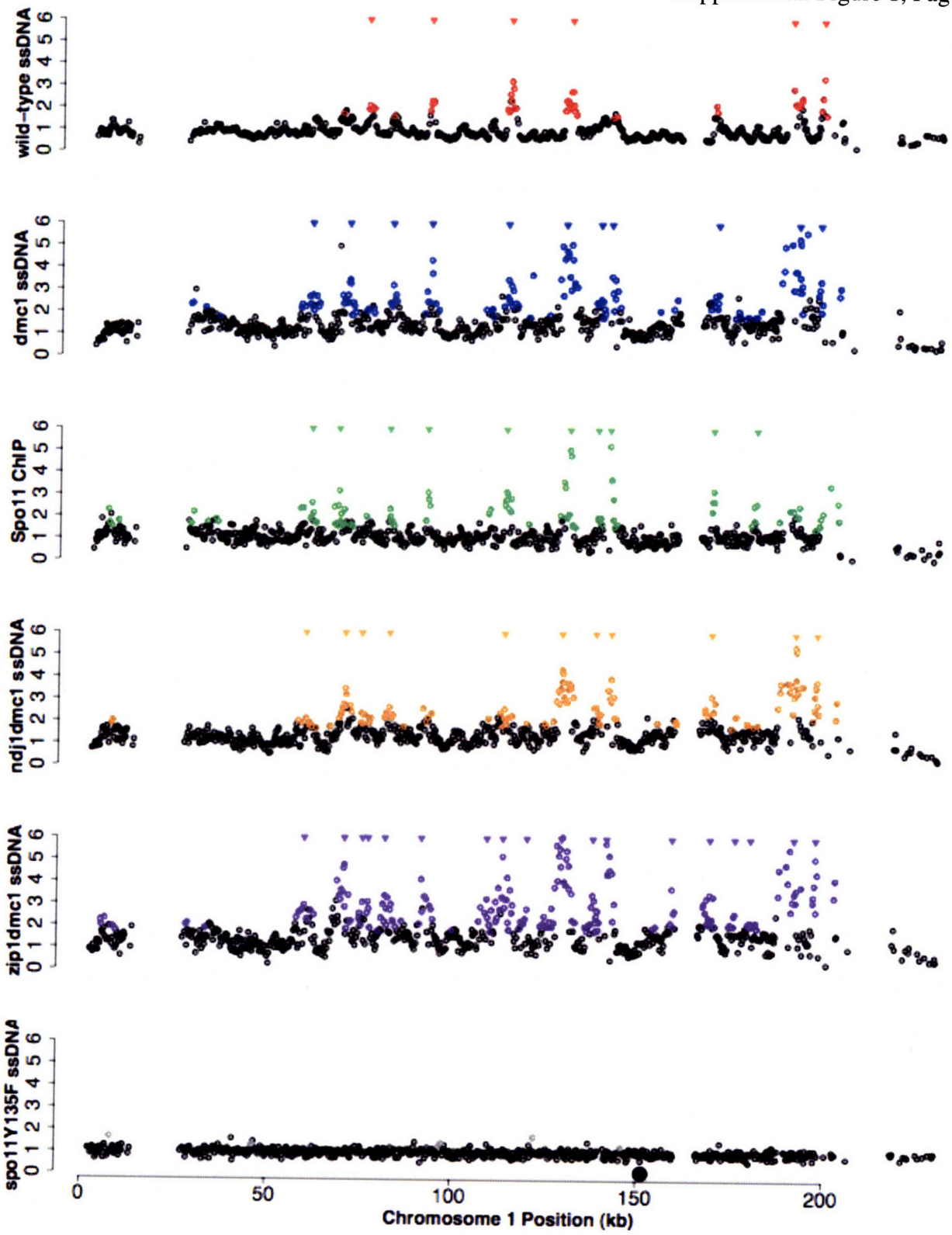
wild-type ssDNA
0 1 2 3 4 5 6
dmc1 ssDNA
0 1 2 3 4 5 6
Spo11 ChIP
0 1 2 3 4 5 6
ndj1dmc1 ssDNA
0 1 2 3 4 5 6
zip1dmc1 ssDNA
0 1 2 3 4 5 6
spo11Y135F ssDNA
0 1 2 3 4 5 6
0
50
100
150
200
Chromosome 1 Position (kb)

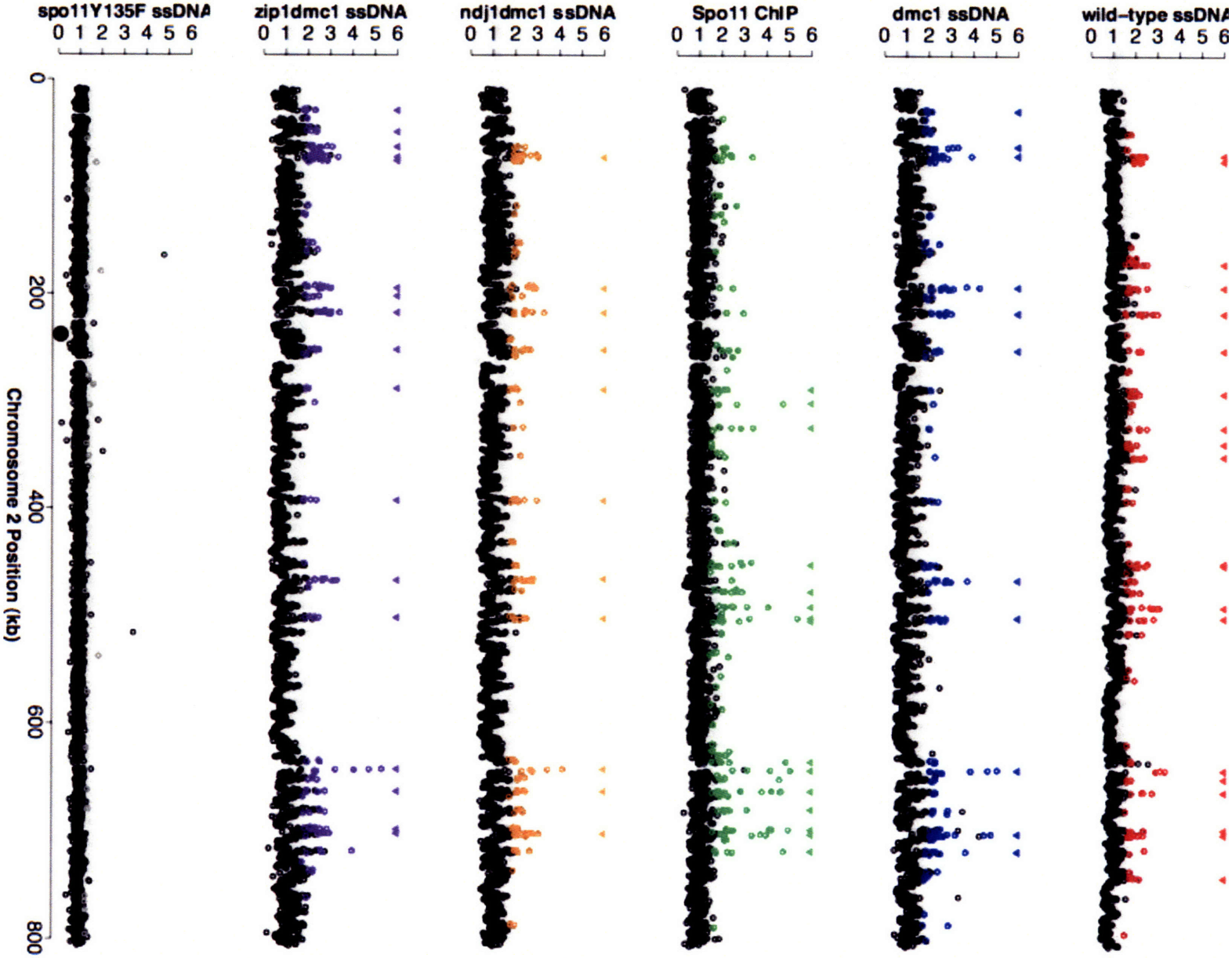
spo11Y135F ssDNA
zip1dmc1 ssDNA
ndj1dmc1 ssDNA
Spo11 ChIP
dmc1 ssDNA
wild-type ssDNA
0 1 2 3 4 5 6
0
200
400
600
800
Chromosome 2 Position (kb)

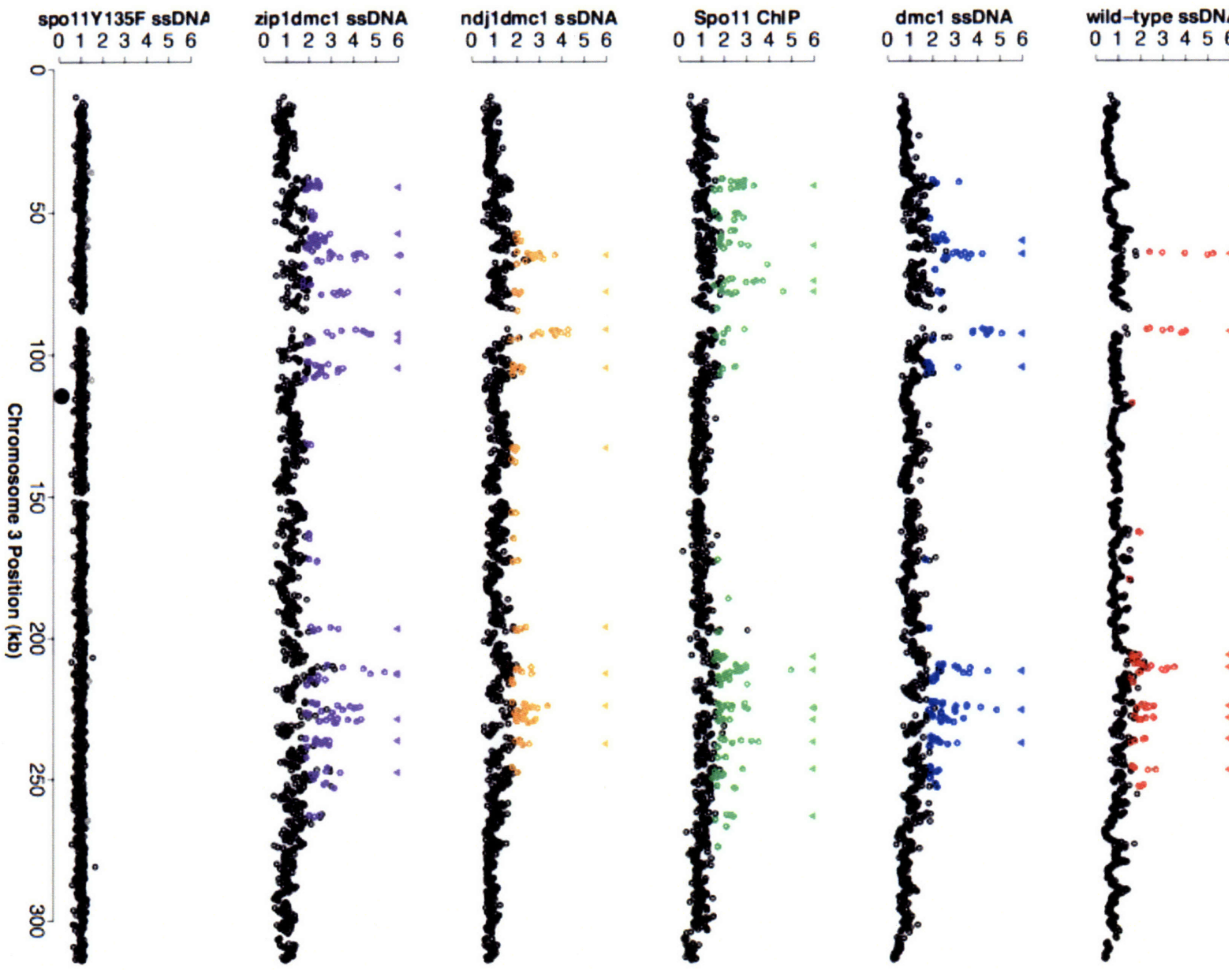
spo11Y135F ssDNA
zip1dmc1 ssDNA
ndj1dmc1 ssDNA
Spo11 ChIP
dmc1 ssDNA
wild-type ssDNA
0 1 2 3 4 5 6
Chromosome 3 Position (kb)
0
50
100
150
200
250
300

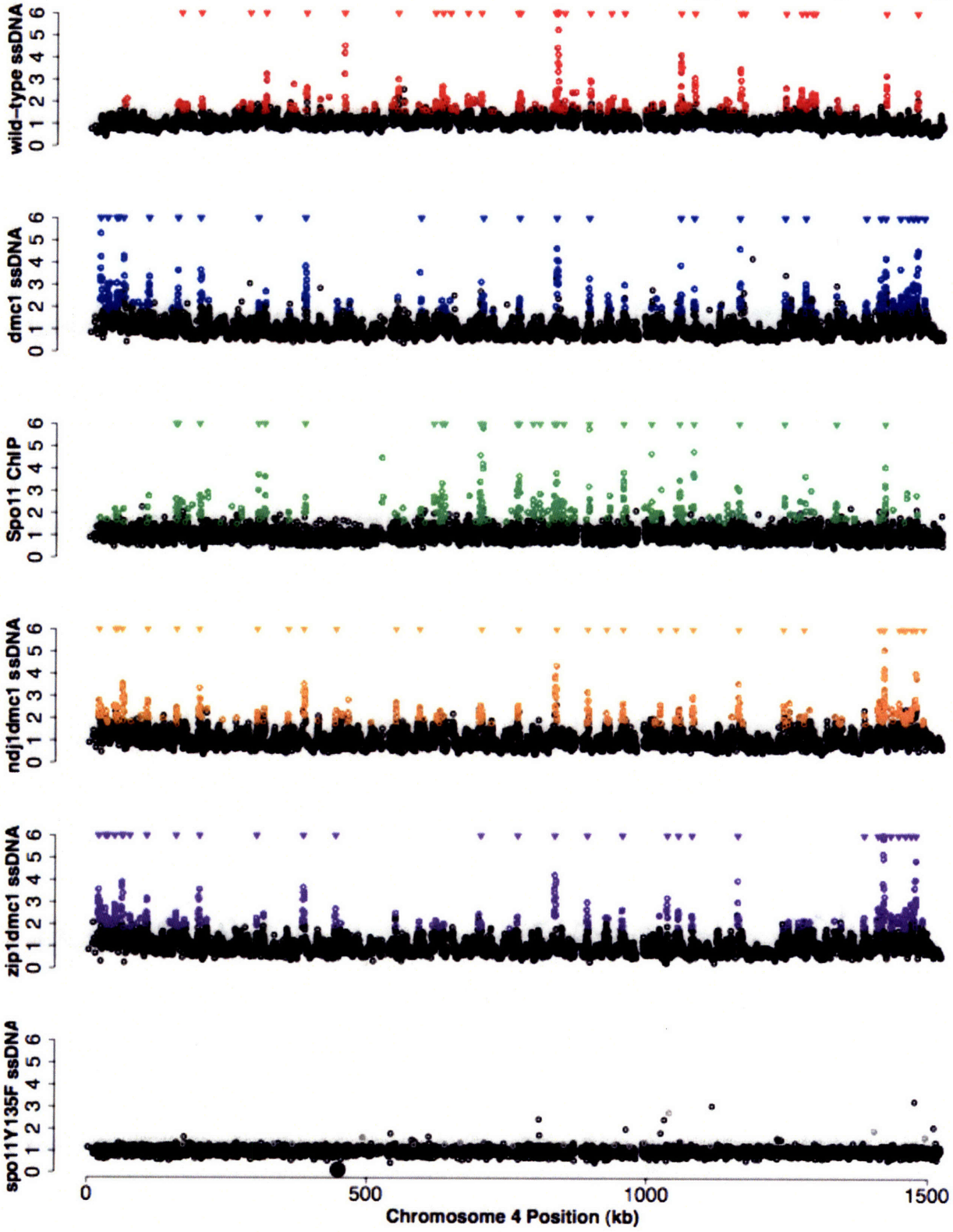
wild-type ssDNA
0 1 2 3 4 5 6
dmc1 ssDNA
0 1 2 3 4 5 6
Spo11 ChIP
0 1 2 3 4 5 6
ndj1dmc1 ssDNA
0 1 2 3 4 5 6
zip1dmc1 ssDNA
0 1 2 3 4 5 6
spo11Y135F ssDNA
0 1 2 3 4 5 6
0
500
1000
1500
Chromosome 4 Position (kb)

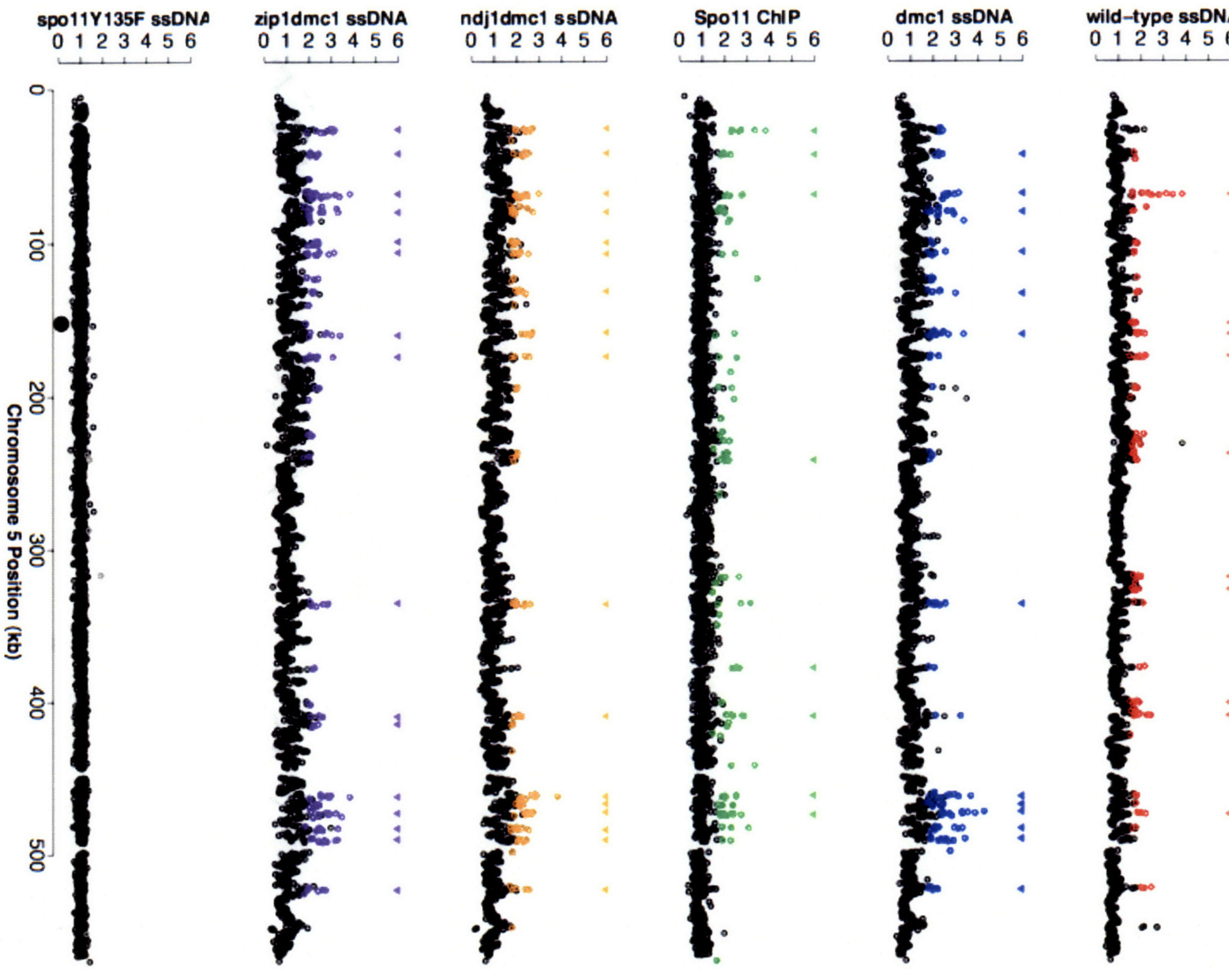
spo11Y135F ssDNA
zip1dmc1 ssDNA
ndj1dmc1 ssDNA
Spo11 ChIP
dmc1 ssDNA
wild-type ssDN
0 1 2 3 4 5 6
0
100
200
300
400
500
Chromosome 5 Position (kb)

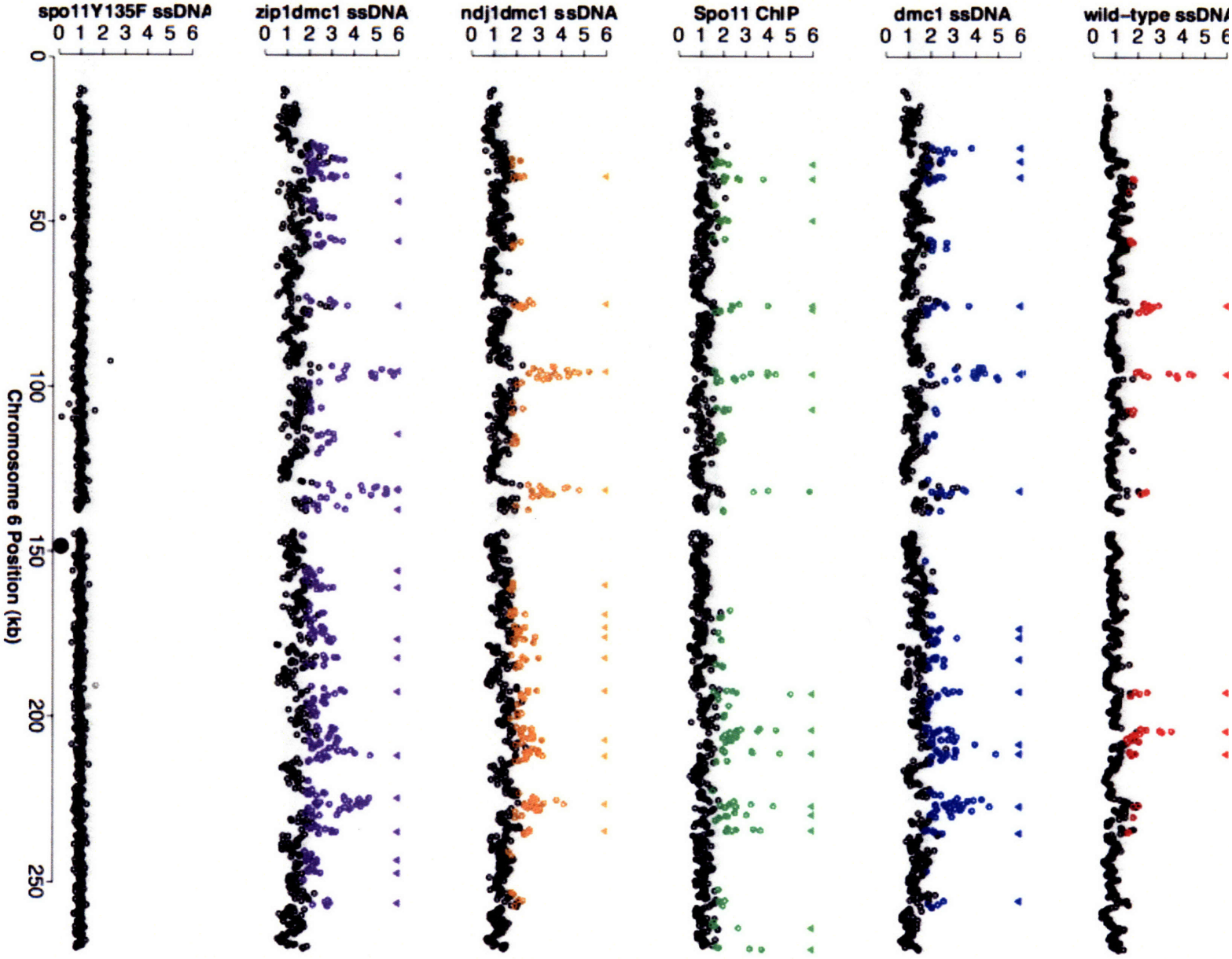
spo11Y135F ssDNA
zip1dmc1 ssDNA
ndj1dmc1 ssDNA
Spo11 ChIP
dmc1 ssDNA
wild-type ssDNA
0 1 2 3 4 5 6
0
50
100
150
200
250
Chromosome 6 Position (kb)

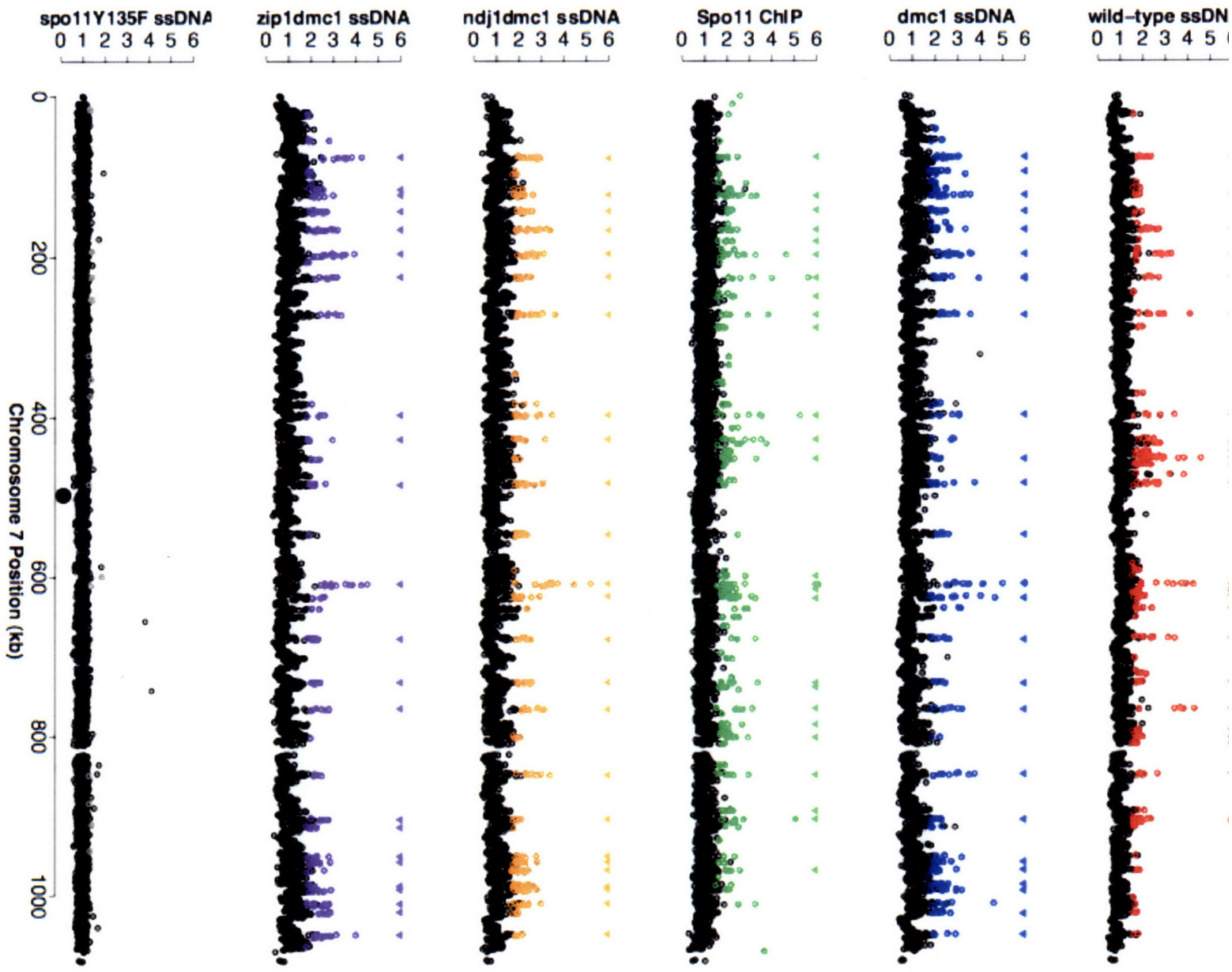
spo11Y135F ssDNA
zip1dmc1 ssDNA
ndj1dmc1 ssDNA
Spo11 ChIP
dmc1 ssDNA
wild-type ssDN
0 1 2 3 4 5 6
0
200
400
600
800
1000
Chromosome 7 Position (kb)

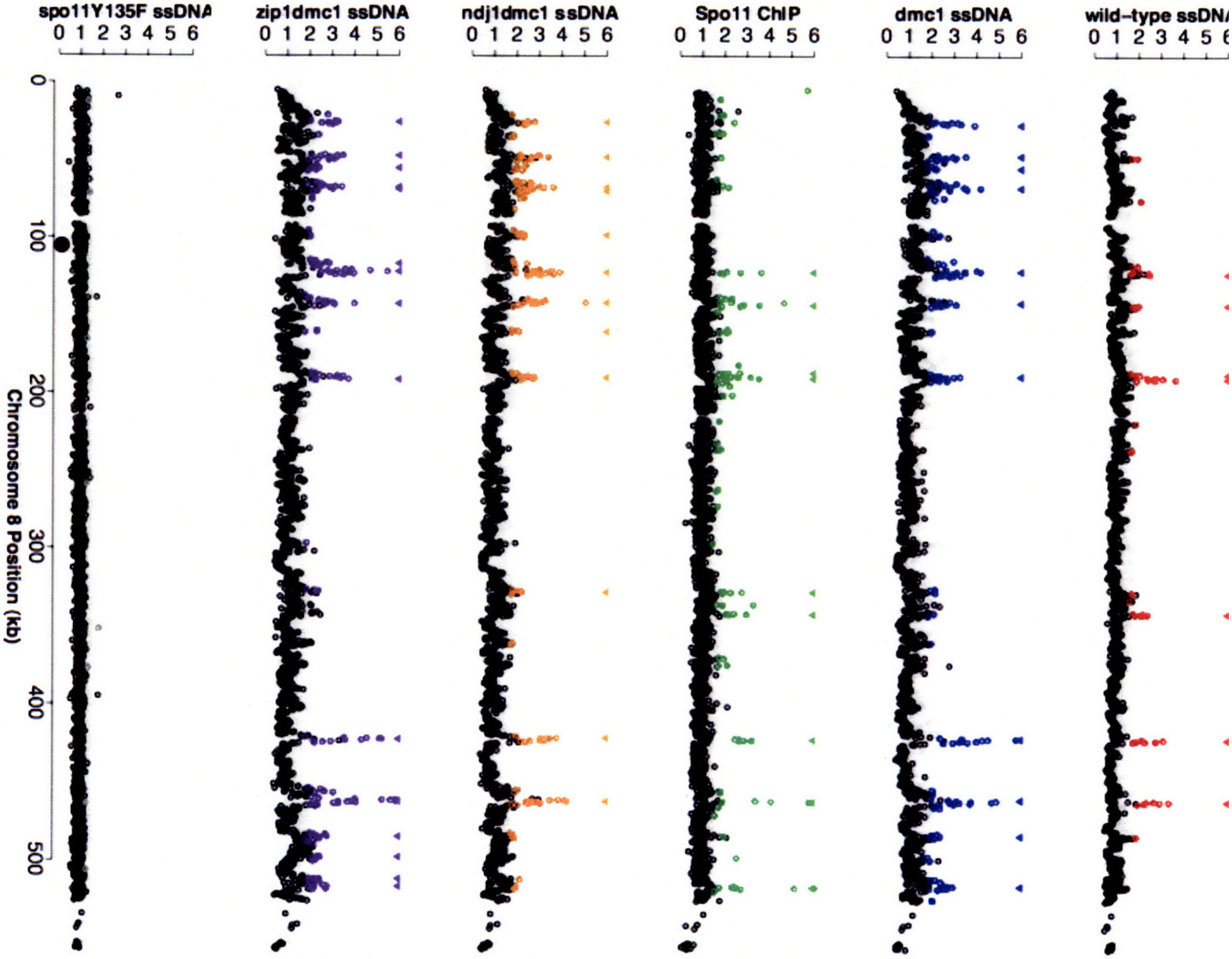
spo11Y135F ssDNA
zip1dmc1 ssDNA
ndj1dmc1 ssDNA
Spo11 ChIP
dmc1 ssDNA
wild-type ssDNA
0 1 2 3 4 5 6
0
100
200
300
400
500
Chromosome 8 Position (kb)

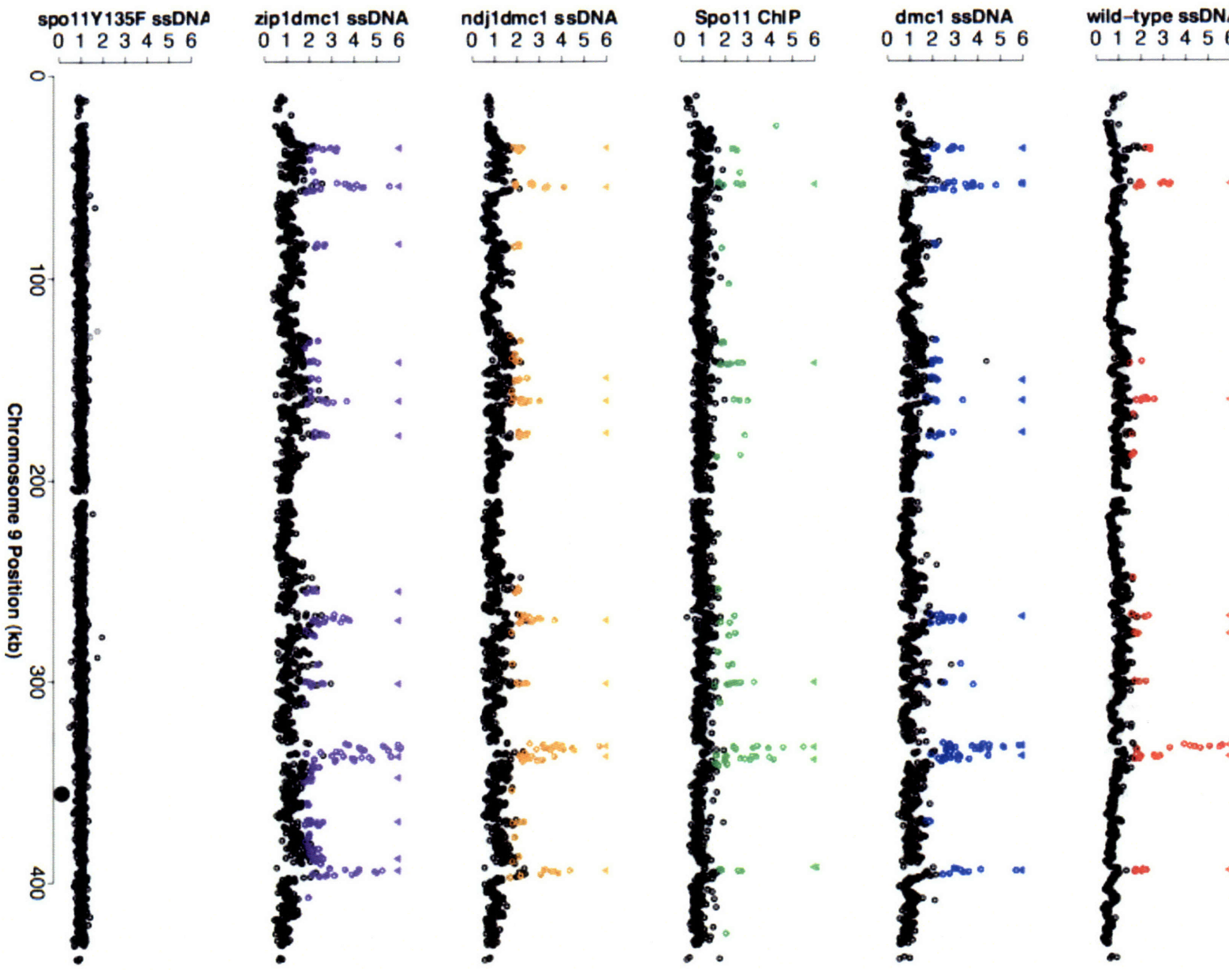
spo11Y135F ssDNA
zip1dmc1 ssDNA
ndj1dmc1 ssDNA
Spo11 ChIP
dmc1 ssDNA
wild-type ssDNA
0 1 2 3 4 5 6
0
100
200
300
400
Chromosome 9 Position (kb)

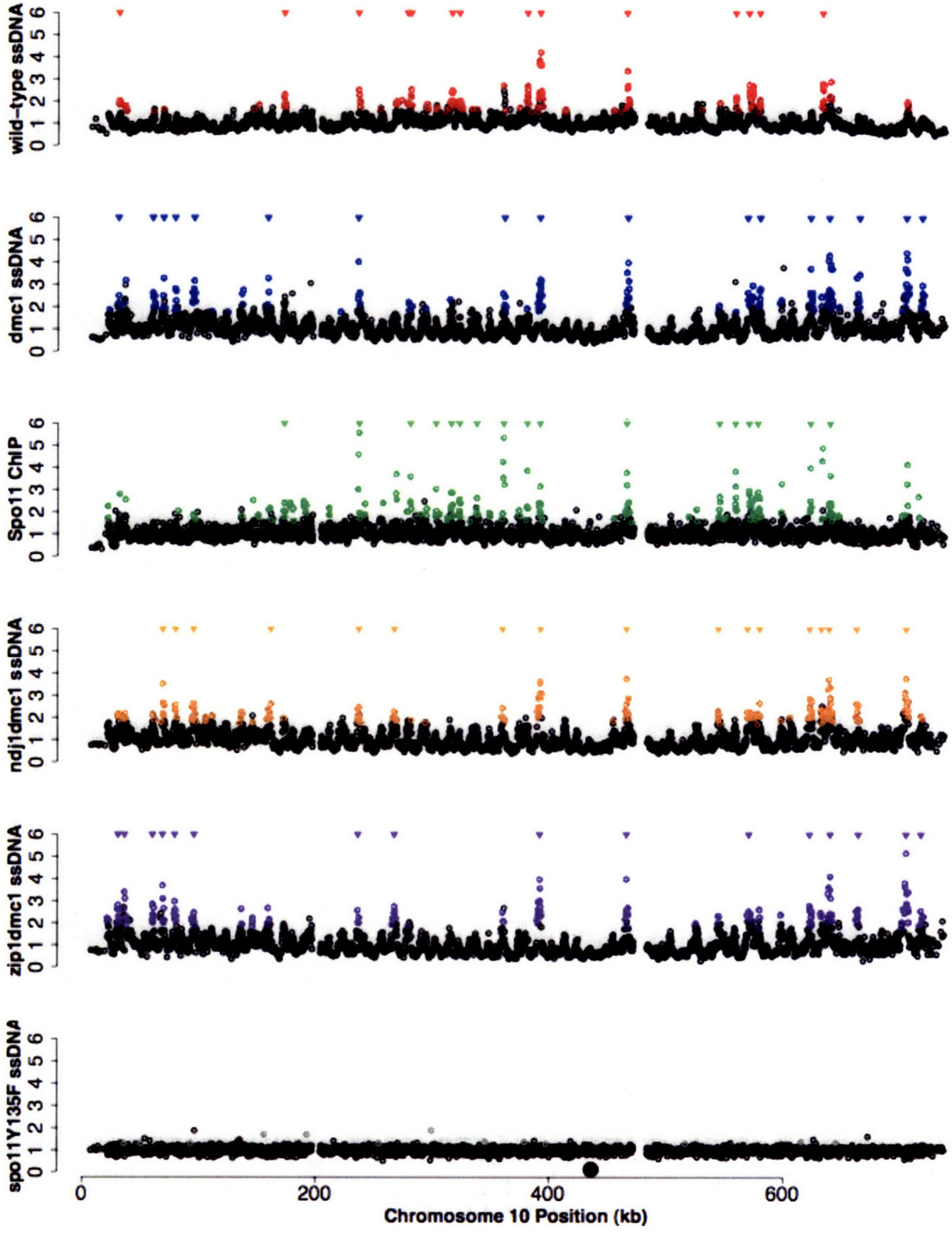
wild−type ssDNA
dmc1 ssDNA
Spo11 ChIP
ndj1dmc1 ssDNA
zip1dmc1 ssDNA
spo11Y135F ssDNA
0 1 2 3 4 5 6
0
200
400
600
Chromosome 10 Position (kb)

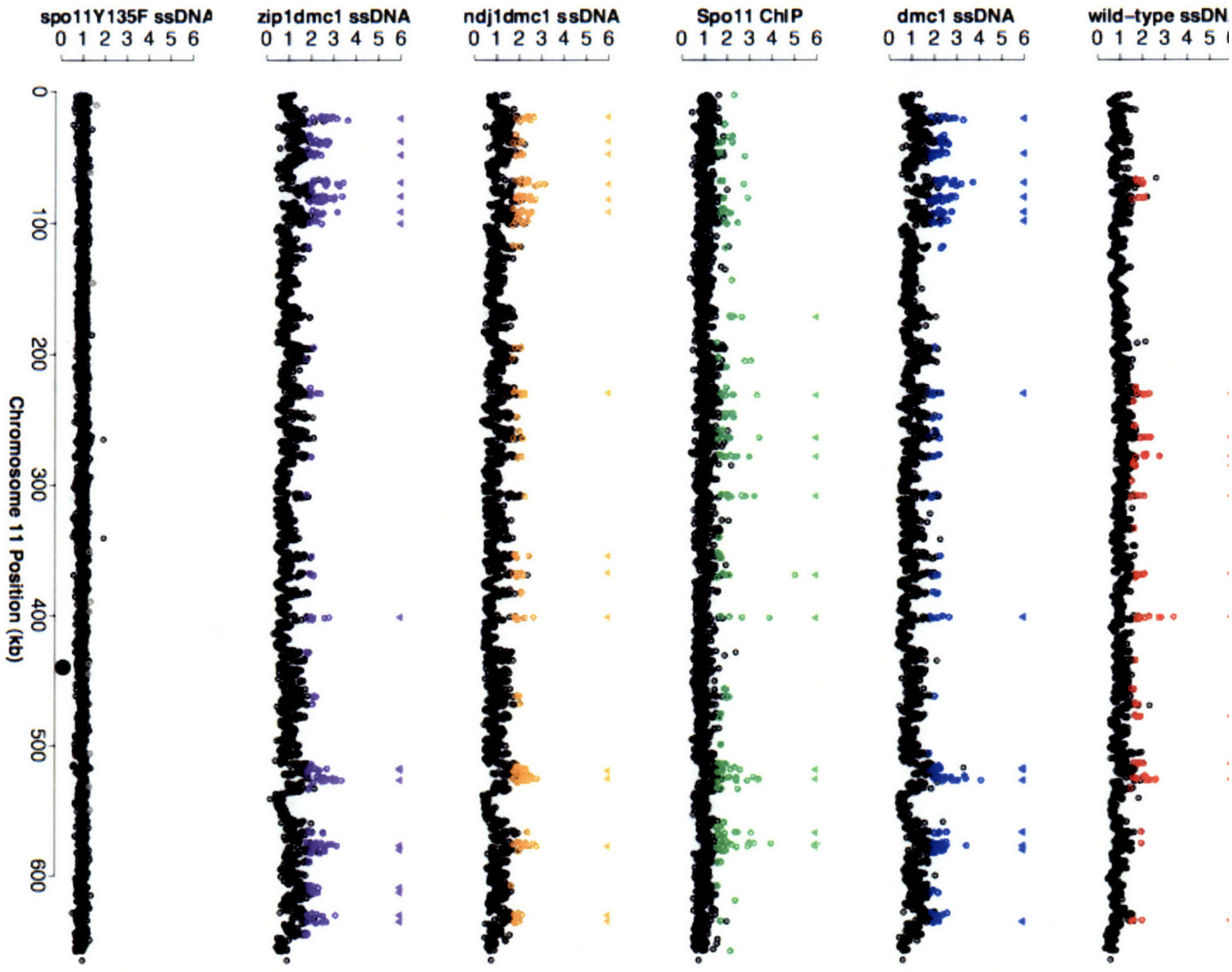
spo11Y135F ssDNA
zip1dmc1 ssDNA
ndj1dmc1 ssDNA
Spo11 ChIP
dmc1 ssDNA
wild-type ssDN
0 1 2 3 4 5 6
Chromosome 11 Position (kb)
0
100
200
300
400
500
600

spo11Y135F ssDNA
zip1dmc1 ssDNA
ndj1dmc1 ssDNA
Spo11 ChIP
dmc1 ssDNA
wild-type ssDNA
0 1 2 3 4 5 6
0
200
400
600
800
1000
Chromosome 12 Position (kb)

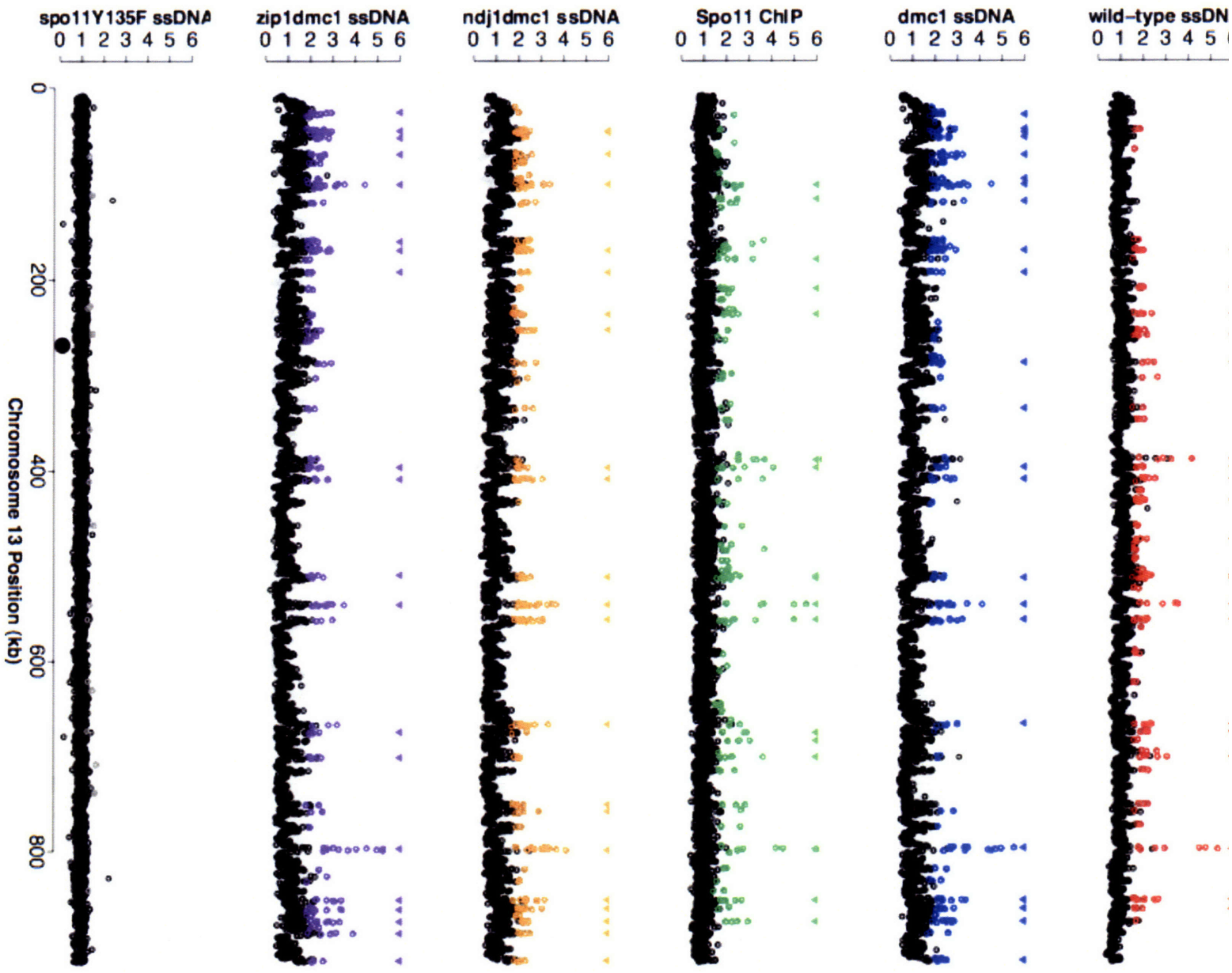
spo11Y135F ssDNA
zip1dmc1 ssDNA
ndj1dmc1 ssDNA
Spo11 ChIP
dmc1 ssDNA
wild-type ssDN
0 1 2 3 4 5 6
0
200
400
600
800
Chromosome 13 Position (kb)

spo11Y135F ssDNA
zip1dmc1 ssDNA
ndj1dmc1 ssDNA
Spo11 ChIP
dmc1 ssDNA
wild-type ssDNA
0 1 2 3 4 5 6
0
200
400
600
800
Chromosome 14 Position (kb)

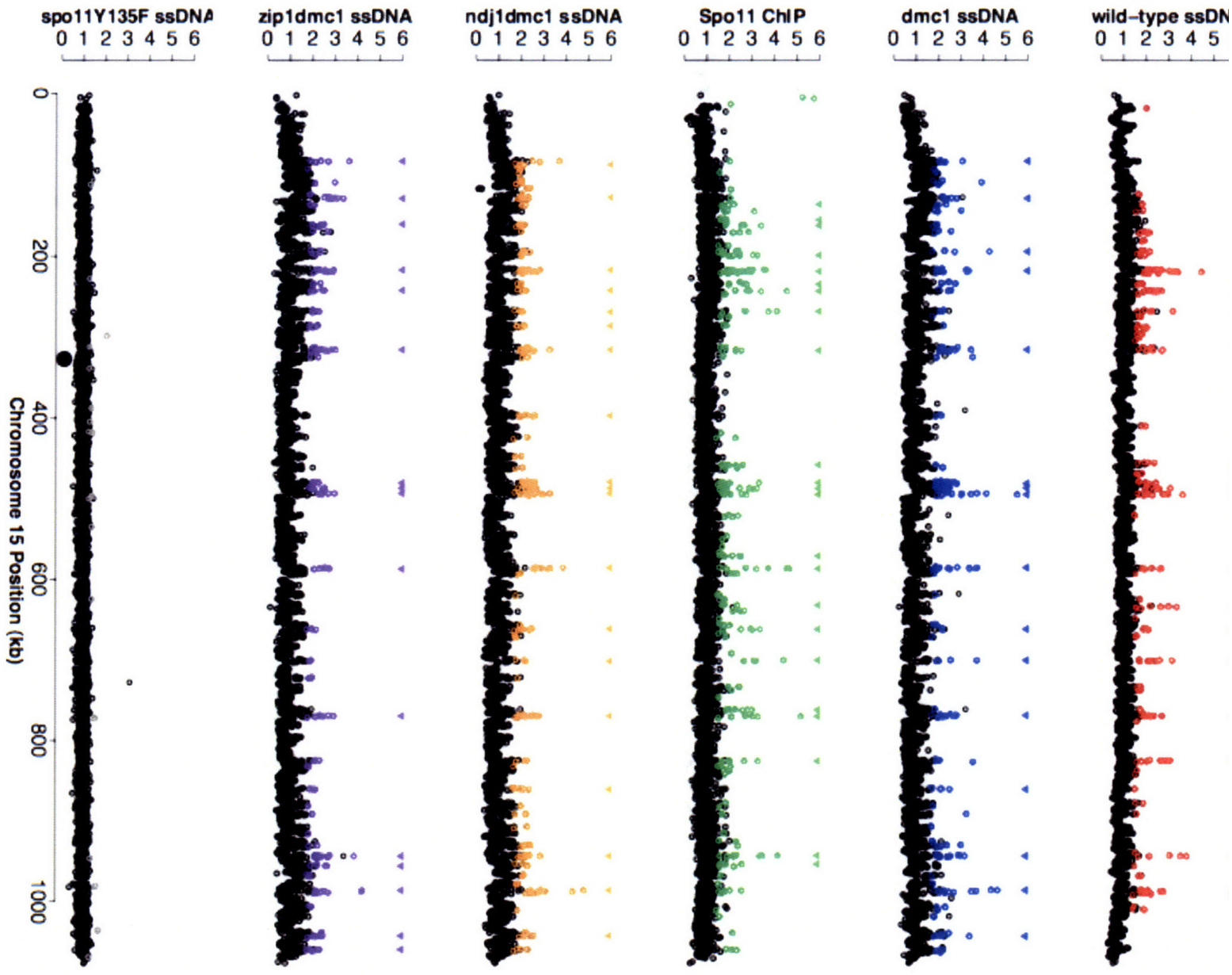
spo11Y135F ssDNA
zip1dmc1 ssDNA
ndj1dmc1 ssDNA
Spo11 ChIP
dmc1 ssDNA
wild-type ssDN
0 1 2 3 4 5 6
0 1 2 3 4 5
0
200
400
600
800
1000
Chromosome 15 Position (kb)

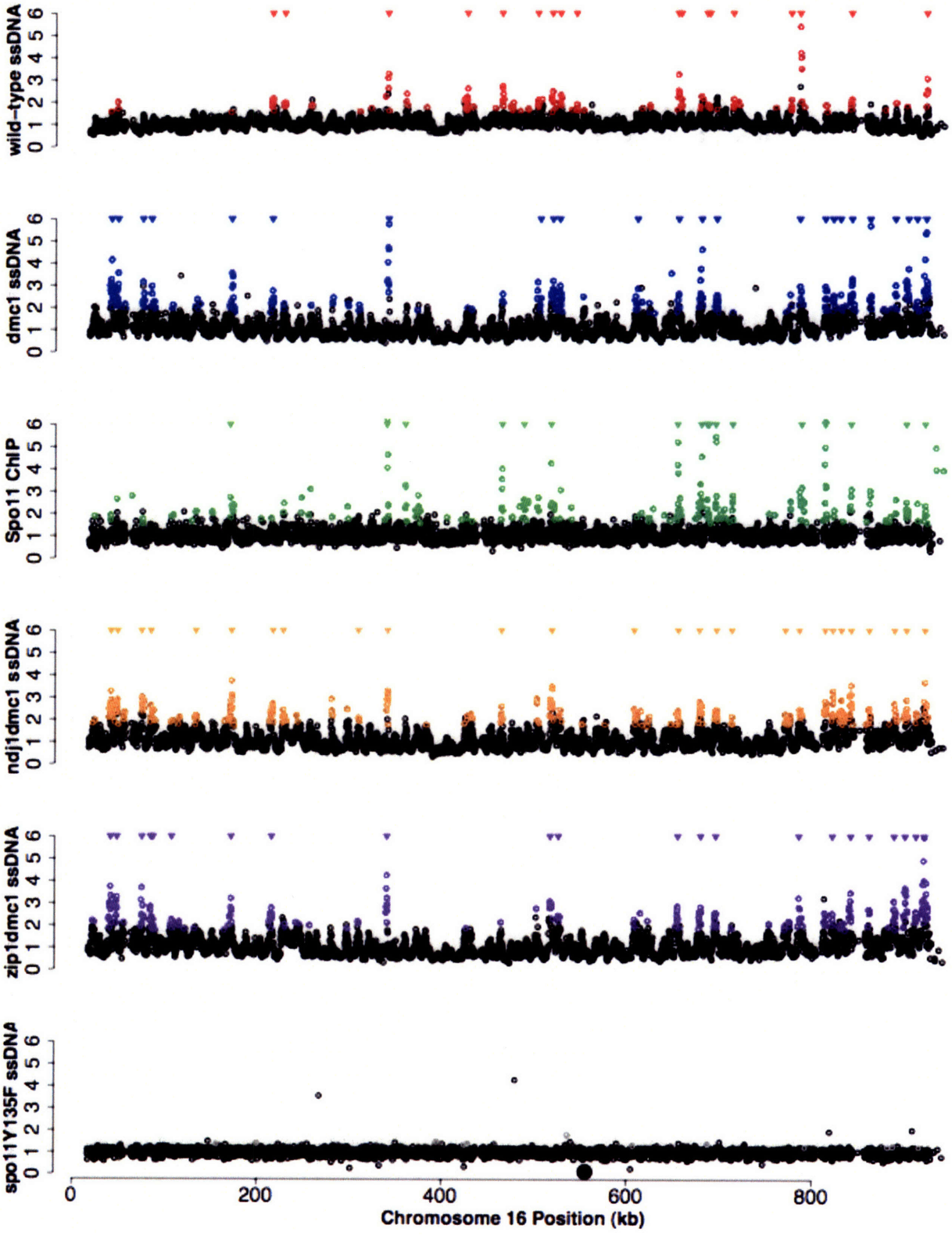
wild-type ssDNA
dmc1 ssDNA
Spo11 ChIP
ndj1dmc1 ssDNA
zip1dmc1 ssDNA
spo11Y135F ssDNA
0 1 2 3 4 5 6
0
200
400
600
800
Chromosome 16 Position (kb)

Supplemental Figure 2

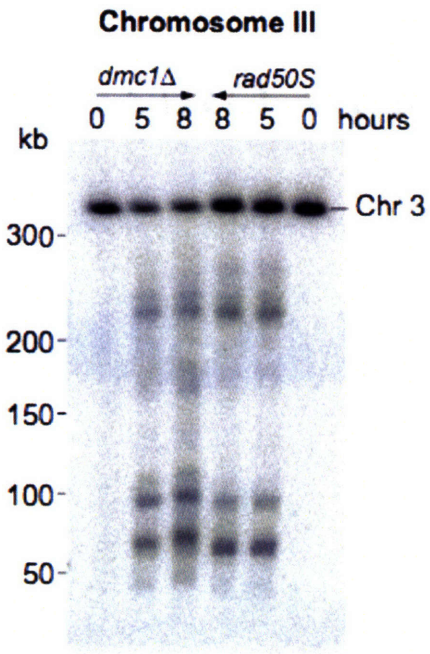

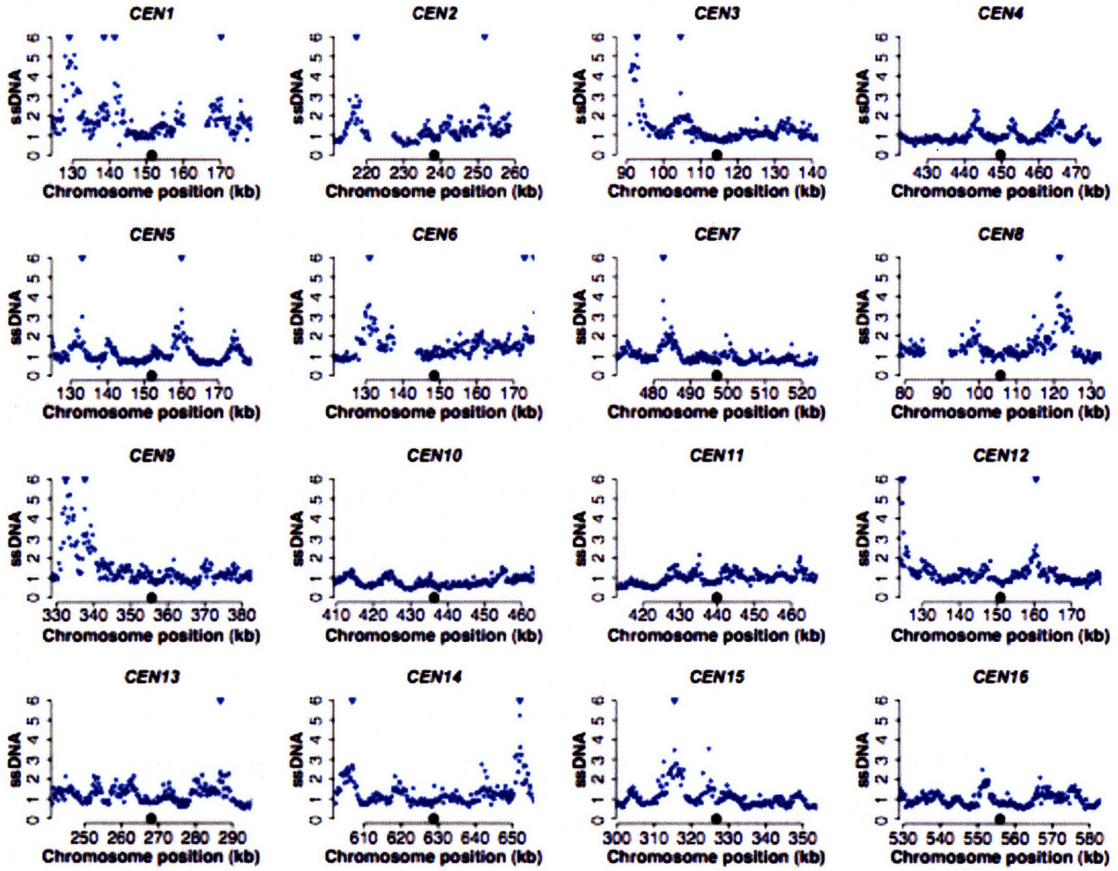
CEN1
CEN2
CEN3
CEN4
CEN5
CEN6
CEN7
CEN8
CEN9
CEN10
CEN11
CEN12
CEN13
CEN14
CEN15
CEN16
ssDNA
0 1 2 3 4 5 6
130 140 150 160 170
220 230 240 250 260
90 100 110 120 130 140
430 440 450 460 470
130 140 150 160 170
480 490 500 510 520
80 90 100 110 120 130
330 340 350 360 370 380
410 420 430 440 450 460
420 430 440 450 460
130 140 150 160 170
250 260 270 280 290
610 620 630 640 650
300 310 320 330 340 350
530 540 550 560 570 580
Chromosome position (kb)

Supplemental Figure 4

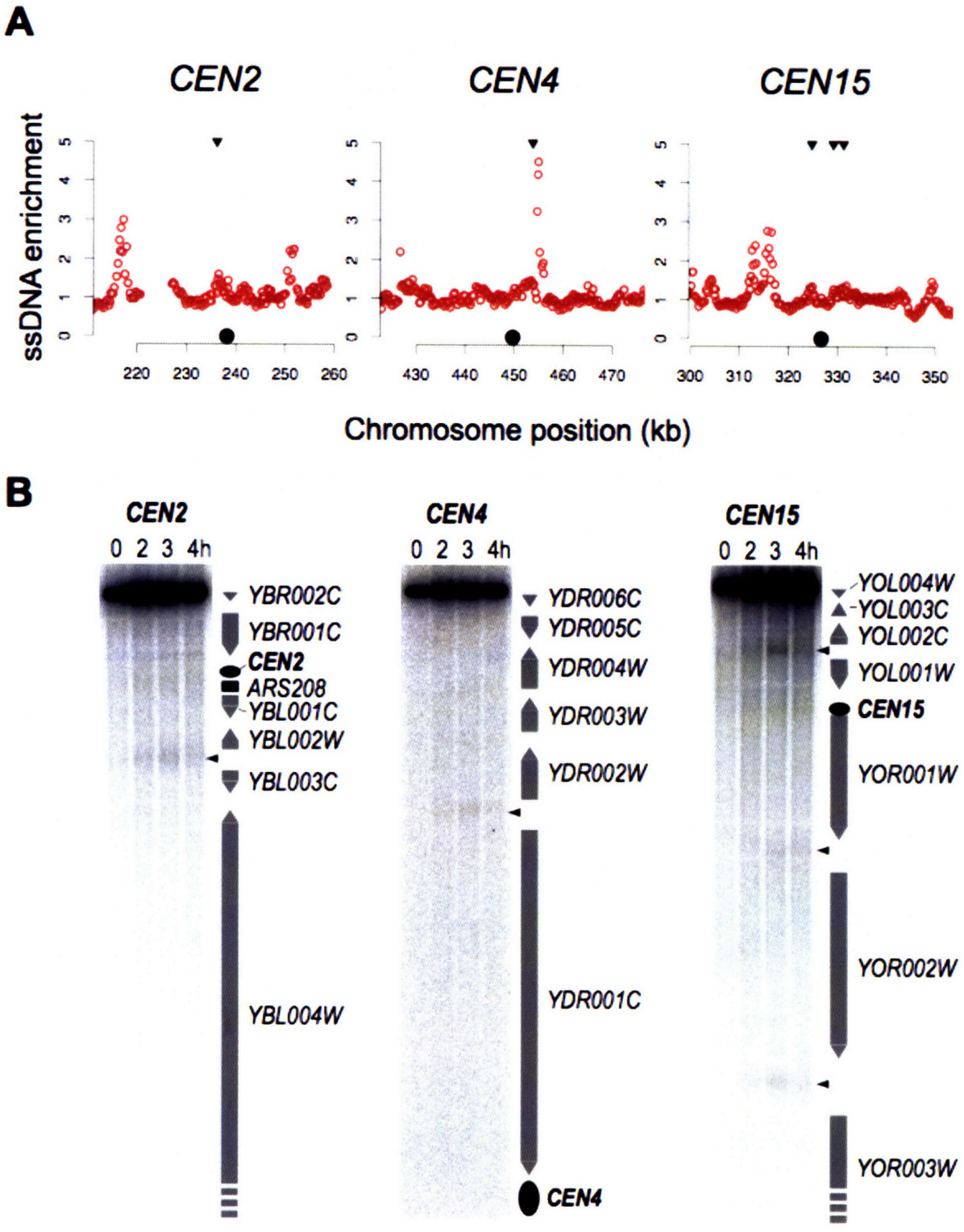

Supplemental Table 2: *dmc1Δ* DSB hotspots.

Information is provided for the 258 DSB hotspots in the *dmc1Δ* (NKY1455) strain, including chromosomal coordinates (bp) for the smoothed peak, and the start and end of the region defined as significantly enriched for each hotspot, the $\log_2$ ratio for the peak maximum, the classification of the genomic region containing the peak used for analysis of DSB localization and the closest genes to each peak. Peaks were classified based on their positions relative to genes as follows; ORF= within the coding region of a gene, DIV = in an intergenic region between two genes that are divergently transcribed, CON = in an intergenic region between two genes that are convergently transcribed, and C = in an intergenic region between two genes that are transcribed in the same direction (on the same strand). Genes were assigned to peaks if the peak was within the ORF of the gene, or if the peak was in the intergenic region containing the promoter of the gene.

Chr.	coordinate	region start	region end	log2 ratio	class	assigned genes
1	60653	59982	62628	1.264651957	ORF	YAL043C
1	70579	68853	72302	1.592503808	DIV	YAL039C,YAL038W
1	83097	81737	83407	1.317857785	ORF	YAL033W
1	92840	91014	94841	1.47888708	DIV	YAL029C,YAL028W
1	113778	112426	116226	1.515909803	ORF	YAL020C
1	129238	127618	132111	2.369071601	DIV	YAL014C,YAL013W
1	138773	137513	139711	1.171863325	C	YAL007C
1	142022	141496	143829	1.544153424	DIV	YAL005C,YAL003W
1	169887	168090	170247	1.273327784	ORF	YAR015W
1	191872	189845	192708	2.052250787	ORF	YAR035W
1	197350	197121	198088	1.486498657	W	YAR050W
2	28637	27562	29435	0.865054028	W	YBL099W
2	62101	61769	63932	1.288402972	ORF	YBL086C
2	70045	68795	72627	1.421374311	ORF	YBL082C
2	192542	192111	195931	1.642232	ORF	YBL016W
2	217912	215450	218213	1.188036983	ORF	YBL005W
2	251863	251007	252977	1.194912434	C	YBR007C
2	466782	464973	468177	1.544423025	DIV	YBR112C,YBR114W
2	502822	500907	503315	1.268804757	ORF	YBR133C
2	642606	642192	644669	2.058622045	DIV	YBR208C,YBR210W
2	701871	701394	703845	1.741571522	C	YBR240C
2	717576	716843	717970	1.26712629	ORF	YBR249C

3	59652	58026	60828	1.250182557	ORF	YCL036W
3	64877	64223	66705	1.797959018	ORF	YCL031C
3	92309	91218	93284	2.114158798	ORF	YCL018W
3	105063	104512	106649	1.064790849	ORF	YCL009C
3	210652	209646	215718	1.612341575	C	YCR046C
3	224400	222837	230179	1.722245188	ORF	YCR060W
3	237342	235294	238851	1.298018661	ORF	YCR068W
4	19389	18705	21974	1.851730679	DIV	YDL243C,YDL241W
4	31847	30864	33463	1.292833128	W	YDL236W
4	48518	47014	49473	1.25814859	C	YDL227C
4	51496	51157	51950	1.168753231	ORF	YDL226C
4	60726	60269	61804	1.556508889	C	YDL223C
4	106348	103356	107455	1.569774534	ORF	YDL197C
4	158044	156537	158338	1.339312596	CON	CON_FLAG
4	198578	198014	201027	1.589157023	C	YDL145C
4	302007	302007	303555	0.968224505	ORF	YDL086W
4	385719	385097	388440	1.539860135	C	YDL037C
4	592629	592046	593375	1.008238719	ORF	YDR073W
4	704398	703368	704855	1.046468355	W	YDR127W
4	768563	768082	769020	1.085763334	ORF	YDR155C
4	835027	833528	837587	1.899806109	ORF	YDR186C
4	892750	892750	894808	1.274931985	W	YDR214W
4	1055546	1054250	1057216	1.312941481	ORF	YDR296W
4	1080213	1079477	1081118	1.171218415	C	YDR309C
4	1162018	1160676	1163700	1.54613173	C	YDR343C
4	1242521	1241126	1242521	1.223214686	DIV	YDR384C,YDR385W
4	1278632	1277158	1279707	1.254522388	W	YDR406W
4	1386534	1384995	1387278	0.810695135	W	YDR463W
4	1410273	1409489	1412499	1.195760056	C	YDR475C
4	1420162	1416467	1421678	1.876737252	ORF	YDR481C
4	1447192	1445993	1448535	1.181344773	DIV	YDR498C,YDR499W
4	1458262	1458262	1460714	1.166237222	ORF	YDR505C
4	1469526	1467343	1470839	1.33252924	ORF	YDR510W
4	1477342	1475590	1478406	1.847794496	ORF	YDR517W
4	1489541	1488979	1490520	0.911500697	CON	CON_FLAG
5	43097	41991	43619	1.14296027	DIV	YEL059C-A,YEL058W
5	68503	68008	69873	1.336171192	ORF	YEL046C
5	79877	79737	80739	1.104025638	ORF	YEL039C
5	107176	106151	108434	0.903237291	DIV	YEL025C,YEL024W
5	131829	131276	133181	0.924969865	ORF	YEL012W
5	159582	157899	161393	1.278191782	ORF	YER004W
5	336277	335314	337374	1.189378608	ORF	YER089C
5	462167	460137	464236	1.608172856	DIV	YER145C,YER146W
5	467493	466366	467822	1.001987672	DIV	YER149C,YER150W
5	472939	472595	475429	1.792220392	ORF	YER152C
5	483412	482444	484948	1.450115882	ORF	YER156C
5	491858	489600	492236	1.252611033	ORF	YER159C
5	523212	522027	523979	0.899071698	DIV	YER168C,YER169W
6	27291	26788	28609	1.335664649	W	YFL052W
6	31030	29764	31030	1.101739947	C	YFL051C
6	36049	35645	37504	1.134087931	DIV	YFL050C,YFL049W
6	75007	74011	75828	1.320285373	DIV	YFL033C,YFL031W
6	95098	93487	97525	2.403175905	DIV	YFL022C,YFL021W
6	130576	130576	132357	1.641361967	ORF	YFL005W

6	173083	172866	173646	1.088454493	ORF	YFR014C
6	176204	175603	177378	1.254164231	ORF	YFR015C
6	181723	181356	182412	1.114458952	C	YFR016C
6	191886	190725	196044	1.446653668	W	YFR021W
6	206367	202689	207806	1.434347375	DIV	YFR026C,YFR027W
6	210512	209342	213482	1.629272214	DIV	YFR028C,YFR029W
6	224696	222007	229760	1.858177162	ORF	YFR033C
6	234657	233397	234657	1.159708483	ORF	YFR040W
6	256183	255101	256929	0.889194178	DIV	YFR053C,YFR055W
7	75959	75090	78114	1.427813355	W	YGL225W
7	93271	92452	93796	1.053064257	W	YGL210W
7	123239	121916	125083	1.422489974	ORF	YGL200C
7	143600	141604	144280	1.121826387	ORF	YGL192W
7	165669	164348	166925	1.316722204	DIV	YGL179C,YGL178W
7	196410	195646	199131	1.621088618	DIV	YGL163C,YGL162W
7	224674	224497	225358	1.113522673	ORF	YGL150C
7	227155	226447	227305	1.329898159	ORF	YGL148W
7	272216	270357	272832	1.460079579	W	YGL125W
7	397707	397098	398763	1.35294654	DIV	YGL056C,YGL055W
7	452158	451288	452638	0.993138314	DIV	YGL023C,YGL022W
7	482867	482489	485233	1.187488283	C	YGL008C
7	547148	545800	548363	1.154518082	ORF	YGR031W
7	609427	608333	611348	2.101627729	W	YGR060W
7	626647	624426	627627	1.51327864	ORF	YGR068C
7	678715	676858	679250	1.140016004	ORF	YGR097W
7	732983	732498	734379	1.033995	DIV	YGR121C,YGR121W-A
7	766606	765228	767989	1.323525978	DIV	YGR138C,YGR140W
7	849026	847235	849912	1.33587324	ORF	YGR177C
7	904923	904585	906277	1.036617743	DIV	YGR202C,YGR203W
7	958717	957757	960399	1.115570115	DIV	YGR233C,YGR234W
7	968793	967617	970904	1.152201881	C	YGR238C
7	986410	986061	988429	1.105691386	ORF	YGR248W
7	994606	992475	995314	1.335705019	DIV	YGR250C,YGR251W
7	1021578	1021149	1023686	1.065655752	ORF	YGR264C
7	1050006	1049434	1050844	1.146187943	C	YGR279C
8	26351	24918	27150	1.568065383	ORF	YHL036W
8	47777	46442	50837	1.508859933	ORF	YHL029C
8	55037	53597	55242	0.883030884	ORF	YHL025W
8	67728	64641	70508	1.732764977	ORF	YHL019C
8	121472	120594	124788	1.861976869	ORF	YHR007C
8	142360	140753	144168	1.677826805	ORF	YHR019C
8	189439	188291	191759	1.444573928	ORF	YHR041C
8	422309	421019	424286	1.991744451	DIV	YHR161C,YHR162W
8	461621	459765	464185	2.187786166	W	YHR179W
8	483284	482625	485004	1.030256411	ORF	YHR188C
8	516316	515697	517949	1.318552649	ORF	YHR207C
9	35811	35370	37219	1.483232832	DIV	YIL164C,YIL162W
9	55034	52958	57155	1.989086043	DIV	YIL154C,YIL153W
9	149749	149296	150812	0.908999022	ORF	YIL114C
9	160784	160370	161294	1.169492122	DIV	YIL109C,YIL108W
9	177264	176658	178924	1.233743935	DIV	YIL101C,YIL099W
9	269517	267033	271604	1.622650696	ORF	YIL046W
9	332755	331180	335513	2.209644181	DIV	YIL013C,YIL011W
9	337607	337006	340348	1.730123016	DIV	YIL009C-A,YIL009W

9	394257	393545	396702	1.903218488	DIV	YIR019C,YIR021W
10	30712	30517	31326	1.071831063	W	YJL213W
10	61353	60088	61955	1.066238108	ORF	YJL198W
10	69209	68054	70074	1.116850437	DIV	YJL196C,YJL194W
10	79813	78789	80538	1.128264599	DIV	YJL187C,YJL186W
10	95759	93745	96415	1.416815753	ORF	YJL174W
10	158885	158283	159368	1.17755254	ORF	YJL134W
10	236532	235809	237291	1.46600447	DIV	YJL101C,YJL100W
10	361668	361380	362644	0.944619793	ORF	YJL042W
10	392474	390045	393628	1.549936752	ORF	YJL026W
10	467442	465399	467961	1.475964495	ORF	YJR019C
10	571795	569467	572296	1.225336539	ORF	YJR072C
10	579564	578386	579988	1.271610656	ORF	YJR078W,YJR079W,YJR080C
10	622565	622010	625082	1.29760843	ORF	YJR104C
10	639545	637496	641672	1.43280524	DIV	YJR113C,YJR115W
10	663144	662351	664703	1.213452281	C	YJR127C
10	704755	702829	706786	1.830717199	ORF	YJR147W
10	718015	717033	719460	1.283678511	W	YJR152W
11	19279	19140	20880	1.236236488	DIV	YKL218C,YKL217W
11	47707	45805	49177	1.00432681	ORF	YKL208W
11	70156	66898	71857	1.607166554	ORF	YKL198C
11	80793	79652	83703	1.375349875	DIV	YKL192C,YKL191W
11	92058	91617	93360	0.955244639	C	YKL187C
11	98208	98208	100402	1.100231262	CON	CON_FLAG
11	230079	229135	230079	1.085017271	DIV	YKL110C,YKL109W
11	401407	400846	402639	1.000993128	ORF	YKL020C
11	517538	515926	517905	1.250428634	W	YKR041W
11	518955	518955	520674	0.988735555	ORF	YKR042W
11	527163	523595	527769	1.61901687	DIV	YKR049C,YKR050W
11	567496	566870	567743	1.08340977	DIV	YKR066C,YKR067W
11	577096	574583	577778	1.245832926	ORF	YKR072C
11	581946	580404	582619	1.018684492	ORF	YKR076W
11	635796	634867	636464	1.031738133	ORF	YKR099W
12	36516	35277	37944	1.293522637	C	YLL053C,YLL052C
12	87325	86902	88730	1.46727218	W	YLL027W
12	98276	98024	98999	1.031236208	ORF	YLL023C
12	109957	107975	109957	1.126700237	ORF	YLL018C
12	113535	111110	115903	1.573230385	ORF	YLL016W
12	125004	123549	126287	1.304762619	DIV	YLL013C,YLL012W
12	160176	159931	160714	1.180950845	ORF	YLR005W
12	341042	340396	342341	1.024299419	DIV	YLR099C,YLR099W-A
12	611021	610208	612288	1.349679052	ORF	YLR234W
12	659580	657434	661324	0.940121513	ORF	YLR257W
12	808727	808107	810342	1.248452831	ORF	YLR341W
12	829297	825940	829896	1.098168951	ORF	YLR350W
12	893509	892205	894738	1.348373655	DIV	YLR385C,YLR386W
12	951915	949431	951915	0.860890598	ORF	YLR413W
12	954204	953267	955374	1.455108247	C	YLR414C
12	1001827	1000799	1002962	1.309014244	DIV	YLR431C,YLR432W
12	1011818	1009762	1014623	1.85640726	ORF	YLR437C
12	1025699	1023368	1026039	1.116974955	ORF	YLR446W
12	1043656	1042097	1044425	1.407441603	DIV	YLR453C,YLR454W
13	26059	25640	27951	1.004382821	DIV	YML123C,YML121W
13	43469	42823	44448	1.308983885	ORF	YML114C

13	46423	45734	46801	0.941730352	W	YML111W
13	51569	50503	52608	1.130979273	DIV	YML110C,YML109W
13	70162	69072	70469	1.230853706	ORF	YML100W-A
13	94773	94773	96896	0.898861582	ORF	YML087C
13	101055	98724	104253	1.551604937	DIV	YML083C,YML082W
13	119706	118182	119706	0.882756762	C	YML075C
13	168917	166573	170522	1.252845515	C	YML054C-A
13	192317	191848	192585	0.930771957	DIV	YML043C,YML042W
13	286667	286425	288955	0.916752717	W	YMR011W
13	334754	334039	336099	0.890297918	DIV	YMR031C,YMR032W
13	396394	395774	397581	0.896101893	DIV	YMR062C,YMR063W
13	409346	406812	410567	1.283757087	ORF	YMR070W
13	512335	511839	513145	1.186717501	W	YMR123W
13	541077	539417	542741	1.369678244	DIV	YMR135C,YMR136W
13	557862	556389	559438	1.181049537	ORF	YMR146C
13	668067	666157	668664	1.173967517	ORF	YMR202W
13	797205	796009	800223	2.067185214	ORF	YMR265C
13	851441	850861	852978	1.384501797	ORF	YMR290C
13	860733	859973	862416	1.161233983	ORF	YMR296C
13	874638	873431	875964	1.36233316	DIV	YMR303C,YMR304W
13	915929	914039	916647	1.125575203	C	YMR319C
14	34875	32959	35942	1.713325959	ORF	YNL321W
14	51847	51485	52989	1.10704683	C	YNL311C
14	79523	79523	82553	1.183650454	ORF	YNL294C
14	90596	88192	91352	1.189710438	ORF	YNL288W
14	116571	116571	118334	1.22528601	W	YNL277W-A
14	121976	121443	123089	1.245825272	ORF	YNL274C
14	187073	186279	189125	1.603070334	C	YNL245C
14	197464	196521	201420	1.68121846	ORF	YNL241C
14	309543	308638	311195	1.169388134	ORF	YNL173C
14	426891	426194	428641	1.223571536	DIV	YNL104C,YNL103W
14	606187	603754	607055	1.218080505	W	YNL014W
14	651801	650666	653510	1.74706962	DIV	YNR013C,YNR014W
14	662701	661220	663138	1.023636372	DIV	YNR016C,YNR017W
15	83510	82764	84616	1.123641855	DIV	YOL126C,YOL125W
15	128181	128181	129133	1.234147825	DIV	YOL101C,YOL100W
15	194304	193466	194756	1.247345978	ORF	YOL073C
15	218065	215599	220032	1.183932843	ORF	YOL059W
15	315432	313877	317956	1.435991962	C	YOL006C
15	480184	478381	482422	1.366792162	ORF	YOR083W
15	487787	485955	488481	1.114506247	ORF	YOR087W
15	493874	492866	496293	1.764847875	ORF	YOR091W
15	585787	584883	588389	1.643243873	ORF	YOR138C
15	662047	661113	662584	1.167248856	DIV	YOR175C,YOR176W
15	700887	700594	701932	1.203080924	C	YOR192C
15	769272	768095	771564	1.42248273	ORF	YOR229W
15	861065	859445	861065	0.985033671	DIV	YOR290C,YOR291W
15	944169	942579	945204	1.314951868	ORF	YOR332W
15	988153	986323	989588	1.46871539	ORF	YOR348C
15	1043527	1042345	1044149	1.089214325	DIV	YOR375C,YOR376W-A
16	40734	38983	41718	1.670679194	W	YPL265W
16	47397	45039	48374	1.46757436	ORF	YPL262W
16	75050	74035	76247	1.334181565	C	YPL250C
16	84707	83706	85928	1.115451226	ORF	YPL246C

16	171417	168944	173879	1.698232363	DIV	YPL201C,YPL200W
16	215708	213203	216388	1.17122684	C	YPL177C
16	340350	339376	340926	2.080210278	ORF	YPL111W
16	504466	504039	505651	0.845621538	ORF	YPL023C
16	518345	516485	520649	1.452964752	ORF	YPL018W,YPL017C
16	526235	525034	528334	1.345591171	ORF	YPL015C
16	609874	607333	610362	0.987272889	ORF	YPR023C
16	654841	653013	654989	1.133880952	ORF	YPR043W
16	677814	676794	680329	1.40673814	ORF	YPR063C
16	695412	693792	697586	1.217805173	C	YPR074C
16	785718	785394	786572	1.207248227	W	YPR124W
16	812627	812042	814246	1.180658673	C	YPR138C
16	821425	820336	822462	1.071741706	DIV	YPR144C,YPR145W
16	828608	828608	830218	0.843106244	DIV	YPR148C,YPR149W
16	841424	839294	841989	1.461175057	ORF	YPR157W
16	861356	860041	862101	1.458207148	ORF	YPR160W
16	888180	887541	888732	1.249438463	ORF	YPR174C
16	899688	899217	902063	1.492538521	DIV	YPR181C,YPR182W
16	911341	911341	913003	0.936317665	ORF	YPR187W
16	921283	918539	922969	1.711378934	W	YPR192W

References

Allers, T. and M. Lichten (2001). "Differential Timing and Control of Noncrossover and Crossover Recombination during Meiosis." Cell 106: 47-57.

Aparicio, O. M., D. M. Weinstein, et al. (1997). "Components and dynamics of DNA replication complexes in S. cerevisiae: redistribution of MCM proteins and Cdc45p during S phase." Cell 91(1): 59-69.

Barton, A. B., Y. Su, et al. (2003). "A function for subtelomeric DNA in Saccharomyces cerevisiae." Genetics 165(2): 929-34.

Baudat, F. and A. Nicolas (1997). "Clustering of meiotic double-strand breaks on yeast chromosome III." Proc Natl Acad Sci U S A 94(10): 5213-8.

Bergerat, A., B. de Massy, et al. (1997). "An Atypical Topoisomerase II from Archaea with Implications for Meiotic Recombination." Nature 386: 414-417.

Birdsell, J. A. (2002). "Integrating genomics, bioinformatics, and classical genetics to study the effects of recombination on genome evolution." Mol Biol Evol 19(7): 1181-97.

Bishop, D. K., D. Park, et al. (1992). "DMC1: a meiosis-specific yeast homolog of E. coli recA required for recombination, synaptonemal complex formation, and cell cycle progression." Cell 69(3): 439-56.

Bishop, D. K. and D. Zickler (2004). "Early decision; meiotic crossover interference prior to stable strand exchange and synapsis." Cell 117(1): 9-15.

Blat, Y., R. U. Protacio, et al. (2002). "Physical and functional interactions among basic chromosome organizational features govern early steps of meiotic chiasma formation." Cell 111(6): 791-802.

Borde, V., A. S. Goldman, et al. (2000). "Direct coupling between meiotic DNA replication and recombination initiation." Science 290(5492): 806-9.

Borde, V., W. Lin, et al. (2004). "Association of Mre11p with double-strand break sites during yeast meiosis." Mol Cell 13(3): 389-401.

Borner, G. V., N. Kleckner, et al. (2004). "Crossover/noncrossover differentiation, synaptonemal complex formation, and regulatory surveillance at the leptotene/zygotene transition of meiosis." Cell 117(1): 29-45.

Cao, L., E. Alani, et al. (1990). "A pathway for generation and processing of double-strand breaks during meiotic recombination in S. cerevisiae." Cell 61(6): 1089-101.

Cha, R. S., B. M. Weiner, et al. (2000). "Progression of meiotic DNA replication is modulated by interchromosomal interaction proteins, negatively by Spo11p and positively by Rec8p." Genes Dev 14(4): 493-503.

Chua, P. R. and G. S. Roeder (1997). "Tam1, a telomere-associated meiotic protein, functions in chromosome synapsis and crossover interference." Genes Dev 11(14): 1786-800.

Conrad, M. N., A. M. Dominguez, et al. (1997). "Ndj1p, a Meiotic Telomere Protein Required for Normal Chromosome Synapsis and Segregation in Yeast." Science 276: 1252-1255.

Copenhaver, G. P., W. E. Browne, et al. (1998). "Assaying genome-wide recombination and centromere functions with Arabidopsis tetrads." Proc Natl Acad Sci U S A 95(1): 247-52.

Dresser, M. E., D. J. Ewing, et al. (1997). "DMC1 functions in a Saccharomyces cerevisiae meiotic pathway that is largely independent of the RAD51 pathway." Genetics 147(2): 533-44.

Feng, W., D. Collingwood, et al. (2006). "Genomic mapping of single-stranded DNA in hydroxyurea-challenged yeasts identifies origins of replication." Nat Cell Biol 8(2): 148-55.

Gerton, J. L., J. DeRisi, et al. (2000). "Inaugural article: global mapping of meiotic recombination hotspots and coldspots in the yeast Saccharomyces cerevisiae." Proc Natl Acad Sci U S A 97(21): 11383-90.

Haber, J. E., P. C. Thorburn, et al. (1984). "Meiotic and mitotic behavior of dicentric chromosomes in Saccharomyces cerevisiae." Genetics 106(2): 185-205.

Hochwagen, A., W. H. Tham, et al. (2005). "The FK506 binding protein Fpr3 counteracts protein phosphatase 1 to maintain meiotic recombination checkpoint activity." Cell 122(6): 861-73.

Huberman, J. A., L. D. Spotila, et al. (1987). "The in vivo replication origin of the yeast 2 microns plasmid." Cell 51(3): 473-81.

Hunter, N. and N. Kleckner (2001). "The single-end invasion: an asymmetric intermediate at the double-strand break to double-holliday junction transition of meiotic recombination." Cell 106(1): 59-70.

Kaback, D. B., V. Guacci, et al. (1992). "Chromosome size-dependent control of meiotic recombination." Science 256(5054): 228-32.

Keeney, S., C. N. Giroux, et al. (1997). "Meiosis-specific DNA double-strand breaks are catalyzed by Spo11, a member of a widely conserved protein family." Cell 88(3): 375-84.

Kiburz, B. M., D. B. Reynolds, et al. (2005). "The core centromere and Sgo1 establish a 50-kb cohesin-protected domain around centromeres during meiosis I." Genes Dev 19(24): 3017-30.

Kitajima, T. S., S. Yokobayashi, et al. (2003). "Distinct cohesin complexes organize meiotic chromosome domains." Science 300(5622): 1152-5.

Kong, A., D. F. Gudbjartsson, et al. (2002). "A high-resolution recombination map of the human genome." Nat Genet 31(3): 241-7.

Lamb, N. E., S. L. Sherman, et al. (2005). "Effect of meiotic recombination on the production of aneuploid gametes in humans." Cytogenet Genome Res 111(3-4): 250-5.

Lambie, E. J. and G. S. Roeder (1988). "A yeast centromere acts in cis to inhibit meiotic gene conversion of adjacent sequences." Cell 52(6): 863-73.

Lichten, M. and A. S. Goldman (1995). "Meiotic recombination hotspots." Annu Rev Genet 29: 423-44.

MacAlpine, D. M., P. S. Perlman, et al. (1998). "The high mobility group protein Abf2p influences the level of yeast mitochondrial DNA recombination intermediates in vivo." Proc Natl Acad Sci U S A 95(12): 6739-43.

Maleki, S. and S. Keeney (2004). "Modifying histones and initiating meiotic recombination; new answers to an old question." Cell 118(4): 404-6.

Mieczkowski, P. A., M. Dominska, et al. (2006). "Global analysis of the relationship between the binding of the Bas1p transcription factor and meiosis-specific double-strand DNA breaks in Saccharomyces cerevisiae." Mol Cell Biol 26(3): 1014-27.

Mieczkowski, P. A., M. Dominska, et al. (2007). "Loss of a histone deacetylase dramatically alters the genomic distribution of Spo11p-catalyzed DNA breaks in Saccharomyces cerevisiae." Proc Natl Acad Sci U S A 104(10): 3955-60.

Petes, T. D. (2001). "Meiotic recombination hot spots and cold spots." Nat Rev Genet 2(5): 360-9.

Petes, T. D. and D. Botstein (1977). "Simple Mendelian inheritance of the reiterated ribosomal DNA of yeast." Proc Natl Acad Sci U S A 74(11): 5091-5.

Petes, T. D. and P. J. Pukkila (1995). "Meiotic sister chromatid recombination." Adv Genet 33: 41-62.

Petronczki, M., M. F. Siomos, et al. (2003). "Un menage a quatre: the molecular biology of chromosome segregation in meiosis." Cell 112(4): 423-40.

Pokholok, D. K., C. T. Harbison, et al. (2005). "Genome-wide map of nucleosome acetylation and methylation in yeast." Cell 122(4): 517-27.

Prieler, S., A. Penkner, et al. (2005). "The control of Spo11's interaction with meiotic recombination hotspots." Genes Dev 19(2): 255-69.

Primig, M., R. M. Williams, et al. (2000). "The Core Meiotic Transcriptome in Budding Yeasts." Nat. Genet. 26: 415-423.

Renauld, H., O. M. Aparicio, et al. (1993). "Silent domains are assembled continuously from the telomere and are defined by promoter distance and strength, and by SIR3 dosage." Genes Dev 7(7A): 1133-45.

Robine, N., N. Uematsu, et al. (2007). "Genome-wide redistribution of meiotic double-strand breaks in Saccharomyces cerevisiae." Mol Cell Biol 27(5): 1868-80.

Rockmill, B., K. Voelkel-Meiman, et al. (2006). "Centromere-proximal crossovers are associated with precocious separation of sister chromatids during meiosis in Saccharomyces cerevisiae." Genetics 174(4): 1745-54.

San-Segundo, P. A. and G. S. Roeder (1999). "Pch2 links chromatin silencing to meiotic checkpoint control." Cell 97(3): 313-24.

Scherthan, H. (2001). "A Bouquet Makes Ends Meet." Nat. Rev. Mol. Cell Biol. 2: 621-627.

Schwacha, A. and N. Kleckner (1997). "Interhomolog bias during meiotic recombination: meiotic functions promote a highly differentiated interhomolog-only pathway." Cell 90(6): 1123-35.

Stahl, F. W., H. M. Foss, et al. (2004). "Does crossover interference count in Saccharomyces cerevisiae?" Genetics 168(1): 35-48.

Storlazzi, A., L. Xu, et al. (1995). "Crossover and noncrossover recombination during meiosis: timing and pathway relationships." Proc Natl Acad Sci U S A 92(18): 8512-6.

Su, Y., A. B. Barton, et al. (2000). "Decreased meiotic reciprocal recombination in subtelomeric regions in Saccharomyces cerevisiae." Chromosoma 109(7): 467-75.

Sun, H., D. Treco, et al. (1991). "Extensive 3'-overhanging, single-stranded DNA associated with the meiosis-specific double-strand breaks at the ARG4 recombination initiation site." Cell 64(6): 1155-61.

Sym, M., J. A. Engebrecht, et al. (1993). "ZIP1 Is a Synaptonemal Complex Protein Required for Meiotic Chromosome Synapsis." cell 72: 365-378.

Sym, M. and G. S. Roeder (1994). "Crossover interference is abolished in the absence of a synaptonemal complex protein." Cell 79(2): 283-92.

Trelles-Sticken, E., M. E. Dresser, et al. (2000). "Meiotic Telomere Protein Ndj1 Is Required for Meiosis-Specific Telomere Distribution, Bouquet Formation and Efficient Homolog Pairing." J. Cell Biol. 151: 95-106.

Turney, D., T. de Los Santos, et al. (2004). "Does chromosome size affect map distance and genetic interference in budding yeast?" Genetics 168(4): 2421-4.

White, M. A., M. Dominska, et al. (1993). "Transcription factors are required for the meiotic recombination hotspot at the HIS4 locus in Saccharomyces cerevisiae." Proc Natl Acad Sci U S A 90(14): 6621-5.

Wu, T. C. and M. Lichten (1994). "Meiosis-induced double-strand break sites determined by yeast chromatin structure." Science 263(5146): 515-8.

Yang, Y. H., S. Dudoit, et al. (2001). Normalization of cDNA microarray data. SPIE BiOS 2001, San Jose, CA.

Zickler, D. (2006). "From early homologue recognition to synaptonemal complex formation." Chromosoma 115(3): 158-74.

Chapter IV

Discussion and Future Directions

Key conclusions

This comprehensive genomic study of meiotic DNA replication and intiation of homologous recombination reveals novel regulatory mechanisms of early meiotic chromosome dynamics. Location analysis for the pre-replicative complex (pre-RC) during meiosis revealed that a subset of yeast origins are located within the coding region of genes and that replication complex assembly at these sites is regulated by transcription of the locus. Measurement of both the kinetics of DNA replication in pre-meiotic and mitotic S phases as well as the extent of replication in cells that were arrested in early S phase by the intra-S phase checkpoint indicated that replication timing is significantly altered at a large number of loci between the two cell divisions. I also observed that the replication inhibitor hydroxyurea (HU) inhibits meiotic entry through the nitrogen-sensing pathway.

Localization of meiotic ssDNA revealed a non-random distribution of double-strand break (DSB) sites in meiosis. DSBs occur most frequently in the promoters of active genes. DSBs are enriched in regions close to chromosome ends, suggesting a mechanism to distribute DSBs to chromosomes of all sizes. Additionally, analysis of DSBs at telomeres, centromeres and the rDNA revealed that although these regions all experience strongly reduced frequency of homologous recombination, the mechanisms of regulation are distinct for each type of locus.

Regulation of replication complex assembly

In this study, I determined the locations of potential replication origins by localization of the pre-RC in the mitotic and meiotic cell cycles. This experiment indicated that the protracted pre-meiotic S phase is not caused by changes in replication complex assembly at potential replication origins. Therefore, the alterations in replication kinetics are due to changes in the regulation of replication initiation and progression. Additionally, I observed a subset of yeast origins that are located within genes, and transcriptional activation of these loci precludes pre-RC formation or dismantles existing pre-RCs. This observation is consistent with previous findings (Snyder, Sapolsky et al. 1988; Tanaka, Halter et al. 1994; Nieduszynski, Blow et al. 2005; Mori and Shirahige 2007). In yeast, most origins are located in non-transcribed intergenic regions, and are particularly enriched at the 3' ends of genes relative to the 5' ends (MacAlpine and Bell 2005; Nieduszynski, Knox et al. 2006). This result implies that both the assembly of transcriptional complexes at promoters and the process of active transcription are incompatible with replication complex assembly. This finding is seemingly incongruent with studies in metazoans, which found that pre-RCs are more likely to be located within gene dense regions, and that such origins initiate replication early in S phase (MacAlpine and Bell 2005). However, these studies did not have the resolution to precisely map either the locations of ORC and Mcm2-7 binding, or the initiation events themselves, which may not occur in transcribed regions. Unlike yeast, higher eukaryotic genomes are rich in repetitive sequence elements and heterochromatin. Therefore, pre-RC assembly and replication initiation may be facilitated in regions of relatively open chromatin structure, but pre-RC binding and replication initiation may occur in non-transcribed sequences.

Regulation of replication timing in meiosis

Replication timing at a large number of loci differs during pre-meiotic and mitotic S phases. Specifically, the initiation of DNA replication is delayed and/or less efficient at a large number of origins during pre-meiotic S phase. To distinguish between these possibilities, more detailed studies of replication initiation and elongation are necessary. Two dimensional gel analysis of replication intermediates from a number of individual origins could be used to measure the efficiency of DNA replication during pre-meiotic S phase. This technique has been used to measure the initiation of replication from origins on chromosomes III and VI during pre-mitotic and pre-meiotic S phases (Collins and Newlon 1994; Mori and Shirahige 2007). However, comparison of the replication profiles on chromosomes III and VI in pre-meiotic and pre-mitotic S phase revealed few changes in replication timing at the origins that were studied. One exception was ARS309, which was less efficient in 2D gel analysis in pre-meiotic S phase and was associated with a smaller peak in the pre-meiotic replication profile and did not initiate replication in HU treated meiotic cells. Therefore, the differences we observed in the replication profiles are confirmed by an independent measure of the efficiency of replication initiation.

Little is known about how replication timing is regulated. Therefore, pre-meiotic S phase is a novel system to study determinants of replication timing. Previous studies have implied that local chromatin may have an effect on replication initiation (Vogelauer, Rubbi et al. 2002; Aparicio, Viggiani et al. 2004). Transcription factors have also been implicated in the efficiency of replication initiation from certain origins (Li, Yu et al. 1998). Although comprehensive genomic studies of transcription factor binding and chromatin modifications have been carried out in mitotically growing cells, no specific relationships between chromatin structure and

replication origin regulation has been reported. During the meiotic cell cycle, chromosomes undergo large changes in gene expression patterns as well as chromosome structure and compaction. Transcription factor binding, histone occupancy and nucleosome modifications have not yet been determined for meiotically dividing cells. It is possible that comparison of the changes in chromatin structure between the mitotic and meiotic cell cycle could reveal mechanisms that regulate DNA replication.

The pre-meiotic and pre-mitotic replication profiles also indicated that the average fork rate is slower in pre-meiotic S phase. This result could be explained by slower fork progression or by inefficient replication initiation at neighboring origins, which would cause forks to travel through a given site in opposite directions in different cells. Therefore, the forks would "cancel each other out" when the average of the population is measured. Two dimensional gel analysis could be used measure the direction of fork movement through non-origin fragments to determine whether relative initiation rates from origins located on either side are altered during pre-meiotic S phase. The rate of DNA synthesis could also be measured by a single cell assay such as DNA combing, in which the DNA in replicating cells is pulse-labeled with a fluorescent nucleotide analog. This method could be used to determine both the average rate of nucleotide incorporation, as well as the distribution of rates in the population. This could distinguish between the models of slower fork progression being due to a lower consistent rate or frequent pausing of replication forks.

The intra-S phase checkpoint in meiosis

I describe here the finding that the replication inhibitor HU blocks meiotic entry in a manner similar to other nitrogen-containing compounds. Cell cycle progression was inhibited through down regulation of meiosis-specific transcription. Hochwagen and colleagues observed a similar effect on transcription when they exposed sporulating cells to the microtubule depolymerizing agent benomyl (Hochwagen, Wrobel et al. 2005). Because the meiotic cell cycle is driven by an altered transcriptional program, the observed inhibition of meiosis-specific transcription could be a conserved mechanism to prevent spore formation when cells are grown in unfavorable conditions. The inhibition of meiotic entry in the presence of HU observed here suggests that the role of the intra-S phase checkpoint in the meiotic cell cycle should be reinvestigated. Studies of a strain with a mutation in the Mec1 gene suggested that the intra-S phase checkpoint preserves viability in yeast sporulated in the presence of low or intermediate levels of HU. Under these conditions, DNA replication was not completely blocked, indicating that meiotic entry was also not blocked. Therefore, it seems likely that the intra-S phase checkpoint functions in meiotic cells.

Particularly, it would be interesting to understand whether the intra-S phase checkpoint regulates the separation and coordination of replication and DSB formation in meiosis. It has been suggested that DNA replication is required for DSB formation, because a *clb5Δclb6Δ* strain failed to undergo both DNA replication and recombination (Dirick, Goetsch et al. 1998; Stuart and Wittenberg 1998; Smith, Penkner et al. 2001). However, cells that did not undergo DNA replication due to a meiotic null allele of Cdc6 made DSBs (Hochwagen, Tham et al. 2005), indicating that replication is not required for DSB formation. Therefore, DSB formation may

require CDK activity independent of DNA replication, through the use recombination-specific CDK substrates. Nine factors other than Spo11 are required to make DSBs. It has been reported that DSB formation requires the phosphorylation of the Mer2/Rec107 protein by Cdc28, probably because this phosphorylation even regulates the association of Mer2/Rec107 with other DSB factors (Henderson, Kee et al. 2006). However, because CDK activity is also required for pre-meiotic DNA replication, another mechanism must exist to prevent DSB formation until DNA replication is completed.

It is possible to test whether the presence of ongoing DNA replication prevents DSB formation by arresting cells in pre-meiotic S phase. DSB formation can be measured in a *cln3Δ* strain that can initiate replication in the presence of HU. If DSBs are prevented in HU, mutations in the checkpoint factors Rad53 and Mec1 can be used to test whether the separation of replication and recombination occurs via the intra-S phase checkpoint. A similar checkpoint-dependent mechanism exists to separate replication and recombination in *S. pombe* (Tonami, Murakami et al. 2005). It will also be interesting to determine whether the intra-S phase checkpoint functions to separate replication and recombination in an unperturbed cell cycle or only in when replication is inhibited. A strain in which one arm of chromosome III experiences delayed replication also experiences delayed DSB formation in the late replicating region. This strain could be used to determine whether Rad53 and Mec1 are required for the inhibition of DSB formation on a local level.

Global distribution of DSB activity

Every chromosome requires at least one crossover to be faithfully segregated during meiosis I. CO formation requires both the initiation of recombination by DSB formation and the repair of the DSB into a mature CO recombinant. The data present here suggest a model for DSB distribution, in which the localization of the majority of DSB activity to a constant region proximal to chromosome ends would ensure that all chromosomes receive a sufficient number of DSBs to initiate at least one CO per chromosome per cell. One problem with the localization of DSBs to the ends of chromosome is that cohesion distal to the CO is required to hold homologs together during metaphase I. In yeast, cohesin binds to chromosomes every ~10 kb, on average ,although level of cohesin association were reported to be lower at chromosome ends than at internal loci (Glynn, Megee et al. 2004). Therefore, the location of the DSB enriched region >20kb from chromosome ends means that there is likely to be a significant amount of cohesin on chromosome arms distal to the break site. Additionally, a mechanism could exist to recruit cohesin to the repetitive telomere elements in meisois. These regions were not examined in any genome-wide studies of cohesin localization.

While the localization of DSBs to a discrete region close to the ends of all chromsomes is a simple and compelling model for DSB distribution in organisms that have multiple chromosomes of different sizes, the mechanism of such DSB placement remains elusive. We eliminated roles for the bouquet, the synamptonemal complex and Sir dependent heterochromatin *SIR2* in determining this non-random distribution of DSBs, through deletion of proteins essential for each of these structures. It is possible that other telomere binding proteins such as yKU70 play a role in the recognition of chromosome ends by DBS factors. Intranuclear

organization may also help to localize DSB factors to chromosome ends. Therefore, it would be interesting to map DSB distribution in mutant cells in which the telomeres fail to localize to the periphery. Human haplotype maps indicate that there are increased levels of recombination close to chromosome ends. Therefore similar mechanisms to distribute DSBs may exists in other organisms. DSB sites have not been mapped in any metazoan systems. The technique described here should permit the localization of DSB sites in mammalian cells.

Suppression of homologous recombination

Sites close to centromeres, telomeres, and the repetitive rDNA have decreased rates of homologous recombination in yeast. The findings described here indicate that the suppression of recombination at these three loci occurs via different mechanisms. We observed no reduction in the rate of DSB formation close to centromeres, indicating that altered DSB repair regulation is responsible for the lack of COs in the pericentromeric regions. We postulated that repair occurs from the sister-chromatid instead of the homolog in this region, and may involve exclusion of the protein Red1 from pericentromeric regions. A similar bias in meiotic DSB repair exists at the rDNA (Petes and Pukkila 1995). Repair from the sister versus the homolog can be tested at individual centromere proximal hotspots, if the homologous chromosomes are differentially marked to allow them to be distinguished. Additionally, it would be interesting to examine the localization of Dmc1, Rad51 and other SC complex components that normally direct or stabilize interactions with the homolgous chromosome.

In contrast to the mechanism that prevents COs close to centromeres, CO recombination close to telomeres and the rDNA is prevent by eliminating the initiating DSBs. Removal of Pch2

revealed DSB hotpots close to the rDNA that are silenced in wild-type cells. While recombination in the rDNA can lead to rDNA loss and death, it is less clear why breaks within single copy sequences 50-100kb away from the rDNA would be deleterious to the cell. *pch2Δ* cells experience increased levels of recombination within the rDNA. It is not known whether this is due to initiating DSBs within the rDNA itself, or whether breaks in the single copy sequence close to the rDNA could lead to ssDNA exposure of rDNA repeat sequence.

An alternative hypothesis for the requirement for Pch2 at the rDNA is that special structures or chromatin at the rDNA are particularly succeptible to DSB formation. We found that Sir2 is required for the increased levels of DSBs close to the rDNA that we observed in *pch2Δ* cells. These data implied that DSBs formation in this region requires Sir2, either through a direct or indirect interaction. While Sir2 does not localize to the single-copy sequence adjacent to the rDNA in mitotic cells (Lieb, Liu et al. 2001), it is possible that in sporulating cells Sir2 itself, or a specialized chromatin structure propagated by Sir2, spreads from the rDNA into the adjacent single-copy regions. These models can be tested by chromatin immunoprecipiation of Pch2, Sir2, and other factors involved in DSB formation. Additionally, chromatin modifications such Sir2-dependent deacetylation can be measured near the rDNA. While the repetitive DNA elements are the exception in the yeast genome, they represent the majority of the DNA content in higher organisms. Therefore the mechanisms that prevent homologous recombination within or close to repetitive DNA may apply to other organisms.

References

Aparicio, J. G., C. J. Viggiani, et al. (2004). "The Rpd3-Sin3 histone deacetylase regulates replication timing and enables intra-S origin control in Saccharomyces cerevisiae." Mol Cell Biol 24(11): 4769-80.

Collins, I. and C. S. Newlon (1994). "Chromosomal DNA replication initiates at the same origins in meiosis and mitosis." Mol Cell Biol 14(5): 3524-34.

Dirick, L., L. Goetsch, et al. (1998). "Regulation of meiotic S phase by Ime2 and a Clb5,6-associated kinase in Saccharomyces cerevisiae." Science 281(5384): 1854-7.

Glynn, E. F., P. C. Megee, et al. (2004). "Genome-wide mapping of the cohesin complex in the yeast Saccharomyces cerevisiae." PLoS Biol 2(9): E259.

Henderson, K. A., K. Kee, et al. (2006). "Cyclin-dependent kinase directly regulates initiation of meiotic recombination." Cell 125(7): 1321-32.

Hochwagen, A., W. H. Tham, et al. (2005). "The FK506 binding protein Fpr3 counteracts protein phosphatase 1 to maintain meiotic recombination checkpoint activity." Cell 122(6): 861-73.

Hochwagen, A., G. Wrobel, et al. (2005). "Novel response to microtubule perturbation in meiosis." Mol Cell Biol 25(11): 4767-81.

Li, R., D. S. Yu, et al. (1998). "Activation of chromosomal DNA replication in Saccharomyces cerevisiae by acidic transcriptional activation domains." Mol Cell Biol 18(3): 1296-302.

Lieb, J. D., X. Liu, et al. (2001). "Promoter-specific binding of Rap1 revealed by genome-wide maps of protein-DNA association." Nat Genet 28(4): 327-34.

MacAlpine, D. M. and S. P. Bell (2005). "A genomic view of eukaryotic DNA replication." Chromosome Res 13(3): 309-26.

Mori, S. and K. Shirahige (2007). "Perturbation of the activity of replication origin by meiosis-specific transcription." J Biol Chem 282(7): 4447-52.

Nieduszynski, C. A., J. J. Blow, et al. (2005). "The requirement of yeast replication origins for pre-replication complex proteins is modulated by transcription." Nucleic Acids Res 33(8): 2410-20.

Nieduszynski, C. A., Y. Knox, et al. (2006). "Genome-wide identification of replication origins in yeast by comparative genomics." Genes Dev 20(14): 1874-9.

Petes, T. D. and P. J. Pukkila (1995). "Meiotic sister chromatid recombination." Adv Genet 33: 41-62.

Smith, K. N., A. Penkner, et al. (2001). "B-Type Cyclins CLB5 and CLB6 Control the Initiation of Recombination and Synaptonemal Complex Formation in Yeast Meiosis." Curr. Biol. 11: 88-97.

Snyder, M., R. J. Sapolsky, et al. (1988). "Transcription interferes with elements important for chromosome maintenance in Saccharomyces cerevisiae." Mol Cell Biol 8(5): 2184-94.

Stuart, D. and C. Wittenberg (1998). "CLB5 and CLB6 Are Required for Premeiotic DNA Replication and Activation of the Meiotic S/M Checkpoint." Genes Dev 12: 2698-2710.

Tanaka, S., D. Halter, et al. (1994). "Transcription through the yeast origin of replication ARS1 ends at the ABFI binding site and affects extrachromosomal maintenance of minichromosomes." Nucleic Acids Res 22(19): 3904-10.

Tonami, Y., H. Murakami, et al. (2005). "A checkpoint control linking meiotic S phase and recombination initiation in fission yeast." Proc Natl Acad Sci U S A 102(16): 5797-801.

Vogelauer, M., L. Rubbi, et al. (2002). "Histone acetylation regulates the time of replication origin firing." Mol Cell 10(5): 1223-33.